

NDOT Research Report

Report No. 531-13-803

**Comparing the Direct Costs and Infrastructure
Implications of Anti-Icing Strategies**

November 2015

**Nevada Department of Transportation
1263 South Stewart Street
Carson City, NV 89712**



1. Report No.		2. Government Accession No.		3. Recipient's Catalog No.	
4. Title and Subtitle COMPARING THE DIRECT COSTS AND INFRASTRUCTURE IMPLICATIONS OF ANTI-ICING STRATEGIES				5. Report Date December 2015	
				6. Performing Organization Code	
7. Author(s) Ning Xie, Xianming Shi, Yan Zhang, Anburaj Muthumani, Laura Fay				8. Performing Organization Report No.	
9. Performing Organization Name and Address Corrosion and Sustainable Infrastructure Lab Western Transportation Institute P. O. Box 174250, Montana State University Bozeman, MT 59717-4250				10. Work Unit No. (TRAIS)	
				11. Contract or Grant No.	
12. Sponsoring Agency Name and Address Nevada Department of Transportation Research Section 1263 S. Stewart Street Carson City, NV 89712				13. Type of Report and Period Covered	
				14. Sponsoring Agency Code	
15. Supplementary Notes					
16. Abstract Field and laboratory investigations were conducted to examine the effects of various deicers along with freeze/thaw cycles on concrete materials. Samples cored from three sites in Nevada were used to evaluate the impact of deicers on the concrete infrastructures. Furthermore, lab testing was carried out to further elucidate the corrosion mechanisms of the deicers on concrete. Eight types of deicers, including KCl, NaCl, CaCl ₂ , MgCl ₂ , KAc, KFm, CaAc ₂ and CaFm ₂ , were used in this study to compare their effects on concrete materials. The lab testing results show that the concrete materials had considerable reduction in mechanical properties with exposure to freeze/thaw cycles and deicers. The reduction in mechanical strength is provided as a rate by deicer type. When the concrete was exposed to MgCl ₂ solution with concentration above 20%, a large amount of white precipitate was found in the MgCl ₂ solution. The chemical and microstructure analysis results show that the molecular formula of the white precipitates are CaMg ₂ Cl ₆ ·(H ₂ O) ₁₂ . These findings elucidate the corrosion mechanism of the concrete materials with exposure to MgCl ₂ solution. The results of the SEM/EDS analysis show that the binder phase in concrete degrade with the exposure of deicers. Notable chemical contents were changed in both field cored and lab prepared samples. In addition to concrete materials, the effects of chloride based deicers, including KCl, NaCl, CaCl ₂ and MgCl ₂ , on asphalt materials were evaluated. Results of the creep stiffness testing determined that the impacts of MgCl ₂ on asphalt material are higher than other chloride based deicers. In addition, the anti-icing performances of high friction polymer coating and overlays were analyzed. Four types of polymers, including epoxy, acrylic resin, methyl methacrylate reactive resin (MMA) and high molecular weight methacrylate polymer (HMWM), were used as anti-icing surface treatment methods on asphalt and concrete pavement. It was found that the epoxy is not a good option as anti-icing overlay because the integrity of the epoxy overlay will be broken when exposed to deicers along with freeze/thaw cycles. By contrast, the acrylic resin performed much better than the epoxy polymer. The results also indicated that both of the MMA and HMWM surface treatments exhibited good performance.					
17. Key Words Deicers, concrete, corrosion, anti-icing, surface treatment			18. Distribution Statement		
19. Security Classification (of this report) Unclassified		20. Security Classification (of this page) Unclassified		21. No. of Pages	22. Price N/A

**COMPARING THE DIRECT COSTS AND INFRASTRUCTURE
IMPLICATIONS OF ANTI-ICING STRATEGIES**

Draft Final Report

November 2015

Disclaimer

This work was sponsored by the Nevada Department of Transportation. The contents of this report reflect the views of the authors, who are responsible for the facts and the accuracy of the data presented herein. The contents do not necessarily reflect the official views or policies of the State of Nevada at the time of publication. This report does not constitute a standard, specification, or regulation.

COMPARING THE DIRECT COSTS AND INFRASTRUCTURE IMPLICATIONS OF ANTI-ICING STRATEGIES

Draft Final Report

by

Ning Xie, Ph.D.
Xianming Shi, Ph.D., P.E.
Yan Zhang
Anburaj Muthumani, P.E.
Laura Fay, P.E.

Western Transportation Institute
College of Engineering
Montana State University
PO Box 174250
Bozeman, MT 59717

for

Nevada Department of Transportation
Research Section
Attn: Manju Kumar
1263 S. Stewart Street
Carson City, NV 89712

and

Federal Highway Administration
400 Seventh Street, SW
Washington, DC 20590-0003

November 2015

SI* (MODERN METRIC) CONVERSION FACTORS

APPROXIMATE CONVERSIONS TO SI UNITS

APPROXIMATE CONVERSIONS FROM SI UNITS

Symbol	When You Know	Multiply By	To Find	Symbol	Symbol	When You Know	Multiply By	To Find	Symbol
<u>LENGTH</u>					<u>LENGTH</u>				
in	Inches	25.4	millimeters	mm	mm	millimeters	0.039	inches	in
ft	Feet	0.305	meters	m	m	meters	3.28	feet	ft
yd	Yards	0.914	meters	m	m	meters	1.09	yards	yd
mi	Miles	1.61	kilometers	km	km	kilometers	0.621	miles	mi
<u>AREA</u>					<u>AREA</u>				
in ²	square inches	645.2	millimeters squared	mm ²	mm ²	millimeters squared	0.0016	square inches	in ²
ft ²	square feet	0.093	meters squared	m ²	m ²	meters squared	10.764	square feet	ft ²
yd ²	square yards	0.836	meters squared	m ²	m ²	meters squared	1.196	square yards	yd ²
ac	Acres	0.405	hectares	ha	ha	hectares	2.47	acres	ac
mi ²	square miles	2.59	kilometers squared	km ²	km ²	kilometers squared	0.386	square miles	mi ²
<u>VOLUME</u>					<u>VOLUME</u>				
fl oz	fluid ounces	29.57	milliliters	ml	ml	milliliters	0.034	fluid ounces	fl oz
gal	Gallons	3.785	liters	L	L	liters	0.264	gallons	gal
ft ³	cubic feet	0.028	meters cubed	m ³	m ³	meters cubed	35.315	cubic feet	ft ³
yd ³	cubic yards	0.765	meters cubed	m ³	m ³	meters cubed	1.308	cubic yards	yd ³
NOTE: Volumes greater than 1000 L shall be shown in m ³ .									
<u>MASS</u>					<u>MASS</u>				
oz	Ounces	28.35	grams	g	g	grams	0.035	ounces	oz
lb	Pounds	0.454	kilograms	kg	kg	kilograms	2.205	pounds	lb
T	short tons (2000 lb)	0.907	megagrams	Mg	Mg	megagrams	1.102	short tons (2000 lb)	T
<u>TEMPERATURE (exact)</u>					<u>TEMPERATURE (exact)</u>				
°F	Fahrenheit	(F-32)/1.8	Celsius	°C	°C	Celsius	1.8C+32	Fahrenheit	°F

*SI is the symbol for the International System of Measurement

ACKNOWLEDGMENTS

The authors acknowledge the financial support for this project provided by the Nevada Department of Transportation (NDOT). They appreciate the guidance provided to this project by the NDOT project manager Manjunathan Kumar and panel members Tyler J. Thew, Matthew L. Nussbaumer, Darin P. Tedford, Kelly H. Yokotake, and Andrew E. Knust. They would also like to acknowledge Dana May and Carla Little of the Western Transportation Institute for editorial review.

DISCLAIMER

This document is disseminated under the sponsorship of the Nevada Department of Transportation and the United States Department of Transportation in the interest of information exchange. The State of Nevada and the United States Government assume no liability of its contents or use thereof.

The contents of this report reflect the view of the authors who are solely responsible for the facts and accuracy of the material presented. The contents do not necessarily reflect the official views of the Nevada Department of Transportation or the United States Department of Transportation.

The State of Nevada and the United States Government do not endorse products of manufacturers. Trademarks or manufacturers' names appear herein only because they are considered essential to the object of this document.

This report does not constitute a standard, specification, or regulation.

TABLE OF CONTENTS

LIST OF FIGURES	7
LIST OF TABLES	12
Chapter 1. Introduction	1
1.1 Problem Statement	1
1.2 Research Objectives	3
1.3 Urgency and Anticipated Benefits	3
1.4 Scope of Work and Report Organization	4
1.5 References	5
Chapter 2. Effects of Deicers on Concrete Infrastructures: State of the Art	6
2.1 Introduction	6
2.2 Anti-Icing Strategies on Bridge Decks and Pavements	6
2.2.1 Rough Surfaces and Physical Bending Pavements	7
2.2.2 High Friction Anti-icing Polymer Overlays	8
2.2.3 Asphalt Pavement with Anti-icing Additives	9
2.2.4 Heated Pavement Technologies	10
2.2.5 Fixed Automated Spray Technology (FAST) System	18
2.2.6. Chemicals Used for Anti-icing Strategies	21
2.2.7. Performance and Cost Comparisons of Anti-Icing Chemicals	21
2.3 Anti-icer Impacts on Highway Infrastructure	28
2.3.1 Impact of Anti-Icing Chemicals on Steel/bare Metals	29
2.3.2 Impact of Anti-icing Chemicals on Concrete Pavement	30
2.3.3 Impact of Anti-icing Chemicals on Asphalt Pavement	33
2.4 Cost Impacts of Anti-icing Chemicals	35
2.5 References	36
Chapter 3. Survey Results from State DOTs	45
Chapter 4. Field Performance of Coring Concrete Samples	55
4.1 Introduction	55
4.2 Methodology	55

4.2.1 Field Sampling.....	55
4.2.2. Compressive Strength.....	56
4.2.3. Splitting Tensile Strength	56
4.2.4 Microstructure Analysis	57
4.3 Mechanical Properties	58
4.3.1 Compressive Strength.....	58
4.3.2 Splitting Tensile Strength	58
4.4 Microstructure Analysis	59
4.4.1 SEM Analysis	59
4.4.2 SEM/EDS Analysis	64
4.5 Key Findings	68
4.6 References	68
Chapter 5. Laboratory Investigation	69
5.1 Materials and Methods	69
5.1.1 Deicing Capability Test of Various Deicers.....	69
5.1.2 Corrosion Resistance Tests of Metals Exposed to Various Deicers.....	70
5.1.3 Preparation of Concrete Specimens.....	71
5.1.4 Freeze-thaw Cycling in the Presence of Deicers	71
5.1.5 Testing Mechanical Properties of Concrete Specimens	72
5.1.6 Microscopic Characterization.....	72
5.2 Results and Discussion.....	73
5.2.1 Deicing Capability of Various Deicers.....	73
5.2.2 The corrosion rate of metals due to exposure to deicers	73
5.2.3 Mass Loss of Concrete Samples Exposed to Deicer Solutions and F/T Cycling	75
5.2.4 Mechanical Properties	81
5.3 Microstructure Analysis	85
5.3.1 SEM Analysis	85
5.3.2 SEM/EDS Analysis	97
5.3.3 TEM/XRD Analysis of the White Precipitates in the MgCl ₂ Solution	111
5.4 Key Findings	113
5.5 References	114

Chapter 6. Laboratory Investigation of Asphalt and High Friction Pavement Exposed to Chloride Based Deicers.....	116
6.1 Introduction.....	116
6.1.1. Epoxy Resins.....	116
6.1.2. Acrylic Ester Polymers.....	119
6.1.3. Advantages and Disadvantages of Various Polymers.....	121
6.2. Materials and methods.....	122
6.2.1 Sample Preparation.....	122
6.2.2 Polymer Coating Procedure.....	122
6.2.3 Bond Strength Testing.....	122
6.2.4 Freeze/thaw Resistance Testing.....	123
6.2.5 Bending Beam Rheometer (BBR) Test.....	123
6.2.6 Surface Friction.....	124
6.2.7 Microscopic Characterization.....	124
6.3. Results and Discussion.....	125
6.3.1 Anti-icing performance of asphalt materials exposed to chloride based deicers.....	125
6.3.2 Impacts of Freeze/Thaw Cycles and Deicers on Polymer Coatings.....	126
6.3.3 Abrasion Resistance of Acrylic Polymer Coatings.....	129
6.3.4 Anti-icing Performance of Crack Sealant Polymers.....	130
6.4 Key Findings.....	136
6.5 References.....	136
Chapter 7. Conclusions.....	138

LIST OF FIGURES

Figure 2- 1 FAST system in action.....	19
Figure 2- 2 Freezing Point of Common Road Chemicals (Rubin, 2010).....	23
Figure 3- 1 Survey results about the training conditions of agency staff.....	49
Figure 3- 2 Main consideration of NDOT highway winter maintenance agencies in choosing anti-icing technologies and/or chemicals.....	50
Figure 4- 1 The setup of the splitting tensile strength test.....	57
Figure 4- 2 Compressive strengths of cored concrete samples from the bridge decks of Creek, Forrest, and Hills.....	58
Figure 4- 3 Splitting tensile strengths of cored concrete samples from the bridge decks of Creek, Forrest, and Hills.....	59
Figure 4- 4 SEM fracture surface morphologies of the samples cored from the Creek site with a) low and b) high magnification.....	60
Figure 4- 5 SEM fracture surface morphologies of the samples cored from the Forrest site with a) low and b) high magnification.....	62
Figure 4- 6 SEM fracture surface morphologies of the samples cored from the Hills site with a) low and b) high magnification.....	63
Figure 4- 7 SEM/EDS of the fracture surface the samples cored from the Creek site with a) SEM image and b) corresponding EDS results.....	65
Figure 4- 8 SEM/EDS of the fracture surface the samples cored from the Forrest site with a) SEM image and b) corresponding EDS results.....	66
Figure 4- 9 SEM/EDS of the fracture surface the samples cored from the Hills site with a) SEM image and b) corresponding EDS results.....	67
Figure 5- 1 The corrosion rates of stainless steel with exposure to various deicers.....	74
Figure 5- 2 The corrosion rates of plain steel with exposure to various deicers.....	74
Figure 5- 3 The corrosion rates of galvanized steel with exposure to various deicers.....	75

Figure 5- 4 The external morphologies of laboratory-fabricated concrete cylinders exposed to various deicer solutions after 3, 7, and 15 F/T and W/D cycles	79
Figure 5- 5 The mass loss of concrete samples exposed to F/T and W/D cycles in various deicer solutions a) after 3 F/T cycles, b) after 7 F/T cycles, and c) after 15 F/T cycles	81
Figure 5- 6 Compressive strength of concrete samples exposed to various deicers with a) 3, b) 7, and c) 15 F/T cycles.....	83
Figure 5- 7 Splitting tensile strength of concrete samples exposed to various deicers with a) 3, b) 7, and c) 15 F/T cycles.....	85
Figure 5- 8 The SEM images of the concrete samples after 15 F/T and W/D cycles in water with a) low and b) high magnification	86
Figure 5- 9 The SEM images of the concrete samples after 15 F/T and W/D cycles in NaCl solution with a) low and b) high magnification	87
Figure 5- 10 The SEM images of the concrete samples after 15 F/T and W/D cycles in MgCl ₂ solution with a) low and b) high magnification	89
Figure 5- 11 The SEM images of the concrete samples after 15 F/T and W/D cycles in MgCl ₂ solution with a) low and b) high magnification	90
Figure 5- 12 The SEM images of the concrete samples after 15 F/T and W/D cycles in KFm solution with a) low and b) high magnification	92
Figure 5- 13 The SEM images of the concrete samples after 15 F/T and W/D cycles in KAc solution with a) low and b) high magnification	93
Figure 5- 14 The SEM images of the concrete samples after 15 F/T and W/D cycles in CaCl ₂ solution.....	94
Figure 5- 15 The SEM images of the concrete samples after 15 F/T and W/D cycles in CaAc ₂ solution with a) low and b) high magnification	95
Figure 5- 16 The SEM images of the concrete samples after 15 F/T and W/D cycles in CaFm ₂ solution with a) low and b) high magnification	96
Figure 5- 17 The SEM/EDS result of the concrete samples after 15 F/T and W/D cycles in water with a) SEM image and b) corresponding EDS element distribution results	98
Figure 5- 18 The SEM/EDS result of the concrete samples after 15 F/T and W/D cycles in NaCl with a) SEM image and b) corresponding EDS element distribution results.....	99

Figure 5- 19 The SEM/EDS result of the concrete samples after 15 F/T and W/D cycles in NaCl with a) high magnification SEM image and b) corresponding EDS element distribution results. *NOTE: The SEM image is a little bit out of focus due to the device limitation on magnification.*..... 100

Figure 5- 20 The SEM/EDS result of the concrete samples after 15 F/T and W/D cycles in MgCl₂ with a) SEM image and b) corresponding EDS element distribution result ... 101

Figure 5- 21 The SEM/EDS result of the concrete samples after 15 F/T and W/D cycles in MgCl₂ with a) high magnification SEM image and b) corresponding EDS element distribution results..... 102

Figure 5- 22 The SEM/EDS result of the concrete samples after 15 F/T and W/D cycles in MgCl₂ with a) SEM image and b) corresponding EDS element distribution results.. 103

Figure 5- 23 The SEM/EDS result of the concrete samples after 15 F/T and W/D cycles in KAc with a) SEM image and b) corresponding EDS element distribution results..... 104

Figure 5- 24 The SEM/EDS result of the concrete samples after 15 F/T and W/D cycles in KAc with a) high magnification SEM image and b) corresponding EDS element distribution results..... 105

Figure 5- 25 The SEM/EDS result of the concrete samples after 15 F/T and W/D cycles in KFm with a) SEM image and b) corresponding EDS element distribution results 106

Figure 5- 26 The SEM/EDS result of the concrete samples after 15 F/T and W/D cycles in KFm with a) high magnification SEM image and b) corresponding EDS element distribution results..... 107

Figure 5- 27 The SEM/EDS result of the concrete samples after 15 F/T and W/D cycles in CaCl₂ with a) SEM image and b) corresponding EDS element distribution results... 108

Figure 5- 28 The SEM/EDS result of the concrete samples after 15 F/T and W/D cycles in CaAc₂ with a) SEM image and b) corresponding EDS element distribution results.. 109

Figure 5- 29 The SEM/EDS result of the concrete samples after 15 F/T and W/D cycles in CaFm₂ with a) high magnification SEM image and b) corresponding EDS element distribution results..... 110

Figure 5- 30 Concrete samples experienced 15 F/T cycles in MgCl₂ (rectangular box) and NaCl (round box) with concentration of a) 20% MgCl₂ and NaCl and b) 1% MgCl₂ and NaCl..... 112

Figure 5- 31 XRD pattern of the white precipitates from MgCl ₂ solution with concentration of 20% after 15 times of F/T cycles of the concrete samples	113
Figure 5- 32 Transmission Electronic Microscopy morphologies of the white precipitates of concrete samples after 15 of F/T cycles in MgCl ₂ solution	113
Figure 6- 1 The chemical structure of epoxy resin	117
Figure 6- 2 The structure and properties of epoxy resins (Osumi, 1987)	117
Figure 6- 3 Anionic mechanism of epoxy reaction (Lee, 1967)	118
Figure 6- 4 The structure of the acrylic ester monomers (Stone, 2010)	120
Figure 6- 5 The polymerization mechanism of the acrylic monomers	120
Figure 6- 6 Bond strength tests	123
Figure 6- 7 British Pendulum Tester.....	124
Figure 6- 8 Creep stiffness of PG 68-22 grade asphalt exposed to chloride based deicers at	125
Figure 6- 9 The m-values of PG 68-22 grade asphalt exposed to chloride based deicers at	125
Figure 6- 10 External failure images of the acrylic polymer coating on asphalt concrete, a) failure of both polymer and asphalt, b) failure of polymer, and c) failure of asphalt.	126
Figure 6- 11 External image of acrylic polymer coating a) before and b) after F/T cycles in water.....	127
Figure 6- 12 External image of epoxy polymer coating a) before and b) after F/T cycles in water.....	127
Figure 6- 13 Bond strength of acrylic polymer exposed to a) water, b) NaCl, and c) MgCl ₂ solution after 15 F/T cycles at various temperatures.	128
Figure 6- 14 Asphalt concrete samples with the acrylic polymer coating a) before and b) after abrasion resistance testing.....	129
Figure 6- 15 Splitting tensile strength of concrete samples with various coatings with exposure to a) NaCl and b) MgCl ₂ solution.....	131

Figure 6- 16 SEM microstructure images of the HMWM coatings after 15 F/T cycles with exposure to MgCl₂ solution a) low magnification, b) high magnification 132

Figure 6- 17 SEM microstructure images of the MMA coatings after 15 F/T cycles with exposure to MgCl₂ solution a) low magnification, b) high magnification 133

Figure 6- 18 SEM microstructure images of the HMWM coatings after 15 F/T cycles with exposure to NaCl solution a) low magnification, b) high magnification..... 134

Figure 6- 19 SEM microstructure Images of the MMA coatings after 15 F/T cycles with exposure to NaCl solution a) low magnification, b) high magnification..... 135

LIST OF TABLES

Table 2- 1 Cost Estimates for Various Heating Systems for Snow and Ice Control (Zhang et al., 2009).....	11
Table 2- 2 Costs of Conductive Concrete versus Conventional Concrete, in 1998 USD (Tuan, 2004).	12
Table 2- 3 Comparison of Different Deicing Systems.....	13
Table 2- 4 Pavement Heating System Costs per Season, in 1972 USD (Murry and Eigerman, 1972).	17
Table 2- 5 Cost Data of a Geothermal Heating System in Virginia, in 2000 USD (Hoppe, 2000).	17
Table 2- 6 Eutectic Temperature vs. Effective Temperature for Several Deicers	22
Table 2- 7 Approximate Cost of Common Deicers	25
Table 3- 1 Number of responses for each title type	45
Table 3- 2 Number of responses for district distribution.....	46
Table 3- 3 Responses on the application of anti-icing technologies.....	47
Table 3- 4 Answers on the chemicals used for anti-icing operations	49
Table 3- 5 Agency’s responses on the cost saving estimation as a result of implementing anti-icing technologies or chemicals.....	51
Table 3- 6 Response on the typical weather maintenance period.....	52
Table 3- 7 Comments on the typical road weather scenarios for winter highway maintenance.	52
Table 3- 8 Response on the significant risk of anti-icing operations to the durability of highway infrastructure.	53
Table 3- 9 Response on the maintenance and replacement costs associated with infrastructure damage due to anti-icing operations.	53
Table 3- 10 The study situations about how to evaluate or mitigate the risk of anti-icing chemicals to infrastructure.....	54

Table 3- 11 Insights on the use of anti-icing strategies for snow and ice control.....	54
Table 5- 1 Lab testing results of the deicing capabilities of various deicers	73
Table 5- 2 Mass loss of concrete exposed to various deicers along with F/T cycles	81
Table 5- 3 Compressive strength (psi) of concrete samples exposed to various deicer solutions along with F/T cycles.....	83
Table 5- 4 Splitting tensile strength (psi) of concrete samples exposed to various deicer solutions along with F/T cycles	85
Table 6- 1 BPN values of acrylic polymer coatings before and after 15 times of F/T cycles exposed to water, NaCl and MgCl ₂ solutions	129

CHAPTER 1. INTRODUCTION

1.1 Problem Statement

Currently, there is a lack of research to systematically examine anti-icing options for NDOT's various bridge decks and pavements. Relevant information based on field experience and reliable testing is needed to assist NDOT in its process to develop anti-icing policies. Anti-icing has proven to be a pro-active approach to maintaining wintery roadways. Relative to deicing and sanding, anti-icing leads to improved level of service (LOS), reduced need for chemicals, and associated cost savings and safety and mobility benefits (Conger, 2005; Staples, 2004). However, the increased use of chemicals may pose a risk to NDOT infrastructure such as decks and pavements and reduce their service life. Research is needed to compare various anti-icing strategies (mobile operations vs. fixed automated spray technology - FAST) and chemicals (granular salt, salt brines, magnesium chloride, potassium acetate, etc.) to determine their effects on infrastructure life-cycle.

Strategies such as high friction anti-icing pavement surfaces may serve as a desirable alternative to FAST systems in terms of cost, reliability and versatility, and their cost-effectiveness is yet to be fully evaluated for NDOT. Preliminary studies have shown the benefits of such alternative anti-icing strategies in accident prevention; but there have been user concerns over their durability. Ultimately, the proposed research addresses three critical research clusters for the Nevada transportation system: Infrastructure and Materials; Data-Driven Decision Making; and Economics. Specifically, it provides the data needed by NDOT to select the anti-icing strategy most suitable for the Nevada highway system that balances safety, infrastructure and environmental goals.

Depending on the road weather scenarios, resources available and local rules of practice, NDOT and other maintenance agencies use a combination of tools for winter road maintenance and engage in activities ranging from anti-icing, deicing (including direct liquid or slurry applications), sanding (including pre-wetting), to mechanical removal (e.g., snowplowing), and snow fencing. A recent study (Ye, 2009) examined the winter maintenance operations used by NDOT and found that the agency spent approximately \$12.8 million for the winter season of 2006-07 and the use of better weather information led to tangible benefits of \$576,000 per season as it enabled more proactive strategies for snow and ice control. In other words, best practices have great potential to significantly reduce the costs of winter maintenance operations.

Over the last two decades, maintenance departments in North America have gradually made two transitions in their snow and ice control strategies. First is the transition from the use of abrasives to the use of more chemicals (Staples, 2004). This is partially owing to the negative impact of abrasives (e.g., sand) to water quality and aquatic species, air quality, vegetation, and soil and the hidden cost of sanding (e.g., cleanup cost). In more recent years, there has been a

transition from mostly deicing to anti-icing wherever possible (O’Keefe, 2005). Anti-icing is defined as “the snow and ice control practice of preventing the formation or development of bonded snow and ice by timely applications of a chemical freezing-point depressant” (Ketcham, 1996). Anti-icing has proven to be a successful method of proactively maintaining roadways during the winter season. Russ et al. (2008) concluded that if forecasts determine winter weather is “likely to affect driving conditions, it is desired to have some form of salt on the road, preferably in the form of dried brine. If there is no or very little salt residue on the road, pretreatment is recommended, except under the following conditions: (a) pretreatment would be rendered ineffective by weather conditions or (b) blowing snow may make pretreated roads dangerous”. A recent Clear Roads study (Peterson, 2010) synthesized the current practices of during-storm direct liquid applications (DLA) and found DLA to be “a valuable asset for the winter maintenance toolbox.”

An environmentally friendly alternative to chemicals used for snow and ice control is pavement/deck layers designed to reduce the bond of ice to pavement or to prevent or treat winter precipitation. Pavement treatments may be used alone or in combination with other strategies for winter roadway maintenance operations. In light of cost considerations, they are most suitable for critical highway locations such as bridge decks, mountain passes, sections prone to frost and/or sensitive to chemicals, and locations featuring sharp change in road conditions. For instance, textured seal coats for pavements or bridge decks (e.g., polymer chip seal and ultra-bounded wear courses) have the potential to prevent dangerous icy or slippery conditions and to significantly reduce the use of chemicals for winter highway maintenance. There are products available on the market (e.g., Cargill’s SafeLane®). Preliminary studies have shown the benefits of such alternative anti-icing strategies in accident prevention; but there have been user concerns over their durability (Adams, 1992; Alger, 2007; Nixon, 2006 and 2007). Continued research is warranted to advance the technology in high friction anti-icing polymer overlays, so as to ensure their long-term durability and anti-icing effectiveness. A comprehensive assessment of antifreezing pavements via rough surface texture or bending found that “the pavement in which grooves were cut and filled with urethane resin and the pavement with cylindrical or doughnut-shaped rubber embedded at regular intervals in the surface had particularly high antifreezing effectiveness.” These two types of pavement were installed at intersections and exhibited positive performance for pedestrians and automobiles. In addition, anti-icing chemicals (mostly calcium chloride) encapsulated in linseed oil have been incorporated in the top course. There are several reports available on the field performance of this product on pavements and, in general, the performance is still inconclusive (Fay, 2013). Other anti-icing additives exist that should be considered, all of which aim to reduce the usage of deicers and improve the efficiency of mechanical removal.

In summary, this work will leverage existing research and address key knowledge gaps for deploying various anti-icing strategies in the State of Nevada where unique challenges exist.

1.2 Research Objectives

The project objectives are two-fold. The research team will synthesize information from existing research on anti-icing for comparison with NDOT practices and test the chemicals and products relevant to NDOT current practices. The research will help NDOT to understand how various anti-icing strategies and chemicals affect NDOT infrastructure and to make more informed decisions accordingly.

The research approaches were modified in consultation with NDOT in order to ensure the success and usability of this research. The research includes six tasks to meet the ultimate objective of this project: *assessing the cost and infrastructure corrosion associated with various anti-icing strategies and chemicals for NDOT.*

1.3 Urgency and Anticipated Benefits

In light of the increased emphasis on the durability of transportation infrastructure and on sustainable winter operations, this research contributes to the infrastructure preservation and anti-icing efforts by NDOT and other agencies. This research also enhances NDOT's winter operating decisions and supports sustainable, cost-effective, and infrastructure-friendly maintenance of wintery roads and bridge decks in Nevada and beyond. The main benefits include the identification of anti-icing strategies and chemicals for improved level of service (LOS) and infrastructure-friendly maintenance practices.

The use of appropriate anti-icing chemicals and strategies helps to preserve the performance and service life of bridge decks and pavements, reduce the need for their costly and difficult repair and rehabilitation, and reduce the life-cycle cost of NDOT infrastructure. Furthermore, the implementation of best practices in anti-icing (with minimal additional cost) has immediate positive impact on the NDOT highway system, including cost savings, enhanced traveler safety, reduced traveler delays, and minimized environmental impacts. Based on a recent NCHRP project completed by the research team, the quantitative benefits of winter highway maintenance by the Minnesota DOT was estimated to be about \$202 million per winter season whereas the cost was about \$36.6 million. The NDOT winter maintenance cost is approximately \$12.8 million per season; as such, it can be estimated that a \$70 million benefit per season can be obtained. Assuming this research improves the NDOT winter maintenance program by a conservative 1%, this would translate to a benefit of \$700,000 per year over a life span of at least three years.

In summary, this research will benefit all DOT maintenance and bridge engineers, local agencies and other stakeholders interested in improving snow and ice removal operations without damaging infrastructure or motor vehicles. The key findings can help to modify the approach used by NDOT to select and implement their anti-icing program and enable them to make informed decisions on protecting their infrastructure from anti-icing chemicals. Additional benefits will be realized once high friction anti-icing pavements make the transition from the *First Application*

(Contract) Field Pilot Stage to the Specification & Standards with Full Corporate Deployment Stage and become widely adapted by NDOT for key highway areas.

1.4 Scope of Work and Report Organization

This research included multiple tasks as follows: (1) a comprehensive literature review that summarized current research on the effects of deicers on concrete constructions, including construction and maintenance methods, property testing and evaluation approaches, and unsolved problems; (2) a systematic laboratory investigation of the performance, including the compressive and splitting tensile strengths of the concrete samples before and after freeze/thaw cycles in eight types of deicer solutions; and (3) microstructure analysis of the cored and lab prepared samples to elucidate the potential deterioration mechanisms. The following chapters present the findings from the NDOT case study on concrete pavement.

Chapter 2 consists of a comprehensive review of the available literature pertaining to the methods and effects of deicers on concrete infrastructure, as well as an assessment of what research remains to be conducted in order to make accurate and informed decisions when choosing whether and how to reduce the negative impacts of deicers on concrete infrastructure. Chapter 3 presents qualitative and quantitative data or records relevant to NDOT anti-icing strategies on bridge decks and pavements; rules of practice; chemicals used and typical application rates under various road weather scenarios; cost and performance of chemical applications, FAST or high friction pavement surfaces; NDOT infrastructure exposed to and at risk of anti-icing chemicals; typical mix design of NDOT bridge decks, overlays, and pavements; typical rebar and dowel bar used; and related data. Two surveys were designed and distributed to gather input from NDOT winter maintenance and bridge/pavement management professionals respectively, in an effort to understand the current and past practices of these practitioners and to identify user requirements for successful anti-icing for NDOT districts. In chapter 4, a summary of the field investigations conducted by the Nevada Department of Transportation is presented. It includes a location report detailing the characteristics of the site and the results from the onsite performance evaluation. Chapter 5 presents the results of the laboratory investigation with respect to the mechanical properties of concrete samples exposed to freeze/thaw cycles in various deicer solutions. An interpretation of those results will also be provided in order to create a more comprehensive view of what is happening in the field. Chapter 6 evaluates the cost-effectiveness of high friction pavement surfaces. This chapter provides information about four polymers used as high friction pavement coating materials that were tested in the laboratory for their anti-icing and friction performance, effectiveness in reducing chloride ingress, mechanical properties, abrasion resistance and other durability properties. Finally, Chapter 7 summarizes and highlights key research findings. It also includes recommendations for the future implementation of pervious concrete under these conditions, based on a comprehensive assessment of all the preceding information.

1.5 References

- Adams, E.E., R.G. Alger, J.P. Chekan, F.D. Williams and R. Valverde., 1992, “Persistence of Reduced Snow to Pavement Shear Strength for Two Aggregate Materials Treated with CMA and NaCl” in Frank M. D’Itri (Ed.), *Chemical Deicers and the Environment* (pp.481-493). Chelsea, MI: Lewis Publishers Inc.
- Alger, R.G., 2007, *Anti-Icing Coatings and Methods* U.S. Patent No. 7279197, October 9.
- Conger SM. 2005. Winter Highway Maintenance: A Synthesis of Highway Practice. NCHRP Synthesis 344. National Research Council, Washington, D.C.
- Fay, L., Akin, M., Shi, X., and Veneziano, D. 2013, Winter Operations and Salt, Sand, and Chemical Management. Final report prepared for the National Cooperative Highway Research Program. NCHRP 20-07/Task 318. March.
- Ketcham SA, Minsk LD, Blackburn RR, Fleege EJ. 1996. Manual of Practice for an Effective Anti-Icing Program: A Guide for Highway Winter Maintenance Personnel. Publication No. FHWA-RD-9-202. Federal Highway Administration, Washington, D.C.
- Nixon, W. 2006, “An Analysis of the Performance of the Safelane™ Overlay during Winter 2005–06” A report submitted to Cargill, May 2006.
- Nixon, W. 2007, A report submitted to Cargill, May 2007.
- O’Keefe K, Shi X. 2005. Synthesis of Information on Anti-icing and Pre-wetting for Winter Highway Maintenance Practices in North America. A final report prepared for the Pacific Northwest Snowfighters Association in Collaboration with the Washington State Department of Transportation. Olympia, WA.
- Özgan, Ercan, Sercan Serin, Hüsnu Gerengi, and Ilhan Arslan. (2013). Cold Regions Science and Technology 87, 59-67
- Peterson, G., Keranen, P., and Pletan, R. 2010, Identifying the Parameters for Effective Implementation of Liquid-Only Plow Routes. A final report prepared for the Clear Roads Pooled Fund. October.
- Russ, A., Mitchell, G.F., Richardson, W., 2008, *Transportation Research Record*, Vol. 2055, 106-115.
- Staples, J.M., Gamradt, L., Stein, O., and Shi, X. 2004, Recommendations for Winter Traction Materials Management on Roadways Adjacent to Bodies of Water. Montana Department of Transportation. Helena, MT, December. FHWA/MT-04-008/8117-19. Prepared by WTI/MSU.
- Ye, Z., Strong, C., Fay, L., and Shi, X. 2009, Cost Benefits of Weather Information for Winter Road Maintenance. Final Report for the Aurora Consortium led by the Iowa Department of Transportation. April.
<http://www.aurora-program.org/pdf/AP200603FinalReport.pdf>.

CHAPTER 2. EFFECTS OF DEICERS ON CONCRETE INFRASTRUCTURES: STATE OF THE ART

2.1 Introduction

The main aim of this section is to synthesize the available literature on existing or ongoing research of 1) anti-icing strategies on bridge decks and pavements 2) chemicals used for anti-icing strategies and 3) corrosive effects on infrastructure and cost comparisons. Over the last two decades, maintenance departments in North America have gradually made two transitions in their snow and ice control strategies. The first transition is from the use of abrasives to the use of more chemicals (Staples *et al.*, 2004). This transition is partially owing to the negative impact of abrasives (e.g., sand) to water quality and aquatic species, air quality, vegetation, and soil and the hidden cost of sanding (e.g., cleanup cost). In more recent years, the strategy of deicing includes more frequent use of anti-icing in cold regions (O’Keefe and Shi, 2005). By replacing the passive strategy with the active one, the anti-icing process is defined as “the snow and ice control practice of preventing the formation or development of bonded snow and ice by timely applications of a chemical freezing-point depressant” (Ketcham *et al.*, 1996). Deicing chemicals, including salts, have been used extensively for anti-icing strategies. Even though deicing chemicals are very effective in anti-icing, it can cause severe damage to the structure of bridges, and environmental impacts. This section will summarize various techniques used for anti-icing operations, performance and cost of various chemicals used for anti-icing and their corrosion impacts on highway infrastructure.

2.2 Anti-Icing Strategies on Bridge Decks and Pavements

This section describes various anti-icing strategies designed to reduce the bond of ice or compacted snow to a pavement/bridge or to prevent or treat winter precipitation. Such pavement treatments present a desirable alternative or supplement to chemical and abrasive usage for snow and ice control, as they would largely reduce the winter maintenance cost for a given Level of Service. They become particularly attractive at extremely cold temperatures (e.g., below 15°F or -9.4°C), where most of the chemical deicers lose their effectiveness and the use of conventional methods (abrasives and snowplowing) become very costly and inefficient.

A recent AASHTO study reported the following benefits after anti-icing test programs were conducted by State DOTs such as Iowa, Missouri, Oregon and Washington (AASHTO, 2009):

- Snow plow trips reduced by roughly one-third, resulting in less wear on equipment.
- Plowing was easier and faster, with snow removal completed up to three hours sooner, resulting in reduced labor cost.

- Fewer chemicals were needed by applying the treatment prior to snowfall, resulting in reduced cost and less chemical stress to the environment.

Kelting and Laxson (2010) reported on a study that was conducted in Boulder Colorado and found that liquid anti-icing chemicals had a total application cost of \$2,500 per lane mile, as compared to \$5,200 per lane mile for conventional de-icing and sanding operations. Idaho DOT reported that anti-icing retrofits showed reduction in annual average use of abrasives, labor hours and vehicle crashes over a five year period (Goodwin and Pisano, 2003).

Pavement treatments can range from anti-freezing pavements that rely on physical action, to high-friction *in situ* anti-icing polymer overlays, to asphalt pavements containing anti-icing additives, to heated pavements using energy transfer systems. Pavement treatments may be used alone or in combination with other strategies for winter highway maintenance operations. In light of cost considerations, they are most suitable for critical highway locations such as bridge decks, mountain passes, sections prone to frost and/or sensitive to chemicals, and locations featuring sharp change in road conditions. Relative to the fixed anti-icing spray technology (Shi *et al.*, 2006), pavement treatments may exhibit higher reliability and incur less capital and maintenance costs.

2.2.1 Rough Surfaces and Physical Bending Pavements

Zhang *et al.* (2008) reported that asphalt pavement can be modified to feature rough surfaces that provide improved skid resistance in icy conditions. The roughening can be achieved through the use of open-graded or half open-graded asphalt concrete overlay and coarse aggregate (e.g., recycled ceramics particles). Such designs also aim to facilitate the breaking and abrasion of an ice layer on pavement. In addition, ordinary asphalt pavement can be modified after construction, by pressing or engraving elastic materials (rubber particles or other polymers) into the pavement surface. Such designs aim to alter the contact between roadway surface and vehicular tires, so as to facilitate the breaking of ice bond to pavement while enhancing surface friction. These modified pavements have been reported to be plagued by durability issues. Takeichi *et al.* (2001) evaluated three types of pavement that provide anti-freezing effects through rough surface texture and another eight types through pavement bending. The study found that “the pavement in which grooves were cut and filled with urethane resin and the pavement with cylindrical or doughnut-shaped rubber embedded at regular intervals in the surface had particularly high anti-freezing effectiveness.” These two types of pavement were installed at intersections and exhibited positive performance for pedestrians and automobiles.

Another type of design for physically bending pavements features the admixing of rubber particles into asphalt pavement during construction, partially replacing aggregate. The admixing of rubber particles makes it difficult for the asphalt to reach sufficient level of compaction (Zhang *et al.*, 2008). PlusRide® features the use of 3-4% granulated tire rubber (1.6-6.4 mm particles) by

weight of the mixture, along with some buffings and chopped fibers in the top course of hot-mix asphalt pavements. It is intended to increase skid resistance and provide “elastic aggregates which flex on the pavement surface under traffic” so as to facilitate the breaking of the bond of ice to pavement (Stuart and Mogawer, 1991). The technology was originally invented in Sweden in the late 1960s and later marketed and field tested in the U.S. It generally doubles the cost of the asphalt mixture. Laboratory testing showed that PlusRide “increased the resistance (of asphalt pavement) to low temperature cracking and decreased the resistance to rutting” and “had a variable effect on (its) moisture susceptibility”. Nonetheless, most field PlusRide pavements surveyed under a FHWA study exhibited “no difference in performance rutting, cracking, and raveling,” relative to control sections. Field tests of PlusRide by Alaska and New Jersey DOTs reported significant benefits in reducing vehicle stopping distances during ice conditions and in improving skid resistance of pavement, relative to control sections (Stuart and Mogawer, 1991). In the northern cold regions of China, the use of crumb rubber asphalt mixture for snow and ice control was evaluated. Adaptability of gradation type, anti-freezing performance, ice-breaking performance, and anti-wearing performance were assessed. It was found that the field performance of asphalt mixture could be improved by crumb rubber, if the appropriate amount of admixture was added. The crumb rubber asphalt mixture was used to pave a high-grade highway in China and exhibited excellent field performance. The method was effective at temperatures above -12°C (10.4°F) and with the ice thickness no more than 9 mm (0.35 inches), but no cost-benefit analysis was conducted (Zhang, 2009). In contrast, a survey response by Alaska DOT in 1998 (Wyant, 1998) reported experimenting with rubber asphaltic mixes to produce a pliable mix that would flex and break the ice as the temperature changes. However, the experimental results were not satisfactory and little benefit was obtained, which seems to contradict the early success with PlusRide.

2.2.2 High Friction Anti-icing Polymer Overlays

Textured seal coats for pavements or bridge decks have the potential to prevent dangerous icy or slippery conditions, and there are products available on the market (e.g., Cargill’s SafeLane®). SafeLane is a surface overlay in which specific polymers are applied to the paved surface and an aggregate is applied over the surface. The aggregate acts like a rigid sponge, serving as a slow-release mechanism for the applied liquid deicers. As such, the overlay can provide residual anti-icing benefits between applications. The technology was patented and commercialized after laboratory tests showed a medium-porosity limestone aggregate and CMA (calcium magnesium acetate) deicer provided impressive residual anti-icing performance. One experiment was conducted at 25°F with repeated applications of compressed snow. The results showed that reduced force was needed to shear the snow for a significantly greater number of snow reapplications, relative to a granite aggregate and NaCl deicer (Adams *et al.*, 1992). A frost experiment conducted at 34°F with aggregate samples cooled to 20°F showed the limestone–CMA combination prevented frost growth (Alger, 2005). Field observations during the 2005–06 winter

season indicated that: SafeLane was generally superior to control sections with 1) reduced snow and ice accumulation, 2) lower chemical applications were needed, and 3) better snow removal when plowing was needed (Nixon, 2006). However, no pavement temperatures below 15°F were observed during that winter season. During the 2006–07 winter season there were still some instances of SafeLane performing better than control sections, but other instances showed performance was either worse or there was no difference. Again, most pavement temperatures were above 15°F. However, during December 7, 2006 when the Mitchell Bridge in Hibbing, MN was -3°F, the SafeLane section was 50 percent frost-covered while the control section was clear (Nixon, 2007). More information and documentation are needed to determine the benefits of SafeLane during extreme cold scenarios. Meanwhile, continued research is warranted to advance the technology in high friction anti-icing polymer overlays, so as to ensure their long-term durability and anti-icing effectiveness.

2.2.3 Asphalt Pavement with Anti-icing Additives

Verglimit® features an additive of anti-icing chemicals (0.1-5 mm flake particles of 95% CaCl₂ and 5% sodium hydroxide) encapsulated in linseed oil or polyvinyl acetate and admixed generally at 5-6% by weight of the mixture in the top course of hot-mix asphalt pavements. It is intended to provide anti-icing benefits throughout the life of the pavement and works best for bridge decks, steep grades, sharp curves, heavily shaded roads, and roads adjacent to water.

Laboratory testing showed that Verglimit® increased the resistance of asphalt pavement to rutting at high temperatures, slightly reduced its temperature susceptibility, and decreased its resistance to moisture damage (Stuart and Mogawer, 1991). Verglimit® has been used in Europe, North America and Japan since the 1970s. There are several reports available on the field performance of Verglimit pavements and, in general, the data were somewhat inconclusive (Burnett, 1985; Maupin, 1986; Kiljan, 1989; Turgeon, 1989; Lohrey, 1992). Specifically regarding its performance at extremely cold temperatures, the following findings are notable:

- Observations by the New York State DOT on a test section installed in Albany, NY in 1978 suggested the overlay performs better during temperatures above 20°F. At lower temperatures, “few or no apparent differences can be discerned” relative to an adjacent control section (Burnett, 1985).
- “Areas such as Western Europe, New York State, and Pennsylvania with relatively warm, wet winters have had positive deicing results; however, areas with colder, drier winters such as Minnesota, Manitoba, and Illinois have not seen deicing benefits” (Turgeon, 1989).
- In Colorado Verglimit® projects, “the deicing action was so slow the effects were often masked by normal salting and sanding operations” (Stuart and Mogawer, 1991).

Stuart and Mogawer (1991) concluded that “Verglimit® generally triples the cost of the mixture and thus is used in selected problem areas. The additional cost is not offset by reductions in sanding and salting operations but may be offset if accidents are reduced”. In the field, some Verglimit® pavements exhibited raveling problems and others did not, which highlights the need for better quality control at the hot-mix plant and during pavement construction (especially compaction).

Due to their ability to absorb moisture from air, Verglimit® pavements may become slippery after construction, which can be mitigated by sand application or water flushing (Stuart and Mogawer, 1991). An article from the Michigan DOT ("Current Deicing Practices and Alternative Deicing Materials", 2014) concluded that Verglimit achieves its effectiveness when the temperature is over 27°F (-3°C). Heavy traffic (at least 5,000 ADT) is required for Verglimit to reach its full deicing potential. Its main advantages include: little environmental risk and significant reduction in salt usage. However, the cost of Verglimit is high (\$109-145 per ton), approximately 33 times the cost of asphalt.

A recent study conducted in Italy used sodium chloride as the dominant additive on the asphalt mixture pavement and found that additives help in the delay in ice formation on the pavement surface, accelerating the melting process, and reducing adhesion between ice and the pavement surface.

Other anti-icing additives that need to be considered include Mafilon® (Japan), IceBane® (China), and WinterPave/ECO-S among others (Lu *et al.*, 2009), all of which aim to reduce the use of chemical deicers and improve the efficiency of mechanical removal. For this technology, the challenge is to balance the need to control-release the encapsulated anti-icing chemical with the risk of degrading the durability performance of the pavement.

2.2.4 Heated Pavement Technologies

One of the most important categories under pavement treatments for snow and ice control features heated pavement technologies, aimed at preventing ice formation or facilitating snow and ice removal. Depending on the relative location of the heating source to the pavement, they can be classified as 1) internal heating [e.g., geothermal heat pumps (Seo *et al.*, 2011), 2) electrical resistive heating (Yehia and Tuan, 1999; Yehia *et al.*, 2000; Chang *et al.*, 2009; Yang *et al.*, 2012)], and 3) external heating (e.g., microwave and infrared heating). Infrared heat lamps and insulating bridge deck with urethane foam were attempted but found to be ineffective (Axon and Couch, 1963; Zenewitz, 1977). Table 2- 1 presents cost estimates by the Iowa DOT for various heating systems (Zhang *et al.*, 2009).

Table 2- 1 Cost Estimates for Various Heating Systems for Snow and Ice Control (Zhang et al., 2009).

Heating	Approximate Capital Cost	Power Consumption	Operating Cost
Infrared Heat Lamp	\$96/m ² (\$8.9/ft ²)	75 W/m ² (7 W/ft ²)	Not available
Electric Heating Cable	\$54/m ² (\$5/ft ²)	323–430 W/m ² (30–40 W/ft ²)	\$4.8/m ² (\$0.45/ft ²)
Hot Water	\$161/m ² (\$15/ft ²)	473 W/m ² (44 W/ft ²)	\$250/Storm, 3-inch snow
Heated Gas	\$378/m ² (\$35/ft ²)	Not available	\$2.1/m ² (\$0.2/ft ²)
Conductive Concrete Overlay	\$48/m ² (\$4.5/ft ²)	516 W/m ² (48 W/ft ²)	\$5.4/m ² (\$0.5 ft ²)

Electrical Resistive Heating

Electric heating cables can be embedded below the pavement surface. The heating is activated by surface mounted sensors or cameras when they detect snow or frost on the pavement. Electrical heating cables were installed as early as the 1960s in Newark, New Jersey. They were abandoned later because of problems with unreliable sensing to activate the heating unit and with electrical cables being pulled out of the overlay by the traffic. The Ladd Canyon Heating Project by the Oregon DOT tested this method on a one-mile section on Interstate Highway I-84 in 2006 (Joerger *et al.*, 2006). Similar problems were observed: two heating cables were dysfunctional due to damage by traffic. The sensors buried in the pavement were unreliable and resulted in wasted energy. The operating temperatures should be over 19°F (-7.2°C) as the system lost its effectiveness when temperature was too low. There were no system failures serious enough to impact the function of the system in keeping the structure and road safe. The low reliability and high operating cost can be two of the major disadvantages of an electric heating cable approach.

Electrically conductive concrete is produced by adding electrically conductive components to a regular concrete mix to attain stable electrical conductivity of the concrete. A thin layer of conductive concrete can generate enough heat due to its electrical resistance. This can be utilized to prevent ice formation on the pavement surface when connected to a power source. The conductive concrete includes two types: 1) conductive fiber-reinforced concrete, and 2) concrete containing conductive aggregates. The two types have both advantages and limitations. Recent advances in this field include electric roadway deicing systems featuring the use of carbon nanofiber paper (Zhou *et al.*, 2011) or carbon/glass fiber hybrid textile (Song, 2009). These new materials are yet to be field evaluated but claim to offer enhanced electrical conductivity, improved heating capacity at low voltage, uniform and rapid heating, reliable performance, low cost, and/or improved service life.

Table 2- 2 Costs of Conductive Concrete versus Conventional Concrete, in 1998 USD (Tuan, 2004).

Material	Cost/lb	Conductive Concrete Cost/yard³	Conventional Concrete Cost/yard³
Steel fiber	\$0.40	\$80.0	0
Conductive material (Coke breeze, steel shaving, etc.)	\$0.10	\$70.0	0
Sand	\$0.0024	\$2.6 ^a	\$2.4
½ in. Limestone	\$0.0024	\$3.9 ^a	\$4.7
Cement	\$4/(sac of 94 lb.)	\$35 ^a	\$32
Total		\$191.5	\$39.1

^a Due to the use of conductive materials, more sand and cement and less limestone were used than in conventional concrete (Tuan, 2004).

Yehia and Tuan (1998) investigated the feasibility of using a conductive concrete overlay for bridge deck deicing through small-scale experiments. They used conductive concrete mixes for heating concrete decks for the Nebraska Department of Roads. Table 2- 2 gives material costs of conductive concrete versus conventional cement concrete. The method was found to be easy to maintain at a lower operating cost relative to the embedded electrical/thermal heating and was a cost-effective method for bridge deck snow and ice control. Following the small-scale experimental study (Tuan, 2004), a concrete mix containing 1.5 percent of steel fibers and 25 percent steel shavings by volume was developed specifically for concrete bridge deck deicing for the Roca Spur Bridge in Roca, Nebraska. The average energy cost was about \$0.8/m² per snow storm. A comparison of conductive concrete technology against other deicing technologies in the literature revealed its potential to become the most cost-effective deicing technology in the future (Tuan, 2004).

Table 2- 3 Comparison of Different Deicing Systems

Deicing System		Initial cost*	Annual operating cost*	Power consumption
Automated System, 2004	Spray	\$600,000	\$12,000	Not applicable
Electric cable, 1961	heating	\$54/m ²	\$4.8/m ²	323 - 430 W/m ²
Hot water, 1993		\$161/m ²	\$250/storm [76 mm snow]	473 W/m ²
Heated gas, 1996		\$378/m ²	\$2.1/m ²	Not available
Conductive concrete, 2003		\$635/m ²	\$0.80/m ² /storm	350 W/m ²

*Cost figures were quoted directly from the literature, and conversion to present worth was not attempted.

As a follow-up, the Roca Bridge deicing system implemented with conductive concrete deck was evaluated from 2003 to 2008. In light of certain drawbacks of the steel shavings used in the previous study, carbon and graphite products were used to replace steel shavings in the conductive concrete mix design. In the storm events, an average of 500 W/m² (46 W/ft²) was used to raise the slab temperature 16°F above the ambient temperature by the conductive concrete. The total construction cost of the Roca Spur Bridge deicing system was \$193,175. The cost per unit of surface area of the conductive concrete inlay was \$59/ft². The construction costs of the various deicing systems are compared in

Table 2- 3. The operating cost of the Roca Bridge deicing system was about \$250 per major snow storm (Tuan, 2008). The author stated that “the most challenging task in the mix design was to achieve the long-term stability of the electrical conductivity. The use of high voltage and high current causes a safety concern”.

The conductive concrete pavement technology has also found its application to airport runways. One such example is the Snowfree® system installed and operated at O’Hare International Airport (Derwin *et al.*, 2003). Snowfree® electrically conductive asphalt pavement uses a unique blend of graphite, asphalt and electricity to heat the runway surface and break the ice bond to pavement. It was installed and operated at O’Hare International Airport for four years starting in November 1994. The installation costs were \$15 per square foot. The conductive asphalt showed similar durability to regular asphalt concrete and “consistently melted snow in all but the most severe conditions.” It was able to increase the pavement temperature 3 to 5°F per hour as designed. A cost/benefit analysis was conducted, which showed that the system will largely help to improve the exits efficiency, which could have a payback of the investment in 3 years. In severe snow storms, Snowfree would expedite the runway reopening after the shutdown, leading to cost savings for airlines and airports and safety benefits. The system was effective even when temperatures went down to -10°F in one of the winter seasons. Its ability to increase the pavement temperature 22°F confirmed its effectiveness in extremely cold weather.

Alternative Heating (Solar, Wind, Microwave and Infrared)

To further reduce the energy consumption by snow removal equipment and to overcome the problems associated with other methods, snow melting systems using natural energy have been under development in Japan. Many renewable heat sources can be used to heat the pavement such as solar energy and wind energy. Hiroshi *et al.* (1998) outlined a number of snow melting systems using natural heat sources in Japan. The approaches include utilizing underground water sources or steam, storing heat underground and circulating it under pavements, and using electricity produced by wind power. Relative to electrical resistive heating systems, such systems entail relatively high capital cost; the savings are expected from reduced maintenance cost (energy savings) as well as environmental conservation.

For microwave and infrared heating, very limited technical information was found during the literature search. The knowledge is still lacking on their performance and cost-effectiveness (Long, 2001; Hopstock and Zanko, 2005). The infrared heaters can be mounted on a truck or on the bridge-side structures to provide heat from the lamps to melt the snow and ice on the bridge deck. In 2001, Switzenbaum *et al.* (2001) described its application on aircrafts. Microwave heating shares similarities in the installation of infrared heaters and can be mounted on a truck or on the bridge-side structures (Johnson, 2006).

A study conducted in Arkansas coupled solar energy with conductive concrete to develop an anti-icing airfield runway. The study developed conductive concrete overlay panels (4 x 10ft) with graphite powder and steel fiber. Solar panels supply energy to the overlay panels and battery storage bank (to provide backup for continuous energy to overlay panels). The study found that renewable energy sources were not sufficient to heat the entire overlay panel thickness and suggested restricting energized pavement sections only to the pavement surface. Due to high implementation cost, investigators suggest implementing this system only to runway pavement sections that are difficult to maintain with heavy equipment. Furthermore, strength characteristics of conductive concrete should be further examined before implementation (Heymsfield *et al.*, 2014).

Geothermal Heating

Geothermal energy has been used to melt ice and snow on roads, sidewalks, bridges and other paved surfaces for years in locations around the world. Either heat pipe technologies or direct geothermal hot water can be used to heat the pavement. Heating airport runways with geothermal heat was claimed to be able to pay for itself in 2-5 years (Athmann *et al.*, 2014). The design was described as “either transfer the heat through pipes in the pavement by a flow of warm liquids or from direct geothermal water or through the use of heat exchanger systems or hot runoff liquids from local industry or power plants.” According to a presentation by Hellström (2007), there were plans to use a Borehole Thermal Energy Storage system to heat the runway at Kallax airport in Lulea, Sweden. The system aimed to utilize waste heat from a local steel plant by “pumping the water down into boreholes that are 65 m (210 ft) deep where it can be stored at an average temperature of 50°C with only approximately 10% heat loss in a volume of one million cubic meters.” As the cost of mechanical snow removal was around \$3 million, it was estimated that the system would pay for itself in 1-2 years if only the runway is heated, and in 5-10 years if the entire surface area is heated.

In Japan, Morita and Tago (2000) introduced and evaluated the Gaia Snow-melting System for melting snow. The Gaia Snow-Melting System utilizes the geothermal heat from the shallow ground and its auxiliary solar heat in the summer. The first system installed in Ninohe, Iwate Prefecture in 1996 has shown that even under very low temperatures for the month of January (averaging 17°F (-8.3°C)), the system was effective in snow and ice melting and environmentally benign. However, modifications would be needed to guarantee its proper operations on very cold days and recommendations on future improvements were proposed to achieve higher performance (Morita and Tago, 2000). In 2006, Yasukawa summarized the advantages of the geothermal heat pump application of the “Gaia System” (Yasukawa, 2007). These include: reduced consumption of fossil fuels (and thus less CO₂ emission), reduced consumption of electricity with higher coefficient of performance, and reduced urban heat island effect with heat exhaust placed underground. Hiroshi *et al.* (1998) reported the use of a snow melting technology utilizing tunnel

spring water and hot spring water on a highway through the Abo Pass, where the average minimum temperature had been around -0.4°F (-18°C) for the 5 years prior to the study, with average annual accumulated snow fall depth of 16.4 ft (500 cm). They concluded that the snow melting system using tunnel spring water and hot spring water are practical ways to melt snow where such thermal energy and large site are available. This is based on their higher construction costs (1.15 to 1.24 times the cost of conventional, electric-powered road heating) and lower operating costs (22 to 46 percent of the conventional systems).

Table 2- 4 Pavement Heating System Costs per Season, in 1972 USD (Murry and Eigerman, 1972).

System Type	Installation Cost (per sq. ft.)	Operating Cost (per sq. ft.)
Fluid Circulation		
Earth Heat Exchanging	Not established	Less than \$.01
Fuel Burning	(Estimated \$6-\$12) \$4	\$.10-\$.15
Electric		
Cable or Mat	\$2-\$4	\$.32-\$.45
Electrically Conductive	\$1-\$3	\$.32-\$.45

Table 2- 5 Cost Data of a Geothermal Heating System in Virginia, in 2000 USD (Hoppe, 2000).

Item	Cost
Construction	\$323/m ² (deck area); \$181,500 total
Retrofit	\$18.73/m ²
Operating	\$18/h (gas); \$312/year (electricity)
Maintenance	\$500/year

In the U.S., geothermal heating technology has also been widely used in bridges and airports as an alternative to traditional methods of snow and ice control. Due to the limited number of geographical locations with geothermal fluids above 100°F, heat pipe technologies are used more commonly in the U.S. As early as 1972, Murray and Eigerman (1972) briefly reviewed some alternative snow and ice control methods (which include pavement heating systems), with their estimated costs in

Table 2- 4. The costs of different geothermal heating technologies are in ascending order as follows: geothermal snow melting without heat pump (around \$20/ft²), ground source heat pumps (\$35/ft² for typical highway bridge deck systems), and “hydronic” geothermal heating system. Total cost for the deck and heating system will run \$100 to \$150/ft². This high cost has limited its usage to only critical areas such as bridge decks and airports (Lund, 2014). In New Jersey, a heat pipe system circulated an ethylene glycol-water mixture between pipes embedded 2 inches below the pavement surface and a horizontal grid buried 3 to 13 feet below the pavement on 2- foot levels. The performance of this ground system was compared to that of a companion 68 Btu/h/ft² electric pavement heating system. The high cost of excavation to place the ground pipes was notable in considering its cost-effectiveness (Lund, 2000). Virginia has chosen a two-lane bridge on Route 60 over the Buffalo River in Amherst County to conduct field evaluation of a heat pipe system using Freon HCFC 123 as the working fluid. The evaluation has shown that applying heat pipe technology to heat bridge decks is feasible and the effectiveness of heating depends largely on the proper working fluid. No construction problem was found for installing the heat pipe system. The cost data of this system are summarized in Table 2- 5 (Hoppe, 2000). Operating costs for the heat pipe system are lower than those for an electrical or hydronic system. The heating system does not seem to have any adverse effects on the durability of the bridge deck.

2.2.5 Fixed Automated Spray Technology (FAST) System

Fixed Automated Spray Technology, or the FAST system, is another technique for anti-icing pavements and bridges, which is typically installed at key and remote locations. Unlike the previously stated anti-icing strategies which focus mainly on changing the pavement materials and heating the pavement surface through different sources, FAST applies the liquid deicers once a road’s conditions or temperature threshold is reached to prevent ice formation.

This system is coupled with road weather information systems (RWIS) and reliable weather forecasts to spray deicers and promote the paradigm shift from being reactive to proactive in fighting winter storms. There are sensitive structures and critical segments of the roadway network that need to be free of snow and ice in a timely manner before the winter maintenance vehicles can travel to the site and treat them.

During the winter season, accidents often occur on bridge decks or shaded areas where the surface temperature tends to be lower than adjacent areas and creates potentially hazardous driving conditions, such as frequent frost and black ice (Friar and Decker, 1999; Barrett and Pigman, 2001). With conventional mobile operations, the levels of service and traffic safety are also difficult and costly to maintain for locations far from winter maintenance sheds (Christillin *et al.*, 1998), or for areas that experience a high traffic volume. In the latter case, traffic congestion may delay the arrival of winter maintenance vehicles to the site in need of treatment (Ward, 2002). In highly trafficked areas, it is difficult to maintain the materials on the road. Thus it is desirable to

apply the anti-icing chemical just prior to the frosting or icing event. FAST is a technological solution designed to provide quick, effective service delivery to such high-risk locations prone to icy conditions and/or with high traffic volumes, while reducing the amount of labor and materials needed through timely prevention of ice formation to the pavement or bonding or packing of snow. Indirect benefits from FAST may include reduced corrosion and environmental impacts and reduced traveler delay and stress. A conceptual study indicated that eliminating even one accident a year would provide a benefit-cost ratio greater than 1 for two automated FAST systems installed on bridges for the Minnesota Department of Transportation (Mn/DOT) (Keranen, 1998). Another study indicated a benefit/cost ratio of 2.36 for a proposed FAST installation on a section of I-90 in Washington State, assuming a 60 percent reduction in snow and ice-related accidents (Stowe, 2001). Figure 2- 1 shows the FAST system in action.



Figure 2- 1 FAST system in action.

FAST systems have been used in Europe more extensively than in North America. Since the mid-1980s, hundreds of automated anti-icing systems have been used throughout Europe as an established tool to battle snow and ice conditions on highways, bridges, and airports. In North America, FAST is a relatively new technology that has gained popularity since the late 1990s (SICOP, 2004). All nine respondents to the FAST survey conducted for this research project installed their first FAST system in 1995 or later, either as a test and evaluation project or based on regional deployment needs. FAST systems aim to deliver the anti-icing chemical to key locations in a controlled manner, using pumps, piping, valves and nozzles (or discs). Ideally, the application should be fully automated, using the pre-programmed logic and real-time input from a number of atmospheric and pavement sensors on-site. When the sensors detect ice presence or an imminent frost or icing event, the nozzles will be automatically triggered to spray the anti-icing chemical at a pre-determined rate and pattern.

While the concept is intuitive, its implementation is complex as the FAST system “integrates sensing technology, fluid mechanics, data processing, and communications technology with the concrete and asphalt of a highway facility” (Bell *et al.*, 2006). To reduce the level of

sophistication and facilitate the implementation of FAST, systems with less automation are often deployed in the United States, particularly those with the capabilities of automatic detection and remote activation. Such systems sacrifice some of the FAST benefits for better system reliability. For instance, the fully automated FAST system may be able to treat short-lived frost events, whereas the remotely activated FAST system cannot. In addition, the fully automated system can improve the level of service at the installation site even when winter maintenance personnel are not available.

A complete FAST system includes the spray subsystem that delivers the anti-icing chemical onto the road surface, and the control subsystem that triggers the spraying action. The spray subsystem consists of the following components:

- Reservoirs to store an appropriate amount of anti-icing chemical in an accessible area.
- A set of pumps to deliver the chemical through the piping of the hydraulic system, which connects the nozzles to the reservoirs through valves.
- A series of spray nozzles that deliver the chemical to various point locations.
- RWIS or atmospheric and pavement sensors on-site for early frost or ice warning.
- A remote processing unit (RPU) that is able to store a certain amount of data preset by the agency as well as observational data collected from the sensors for an extended period of time.
- A software application to display the FAST data in graphic and tabular formats and to manage users and their privileges.
- Electronically controlled automated and manually operated triggering devices to spray deicers.

In conclusion, FAST is not a solution for the entire road network, but rather for key locations where it can derive the maximum benefits. Selection of the proper site is crucial to the success of any FAST system installation. The site should have unique characteristics such as high winter accident statistics, remote location away from the regular maintenance routes, or very high traffic volumes (CERF, 2005). A report summarizing the experience of the Kentucky Transportation Cabinet recommended that the FAST system be used in the following areas and/or conditions: (1) crash-prone areas, (2) isolated structures that require the deicing truck to travel an unreasonable distance to treat, (3) remote areas that are difficult to reach in bad weather, or (4) bridges over water which may be more susceptible to freezing moisture (Barrett and Pigman, 2001). A methodology and a decision support tool were developed for the Nebraska Department of Roads to prioritize candidate bridge deck FAST installations, which considered accident history, bridge alignment, weather, traffic, and bridge distance from maintenance yard, among others (Khattak *et al.*, 2003).

2.2.6. Chemicals Used for Anti-icing Strategies

The important characteristic of anti-icing chemicals is to reduce the freezing point of water thereby slowing down the formation of ice, weakening the ice formation, or preventing the formation of bond between road surface and ice. The freezing point depression of road anti-icing chemicals is therefore often determined experimentally (ASTM, 2003). Liquid chemicals are most commonly used as anti-icers while it is possible to use solid chemicals under certain circumstances. There are primarily five types of chemicals available in North America for anti-icing operations, i.e., sodium chloride (NaCl), calcium chloride (CaCl₂), magnesium chloride (MgCl₂), potassium acetate (KAc), and calcium magnesium acetate (CMA). In addition, a variety of agro-based (agriculturally derived) chemicals have been used either alone or as additives to other chemicals (Nixon and Williams, 2001). Due to corrosion impact of the anti-icing chemicals on highway infrastructure such as reinforced or pre-stressed concrete and steel bridges, it is a popular practice to add corrosion inhibitor(s) or other additives in anti-icers to reduce corrosive effects. Selection of the suitable anti-icing chemicals and application rate are based on the performance of various anti-icing chemicals and the agencies' requirements. In addition, agencies have to decide on anti-icing chemicals based on the cost such that benefits of chemicals outweigh the additional cost associated with them. In interviews, maintenance personnel from Kansas and New Jersey estimated that 15-20% in cost savings could be realized by using anti-icers (Coleman, 2014). In addition to cost savings, Coleman (2014) emphasized various benefits such as easy plowing, better roads conditions for customers, and safety. However, applying anti-icers in extreme low temperatures can make the road conditions worse due to the re-freezing of chemicals when temperatures are beyond anti-icers' eutectic temperature.

2.2.7. Performance and Cost Comparisons of Anti-Icing Chemicals

Chloride-based salts are the most common chemicals used as freezing-point depressants for winter road maintenance applications. According to a 2007 survey, most state DOTs continue to rely on chloride salts and abrasives for winter highway maintenance (Fay *et al.*, 2008). NaCl, or rock salt, is the most widely used chemical due to its abundance and low cost (Fischel, 2001). Other than using it as salt brine for anti-icing, it can also be used as rock salt for de-icing or added to sand or other abrasives to prevent freezing. The Salt Institute suggested application rates of NaCl at 100 to 300 pounds per lane mile (30 to 90 kg per lane km) of solid material, and at 45 to 165 gallons per lane mile (105 to 388 liters per lane km) of 23% liquid salt brine. However, NaCl is rarely used and minimally effective below pavement temperatures of 10°F (Salt and Deicing, 1991).

Eutectic temperature is the minimum temperature a deicing solution remains in liquid form, which depends on the concentration of the deicer (usually expressed as percent weight of the

solution). During the process of melting snow or ice, additional water is produced and the deicer is diluted, which may cause the solution to re-freeze. Thus, the eutectic temperature can be significantly different from the effective temperature for a deicer. Table 2- 6 presents the comparison of eutectic and effective temperatures for some common deicers. Most chemicals cease to be effective long before the eutectic temperature is reached. As temperatures drop below 15°F, NaCl and CMA are no longer as cost-effective and other deicers may be needed for snow and ice control. Other options used in the U.S. and Nordic countries include the use of NaCl blended with liquid MgCl₂ or CaCl₂. Additionally, rock salt blended with a carbohydrate by-product, such as corn derivative or sugar beet, has been proven to enhance traction. Cold temperature modified and high performance brines may need to be developed when winters get more severe (Wieringa, 2010).

Table 2- 6 Eutectic Temperature vs. Effective Temperature for Several Deicers

Deicer (Eutectic Concentration, Eutectic Temperature)	Minimum Effective Temperature (°F)	Reference
Sodium chloride, NaCl (23.2%, -6°F)	15	(Anonymous, 2003)
	14	(S Yehia and Y Tuan, 1998)
	17.6	(Norem, 2009)
	14	(Zhang <i>et al.</i> , 2009)
Magnesium chloride, MgCl ₂ (21.6%, -28°F)	-4	(Resource Concepts Inc, 1992)
	5	(Anonymous, 2003)
	5	(S Yehia and Y Tuan, 1998)
Calcium chloride, CaCl ₂ (30%, -60°F)	5	(Shi <i>et al.</i> , 2009c)
	-20	(Anonymous, 2003)
	-13	(S Yehia and Y Tuan, 1998)
Potassium acetate, KAc (50%, -76°F)	-13	(Shi <i>et al.</i> , 2009c)
	-15	(Anonymous, 2003)
Calcium magnesium acetate, CMA (33%, 14°F; or granular, - 18.4°F)	-26	(Myhra, 2012)
	14	(Resource Concepts Inc, 1992)
	23	(Shi <i>et al.</i> , 2009c)

Figure 2- 2 presents the eutectic curves of some common deicers, i.e., their freezing point temperature as a function of their aqueous solution concentration. It shows that NaCl generally performs best for melting ice above 15°F and stops melting altogether at -6°F. At extremely cold temperatures (15°F and lower), other chlorides and acetates are often used to supplement NaCl for ice-melting as they have a lower freezing point (Rubin et al., 2010). A recent study was done to study the physical mechanism of wet pavement anti-icing using NaCl. In comparison to freezing

point theory values, the study found that 60% less salt concentration is sufficient for anti-icing operations (Klein-Paste and Wåhlin, 2013). This discrepancy is attributed to role of chemicals to weaken the ice bond with the pavement such that the ice formed on the pavement after anti-icing operations is weak enough to break with the mechanical load caused by traffic. CaCl_2 and MgCl_2 that exhibit better ice-melting performance than salt brine at cold temperatures are used by many DOTs as brine solutions for anti-icing or to pre-wet rock salt (Baroga, 2005). However, CaCl_2 and MgCl_2 are more costly than NaCl , and can be more difficult to handle. At low relative humidity, their residue on roads can attract more moisture than NaCl , which can lead to dangerous, slippery conditions under certain circumstances (Perchanok *et al.*, 1991; Center for Watershed Protection, 2003; Wasstrom, 2007).

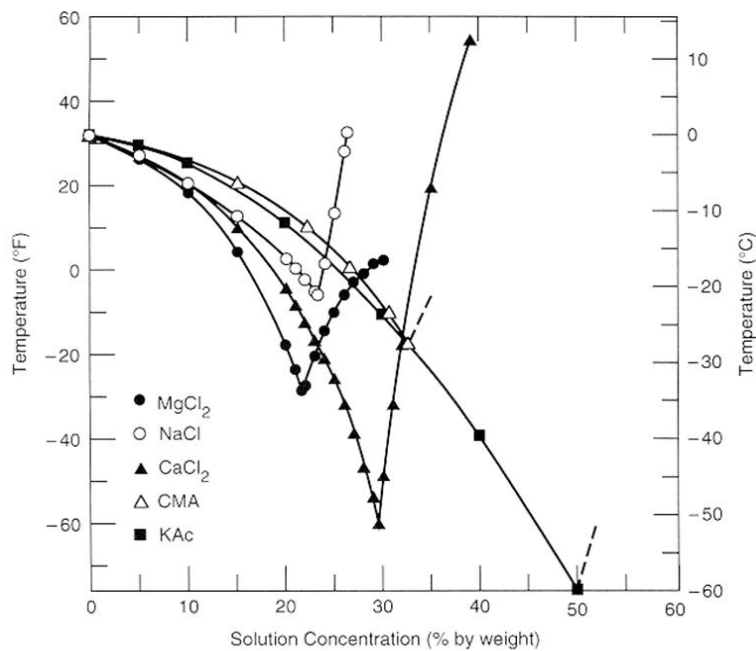


Figure 2- 2 Freezing Point of Common Road Chemicals (Rubin, 2010)

Field studies have shown that CaCl_2 can be more effective than NaCl , owing to its ability to attract moisture and stay on the roads (Warrington and Phelan, 1998). The Maine DOT conducted a field evaluation of various approaches to treating an Interstate highway during a low-temperature January 2011 snowstorm that lasted about 7 to 8 hours (CTC & Associates, 2011). The agency found that applying pre-wetted sand with a 70/30 blend of salt brine and Ice B’Gone (a proprietary MgCl_2 blend) was more cost-effective relative to two other approaches (three applications of salt, or early salting followed by sanding). In Alberta, Canada, when temperatures

fall between 0°F to 10°F, crews apply salt mixed with a small percentage of sand plus a heavy application of liquid deicer (MgCl₂ or CaCl₂) to melt the ice on the road.

Laboratory data demonstrate that, relative to NaCl, the use of CaCl₂ for comparable deicing performance between 0 and 10°F within 1 hour, would introduce five times fewer chloride anions and ten times fewer cations (Brandt, 1973). Another laboratory study demonstrated that at 15°F and 5°F CaCl₂ produced more undercutting of ice on pavement materials than NaCl (Blackburn *et al.*, 1991). Yet another laboratory study demonstrated that at 23°F the relative area deiced by chemicals followed the order of NaCl>CaCl₂>CMA>Urea, whereas their relative rate at which the chemicals debonded ice from pavement followed the order of CaCl₂>NaCl>Urea>CMA (Trost *et al.*, 1987). Granular CaCl₂ can be combined with NaCl to increase the effectiveness of NaCl in cold conditions, as CaCl₂ acts quickly, gives off heat, and forms a brine utilizing moisture from the air (Wisconsin Transportation Information Center, 1996). Mitchell *et al.* (2006) reported on an Illinois case study to find the effectiveness of salt when mixed with 10-15% CaCl₂. The study found that the additives increased the effective life of brine and reduced the minimum effective temperature. Another field study was conducted to study the difference in effectiveness of straight salt brine and a mixture of salt brine and CMA. The researchers observed that salt brine with CMA lasted longer on the road. In addition, a study was conducted in Baltimore that suspended the use of MgCl₂ for anti-icing operations due to slippery road conditions.

In a survey sponsored by the Colorado DOT, respondents stated that magnesium chloride (liquid), calcium chloride (liquid), Clearlane, potassium acetate, Ice B'Gone, De-ice, unspecified Agro-based, and sodium acetate have the lowest effective temperature. By contrast they considered abrasives, potassium formate and sodium chloride to be the least effective products (Shi *et al.*, 2009b).

Coleman (2014) found that KAc -based liquids and calcium magnesium acetate work well as anti-icers even at temperatures significantly below zero. A survey conducted in 1997 in Virginia found that liquid MgCl₂ and CaCl₂ were used for anti-icing operations and were found to be beneficial for clearing snow (Roosevelt, 1997). For many anti-icing products an increase in effectiveness results in an increase of the cost. Coleman (2014) found that traditional salt brine cost about 5 cents per gallon, while CaCl₂ and MgCl₂ cost about 40 to 50 cents per gallon. There is a clear increase in cost as the effectiveness of chemicals increases. Furthermore, KAc based products cost about \$2.5 per gallon, and they are generally used on important infrastructures (bridges) due to their anti-corrosive properties to metals (Coleman, 2014). In general, KAc and CMA can be more effective, less corrosive to carbon steel, and have reduced environmental impacts when compared to chlorides. A mixture of different chemicals can be used to find the right balance between cost and effectiveness. Approximate costs of common deicers from several references are compiled in Table 2- 7.

Table 2- 7 Approximate Cost of Common Deicers

Deicer	Approximate Cost/Weight	Reference	Application Rate, Cost/Area
Sodium chloride (NaCl)	\$26/ton	(Zhang <i>et al.</i> , 2009)*	170-890 lbs/12-ft lane mile (13-68 g/m ²), \$0.0003/m ²
	\$36/ton	(Levelton Consultants Limited, 2007)	
	\$20–42/ton	(Shi <i>et al.</i> , 2009b)	
	\$66–79/ton	(Rubin <i>et al.</i> , 2010)	
Magnesium chloride (MgCl ₂)	\$95/ton	(Zhang <i>et al.</i> , 2009)	100-150 lbs/12-ft lane mile (8-11 g/m ²), \$0.0002/m ²
	\$95/ton	(Levelton Consultants Limited, 2007)	
Calcium chloride (CaCl ₂)	\$294/ton	(Zhang <i>et al.</i> , 2009)	Used along with NaCl in U.S., \$0.03/m ²
	\$120/ton	(Levelton Consultants Limited, 2007)	
	\$267/ton	(Rubin <i>et al.</i> , 2010)	
Calcium magnesium acetate (CMA)	\$670/ton	(Zhang <i>et al.</i> , 2009)	200-500 lbs/12-ft lane mile (15-39 g/m ²), \$0.004/m ²
	\$1280/ton	(Levelton Consultants Limited, 2007)	
Potassium acetate (KAc)	NA	(Zhang <i>et al.</i> , 2009)	0.9 to 9.1 gal/1000 ft ²
Salt mixed with Calcium Chloride (NaCl and CaCl ₂)	\$98/ton	(Zhang <i>et al.</i> , 2009)	5 to 12 gal CaCl ₂ /ton of NaCl, \$0.01/m ²

* Cost reported in 2009 US dollars. NA: Not Available.

Additives such as agricultural by-products (ABPs) or organic by-product enhancers are also blended with these primary chemicals to improve their performance in snow and ice control. Known additives are corn syrup, corn steep, and other corn derivatives; beet juice-sugared or de-sugared; lignin/lignosulfonate; molasses (usually from sugar cane); brewers/distillers by-product; and glycerin. A variety of agro-based chemicals are being used either alone or as additives for other winter maintenance chemicals (Nixon and Williams, 2001). Agro-based additives increase cost but may provide enhanced ice-melting capacity, reduce the deicer corrosiveness, and/or last longer than standard chemicals when applied on roads (Kahl, 2004). Furthermore, agro-based additives utilize renewable resources and have low environmental impact. Alkoka and Kandil (2002) examined a deicing product named Magic, which was a blend of ABPs and liquid $MgCl_2$. The working temperature of the product was found to be down to $-20\text{ }^\circ\text{F}$ (Alkoka and Kandil, 2002). Pesti and Liu (2003) evaluated the use of salt brine and liquid corn salt on Nebraska highways and found liquid corn salt to be more cost-effective because it achieved bare pavement conditions quicker than salt brine and contributed to more significant road user savings (Pesti and Liu, 2003). Fu *et al.* (2012) conducted field testing in the City of Burlington, Canada of two different beet molasses based materials (30% beet juice + 70% salt brine) and regular salt brine (23% NaCl) used as pre-wetting and anti-icing agents over nine snow events. The results indicated organic materials for pre-wetting under low temperatures did not perform significantly better. With a higher cost than regular brine, organic materials can reduce the amount of chlorides released into the environment. However, the results from this study are limited to the application rates and the observed winter conditions (Fu *et al.*, 2012). The Swedish National Road and Transport Institute evaluated the friction characteristics of three types of mixtures. A brine made with 30% sugar beet flour used to pre-wet salt resulted in no significant friction improvement. Longer term performance was observed with sand mixed with hot water (Möller, 2007). Fay and Shi (2010) developed a systematic approach to assist maintenance agencies in selecting or formulating their deicers, which integrates the information available on various aspects of deicers and incorporates agency priorities.

Recently, bio-derived freezing point depressants have been developed for airport runway and roadway applications. For each gallon of biodiesel produced, approximately 0.76 lb (0.35 kg) of crude glycerol is also produced, and there is an urgent need to better utilize this by-product with added value (Pachauri and He, 2006; Thompson and He, 2006). Crude glycerol is also very cost-effective as it is available at \$0.02 per gallon, but it may need to be purified before used for snow and ice control. The addition of succinate salts and glycerol to salt brine will enhance anti-icing performance at cold temperatures to the level comparable to $MgCl_2$ or KAc at reasonable costs, while producing substantial savings through reduced application rates, reduced corrosion to metals, and reduced impact on concrete or asphalt materials. These chemical blends can be very cost-effective for certain road weather scenarios. For instance, a “Supermix” (85% salt brine, 10% De-ice, and 5% $CaCl_2$) was found to exhibit positive field performance when used for anti-icing

above 15°F at 40 gallons per lane-mile or for pre-wetting above 2°F at 10 gallons per ton (DeVries and Hodne, 2006). Some Ohio counties have found that blending salt brine with 10–15% agro-based product or less than 10% CaCl₂ “can provide a significant increase in the residual of salt on higher volume roads when anti-icing and lower the effective working temperature of brine when pre-wetting at the spinner” (Ohio DOT, 2011). Taylor *et al.* (2010) evaluated the brines made of glycerol, NaCl, MgCl₂, and commercial deicers individually and in combination and concluded that the blend of 80% glycerol with 20% NaCl showed the greatest promise in good laboratory performance and low negative impacts (Taylor *et al.*, 2010). Nonetheless, this finding should be considered with caution, because this blend has very high viscosity and its dilution allows anti-icing application but reduces effectiveness. Furthermore, the use of glycerol may pose potential risk to water quality.

Developing deicer compositions using sustainable resources such as by-products of agricultural processes offers many advantages. This approach is beneficial to the environment by reducing wastes, decreasing impact, and creating environmentally safe deicers. Janke and Johnson Jr (1997) developed an environmentally friendly deicer or anti-icing agent from a by-product of a wet milling process of corn called steepwater. The deicer formulation is noncorrosive, inexpensive, water soluble, and readily available in large quantities. Tests have shown that successful inhibition is achieved with the addition of these steepwater solubles to chloride salts (Janke and Johnson Jr, 1997). Similarly, Kharshan *et al.* (2012) demonstrated the successful increased corrosion protection of carbon steel using corn extracts (Kharshan *et al.*, 2012). It is suggested that an amount of 20 to 60 gallons per lane mile of the steepwater deicer be applied to effectively clear snow and ice from roadways. When applied to roadways, the steepwater deicer is not easily removed by passing vehicles or wind and remains in contact with the road, which provides continued deicing performance with decreased application rates. Ice melting tests were conducted on 3.5-inch-thick snow comparing steepwater concentrated at 50% by weight of dry substance to an industrial salt/sand mixture. The steepwater demonstrated higher melting performance than the salt/sand mixture with respect to both duration and strength. In addition, the steepwater deicer also showed active ice melting at temperatures as low as 7.5°F, whereas the salt/sand mixture ice melting stopped around 20°F (Janke and Johnson Jr, 1997). Montgomery *et al.* proposed a deicer formulation, derived from corn steepwater, in which glucose and corn steepwater is combined with sodium hydroxide to form a biodegradable deicer solution with a freezing point around -15°F (-26°C) (Montgomery and Yang, 2003). Furthermore, corrosion testing resulted in little effect on mild steel. Mild steel bolts were immersed in and sprayed with various concentrations of steepwater and showed no oxidation after four months (Janke and Johnson Jr, 1997). Janke and Johnson Jr. (1998) proposed a noncorrosive, environmentally safe deicer composition made from vintners condensed solubles acquired from the processing of wine. This wine by-product deicer has a freezing point of -20°F and is primarily carbohydrate-based (Janke and Johnson Jr, 1998).

Manitoba's search for alternative environmentally friendly deicing agents led to an alcohol by-product produced by a nearby Crown Royal plant that was found to be effective. Other deicing agents containing sugar beet by-products are also being explored (CTC & Associates, 2011). A two-year study for the Colorado DOT found NaCl (liquid brine or solid), abrasives (non-volcanic), and Ice B'Gone have the lowest cost per lane mile, whereas, pre-wet abrasives, CMA, potassium acetate, and potassium formate were considered to be more costly per lane mile. Moreover, a CDOT staff survey respondent mentioned that Clearlane had been very useful because it worked in very cold temperatures (Shi *et al.*, 2009b). Cuelho *et al.* (2010) established best practices for removing snow and ice from roadways through laboratory and field experiments (Cuelho *et al.*, 2010). The work found that anti-icing materials improved the ability of a plow to remove snow from the pavement surface, even at temperatures lower than 14 °F. CaCl₂ performed best on asphalt surfaces at all temperatures, while KAc performed best on concrete at all temperatures (0 °F, 10 °F, 15 °F and 30 °F) (Cuelho *et al.*, 2010).

2.3 Anti-icer Impacts on Highway Infrastructure

Anti-icing operations performed with chemicals provide various benefits for snow and ice control operations. However, another concern of these chemicals is corrosion to the highway infrastructure. It is difficult, however, to determine the extent of damage caused by such materials, or to compare the corrosiveness of different products in the field where many variables come into play. New products are continually tested and introduced so that agencies can provide safer alternatives for snow and ice control. For example, many transportation agencies have moved toward the use of more advanced chemical products in response to public and environmental concerns about abrasives and salt. Compared with traditional methods of using abrasives and road salt, extensive research has shown these chemical products:

- Do not damage car windshields and paint like abrasives;
- Are less corrosive to infrastructure than salt, especially when blended with corrosion inhibitors.

Snow and ice control operations may cause damage to the highway infrastructure, including: concrete deterioration due to corrosion of the reinforced steel, surface deterioration known as scaling, and degradation of the concrete matrix. Large span supported structures, steel bridges, parking garages and even paved surfaces are susceptible to corrosion derived from winter maintenance chemicals. This section will summarize the corrosion impact of anti-icing chemicals on steel and other bare metals, concrete pavement, and asphalt pavement, and bridge decks.

2.3.1 Impact of Anti-Icing Chemicals on Steel/bare Metals

Chloride-based chemicals for winter maintenance may result in deterioration of reinforced concrete structures, the major cause of which is the corrosion of steel following the diffusion of chloride ions into concrete (Transportation Association of Canada, 2003). Chloride ingress, either from marine environments or from chloride-based anti-icers, is one of the primary forms of environmental attack for reinforced concrete structures (Samples and Ramirez, 1999; Poonguzhali et al., 2008), which leads to rebar corrosion and a subsequent reduction in the strength, serviceability, and aesthetics of the structure. The chloride permeability of concrete is thus considered a critical intrinsic property of the concrete (Wee et al., 2000). Premature deterioration of bridge decks, as well as the contamination of parking garages due to the application of deicing salts has been reported (Salt and Deicing, 1991). The remediation of concrete bridges in the U.S., undertaken as a direct result of chloride-induced corrosion of the reinforcing steel, would cost U.S. highway departments \$5 billion per year (Federal Highway Administration, 1999). In the snowbelt region, the synergy of freeze-thaw cycles and corrosion of reinforcing steel can lead to serious problems for reinforced concrete structures. When comparing $MgCl_2$ with NaCl, research has determined that the chloride diffusion coefficients for $MgCl_2$ are two to three times greater than NaCl (Hondo *et al.*, 1974; Deja and Loj, 1999; Mussato *et al.*, 2004), which may reduce the time to initiate corrosion by 10 to 15 years for concrete embedded with reinforcing steel (Mends and Carter, 2002).

Compared to chlorides, acetate and formate based anti-icers are less corrosive to highway infrastructure. Acetate-based deicers such as KAc, NaAc, and CMA have been used on some winter roadways as non-corrosive alternatives to chlorides. In addition, acetate and formate-based anti-icers are widely used on airport pavements, despite their possible role in accelerating corrosion via increased electrolyte conductivity (Levelton Consultants Limited, 2007). It was found that changing from NaCl to an acetate based deicer decreased the corrosion rate of steel rebar in a simulated concrete pore solution by more than a factor of ten (Man *et al.*, 1990). However, potassium formate was reported to cause serious corrosion to landing gear and associated wiring of some Boeing airplane models and the corrosion risk of acetate and formate-based deicers to cadmium-plated steel has raised concerns by aircraft manufacturers and airlines (Shi, 2008). Another study conducted revealed that while NaAc- or KAc-based deicers were non-corrosive to mild steel, they were comparably as corrosive as chloride-based deicers to galvanized steel (Salt Institute, 2008).

CMA is generally considered to be less corrosive to metals than NaCl (TRB, 1991a), even though this consensus is mostly based on existing laboratory studies involving the direct exposure of rebar or steel coupons to CMA solutions, which may not represent the case where the rebar is embedded in concrete (Levelton Consultants Limited, 2007). Electrochemical and weight loss tests of 14-17 month duration indicated that bridge structural metals, including steel, cast iron,

aluminum, and galvanized steel corroded considerably less in CMA solutions than in NaCl solutions (Kennelley, 1986). Full and half immersion, vapor space, sprays, and dip testing of ASTM A-36, A-325, and A-588 steel, gray cast iron, and aluminum indicated that CMA solutions were less corrosive to all the metals tested than NaCl solutions (Locke *et al.*, 1987). However, similar to NaCl, CMA caused a substantial shift of the potential of steel in mortar, simulated pore solutions, and concrete slabs, indicating the increased risk for steel corrosion (Locke *et al.*, 1987). This may be attributed to the fact that CMA reduced the pH of simulated pore solutions, by precipitating OH⁻ ions as Ca(OH)₂ and Mg(OH)₂ (Locke *et al.*, 1987). It is noteworthy that in another study, the steel embedded in concrete ponded with CMA solutions did not show any significant potential shifts or corrosion, whereas the steel embedded in concrete ponded with NaCl solution did (Chollar and Virmani, 1988). In CMA solutions of 2 wt.% and higher, reverse polarization scans indicated that an unusual electrochemical behavior occurred. It is suggested that carbon dioxide is formed as a consequence of an electrochemical reaction involving the acetate ion. The carbon dioxide then dissolved in the solution, leading to the precipitation of insoluble carbonates at cathodic sites on the steel surface (Kennelley and Locke Jr, 1990).

Currently there are conflicting data as to whether CMA can be used as an effective corrosion inhibitor for chloride-induced corrosion of reinforcing steel. The ASTM G 109 ponding test results suggested that CMA as an additive to NaCl (in a ratio of 1 to 2) did not inhibit the rebar corrosion in concrete (Callahan, 1990). One study confirmed that sodium acetate, urea and CMA were only marginally effective as corrosion inhibitors for rebar in concrete, by examining the electrochemical behavior of iron in cured cement pastes (Ushirode *et al.*, 1992). In contrast, another study indicated that adding CMA to a steel-concrete system undergoing active chloride-induced corrosion slowed corrosion after 30 days and stopped corrosion after 60 days (Fritzsche, 1992). Compared with salt solution made with pure NaCl, a solution made with a 20:80 blend of NaCl:CMA mixture (wt. %/wt. %) was 45 percent less corrosive to steel (Ihs and Gustafson, 1997). The impedance and voltammetric measurements confirmed that adding CMA to a simulated pore solution diminished the corrosion rate and increased the protectiveness of surface films (Flis *et al.*, 1998).

2.3.2 Impact of Anti-icing Chemicals on Concrete Pavement

A Transportation Pooled Fund study investigated the effects of concentrated brines of NaCl, CaCl₂, MgCl₂ and CMA on Portland cement concrete (PCC) and concluded that both physical and chemical interactions occur within concrete when it is exposed to freeze/thaw conditions and chemicals (Sutter and Dakota, 2008). Based on the ASTM C666 freeze/thaw test results, concrete prisms of 10cm diameter by 5 cm height subjected to 300 freeze/thaw cycles in 14% MgCl₂ and 15% CaCl₂ reported considerable expansion (0.17% and 0.18% length change, respectively), mass change (3.5% and -3.5%, respectively) and loss in the dynamic modulus of

elasticity (50% and 40%, respectively). In contrast, those exposed to 18% NaCl did not expand more than 0.04% and reported 0.5% mass gain and approximately 5% loss in the dynamic modulus of elasticity. Significant evidence existed that MgCl₂ and CaCl₂ chemically reacted with hardened cement paste, as indicated by the dissolution of the cement paste and formation of expansive oxychloride phases. These mechanisms were assumed responsible for the observed expansive cracking, increased permeability, and significant loss in compressive strength of the concrete (Sutter and Dakota, 2008). Exposure to NaCl, however, did not result in noticeable chemical interaction or related distress in concrete mortar or concrete (Sutter and Dakota, 2008).

Another study investigated the effects of diluted deicers on PCC, assuming a 100-to-3 dilution ratio for all liquid and solid deicers (Shi *et al.*, 2010). De-ionized water, CMA solid deicer, and MgCl₂ liquid deicer were found to be benign to PCC durability, based on the gravimetric and macroscopic observations of freeze-thaw specimens following the SHRP H205.8 laboratory test. In contrast, KFm and the NaAc/NaFm blend of deicers showed a moderate amount of weight loss and noticeable deterioration of the concrete. NaCl, the NaCl based anti-icer, and the KAc-based anti-icers were the most deleterious to the concrete. In addition to exacerbating physical distresses, each investigated chemical or diluted deicer chemically reacted with some of the cement hydrates and formed new products in the pores and cracks. Such physiochemical changes of the cement paste induced by the deicers pose various levels of risks for the concrete durability (Shi *et al.*, 2010).

Yet another laboratory study investigated the effects of both diluted and concentrated deicers on PCC. Concrete specimens were exposed to weekly cycles of wetting and drying in distilled water and in solutions of NaCl, CaCl₂, MgCl₂, and CMA with either a 6.04 molar ion concentration (equivalent to a 15% solution of NaCl), or a 1.06 molar ion concentration (equivalent to a 3% solution of NaCl), for periods of up to 95 weeks. At lower concentrations, NaCl and CaCl₂ showed a relatively small negative impact on the properties of concrete, whereas MgCl₂ and CMA caused measurable damage to concrete. At high concentrations, NaCl showed a greater but still relatively small negative effect, whereas CaCl₂, MgCl₂ and CMA caused significant loss of material and a reduction in stiffness and strength of the concrete (Darwin *et al.*, 2008).

In addition to chlorides, the detrimental effects of CMA on PCC have also been confirmed. In a recent laboratory study, cement mortar samples (water to cement ratio (w/c)=0.485) were reported to lose cohesiveness and disintegrate completely after 30-day exposure to 28% CMA solution at room temperature, and the formation of calcium acetate hydrate phases were confirmed by X-ray diffraction results (Sutter and Dakota, 2008). In another laboratory study (Santagata and Collepardi, 2000), eight-month continuous exposure of good-quality concrete (w/c=0.45 and air entrained) to concentrated CMA solutions (25%) caused a significant decrease in load capacity, mass loss and severe visual degradation of the concrete. The use of 40% blast furnace slag along with a Portland clinker was found to be effective in mitigating such impacts of CMA (Santagata

and Collepari, 2000). The deleterious effects of CMA were also reported in earlier studies (Santagata and Collepari; Peterson, 1995), involving a delamination process of the cement matrix likely associated with leaching of the calcium hydroxide.

Physical mechanisms of attack by deicers can lead to damage of PCC in the common forms of scaling, map cracking, or paste disintegration (Sutter and Dakota, 2008). Scaling refers to the local peeling of the hardened concrete surface, often as a result of cyclic freezing and thawing (ACI Committee, 2004). Scaling can occur on concrete surfaces independent of chemical application, as the aqueous solution in the concrete pores near the surface freezes and thaws due to temperature fluctuations. Freezing of water in saturated concrete exerts tremendous expansive forces that consequently lead to scaling off of concrete surfaces, especially when the concrete surface is not adequately protected with entrained air.

Many research studies have shown that chloride-based anti-icing salts can exacerbate the scaling problem as concrete experiences freeze/thaw cycles. Moisture tends to move toward zones with higher salt concentrations via osmosis. Accordingly, the osmotic pressure adds to the normal hydraulic pressure if salts are present in the pore solution, which increases the risk for physical deterioration of concrete. In addition, the application of salts to pavements increases the rate of cooling, which increases the number of freeze/thaw cycles and thus the risk for freeze/thaw deterioration. However, the presence of deicers can be beneficial as it widens the temperature range in which phase transitions occur. These opposing effects define the physical distress in concrete caused by deicers, and a pioneering laboratory study revealed the worst conditions at a low deicer concentration (5% NaCl) and optimum conditions at a moderately high concentration (13% NaCl) (Litvan, 1975). Another study suggested that concrete containing relatively high concentrations of dissolved salts can provide better resistance to scaling than concrete with plain water in its pores (Korhonen, 2002).

The scaling of concrete in the presence of deicers, referred to as “salt scaling,” has been recognized as the main cause of frost-related concrete deterioration, and has been found closely related to concrete quality (e.g., air entrainment level), weather conditions, and the number of freeze/thaw cycles (Marchand *et al.*; Transportation Association of Canada, 2003; Mussato *et al.*, 2004; Pigeon and Pleau, 2010). Concrete damage from salt scaling was found to be significantly dependent on the salt type (sodium, potassium, magnesium or calcium chloride), and salts containing potassium seemed to cause more scaling damage for unknown reasons (McDonald and Perenchio, 1997). A study conducted by Šelih (2010) found that CaCl_2 solution has the most destructive effect and MgCl_2 has the least deterioration based on the scaling tests. A literature review conducted by Sumsion and Guthrie (2013) found that regardless of testing method and specimen characteristics, specimens exposed to NaCl experienced minor deterioration and specimens exposed to CaCl_2 , MgCl_2 , or CMA experienced significant deterioration which includes scaling, cracking, mass loss, and compressive strength loss. Another study conducted in our

laboratory found that the effect of anti-icers on concrete pavements had been mild until the introduction of acetate and formate based chemicals (Shi *et al.*, 2009a).

KAc was reported to cause minor scaling associated with alkali carbonation of the surface layer of concrete (Wang *et al.*, 2006). Recently, however, the treatment of PCC with sodium acetate solutions was claimed to be a promising technology to grow crystals inside the pores to reduce water penetration into concrete and thus extend the service life of concrete (Al-Otoom *et al.*, 2007). Such beneficial effect was demonstrated in the treatment of a poor-quality concrete ($w/c=0.65$ and non-air-entrained).

Early research argued that the best protection against "salt scaling" would be reduction of porosity (Litvan, 1975). It is now generally believed that the use of properly cured, air entrained PCC would prevent physical damage by the freeze/thaw cycles. For instance, high-quality concrete with 5-7% entrained air has been found more resistant to freeze/thaw cycles and scaling (Williams, 2003). Entrained air provides spaces within the concrete mass for expanding water to move into, thereby reducing the potential stress and associated deterioration. For an air-entrained concrete, the spacing factor seems to be a key air void characteristic to allow sufficient resistance to salt scaling (Frost-Tausalz-Widerstand *et al.*, 2006). It should be noted that air entrainment only slows the freeze-thaw process instead of preventing it (Korhonen, 2002).

The use of supplementary cementitious materials, particularly fly ash, has been widely reported to have detrimental effects on the scaling resistance of properly air-entrained concrete, as it tends to refine porosity and increase the non-evaporable water content (Marchand *et al.*, 1997). One study suggested that the key was to allow sufficient time for high-volume fly ash concrete to develop strength before subjecting it to salt scaling (Naik *et al.*, 2005). In contrast, the use of some cementitious material may improve the resistance of mortars and concretes to the combined action of frost and deicer, as in the case of a magnesium phosphate cement-based binder prepared by mixing magnesium oxide (MgO) with mono-ammonium phosphate, borax, and fly ash (Yang *et al.*, 2002).

2.3.3 Impact of Anti-icing Chemicals on Asphalt Pavement

It is generally believed that asphalt pavement is less affected by deicers. This is attributable to the relatively high chemical resistance that asphalt binder demonstrates in the presence of chloride-based deicers. Thus far, there are no specific guidelines established in the United States for application of deicers on asphalt pavements and little fundamental research carried out in investigating the asphalt/bitumen deicer reaction.

Thermal cracking, differential heaving, and loss of bearing capacity during spring thaw are often identified as the main mechanisms of pavement deterioration in cold climates. Frost action within the pavement granular layers can be aggravated by an ice enrichment process and

differential freezing conditions associated with the contamination of the base material by deicing salt (Li *et al.*, 2011).

A comprehensive laboratory study evaluated the relative destructive effects of various deicers on asphalt pavement, considering the effect of freeze/thaw cycles (Hassan *et al.*, 2001; Hassan *et al.*, 2002). This study involved actual aggregates and asphalt specimens cored from the field, as well as four types of deicers used on both highway and airport pavements, namely, urea, NaCl, NaFm, and KAc. Various degrees of material disintegration as a combined result of frost action and deicers were observed, revealing that the effect from freeze/thaw cycling was significant whereas the effects of different deicers on both the aggregates and the asphalt concrete mixes varied. The extent of damage due to freeze/thaw cycling in distilled water was less than that caused by any deicer used. A critical range of deicer concentration was found to exist between 1% and 2% by weight of solid deicer to deicer solution, in which the maximum damaging effect of deicers to the aggregate was observed. The limestone aggregates showed a higher resistance to disintegration than the quartzite aggregates when subjected to freeze/thaw cycles in the presence of the deicers. The urea was found to have the highest damaging effect among all the deicers on both the aggregates and asphalt concrete samples, while the least damaging deicer for limestone was NaCl and for quartzite was KAc.

Additionally, the indirect tensile strengths (ITS) of the samples exposed to deicers were mostly higher than those exposed to distilled water, while all of them were found to be significantly lower than those of the intact samples. However, there was no significant deterioration identified for the mechanical properties of the samples exposed to KAc, NaFm, or NaCl, relative to distilled water. Conditioning asphalt samples using freeze-thaw cycles in the presence of a deicer solution also caused a decrease in the modulus of elasticity. The lowest average elastic modulus was associated with the samples in urea, and visual inspection indicated significant damage by urea (Hassan *et al.*, 2002). Based on weight measurements and density calculations, asphalt mix samples immersed in NaFm experienced the most disintegration after 25 cycles, whereas urea (followed by KAc) was the most detrimental deicer after 50 cycles (McCutchon *et al.*, 1998). Exposure to freeze/thaw cycles and deicers was found to affect the viscosity of the recovered asphalt binder and the gradation of recovered aggregates. The freeze/thaw cycles seemed to result in soft asphalt binder, while the deicers caused asphalt hardening. However, the authors noted that these findings were inconclusive due to the difficulties involved in testing and the inaccuracies in measuring viscosity of the recovered asphalt. Overall, this laboratory investigation found urea to be the most detrimental deicer, while the other deicers “induced relatively small damage, comparable to that caused by distilled water” (Hassan *et al.*, 2001). It should be noted that chemical reactions might have been slowed by the low temperatures involved in this study and that damage in the field could occur as a result of reactions between deicer residues and asphalt during hot summer temperatures (Hassan *et al.*, 2001).

A follow-up study was conducted at higher temperatures on asphalt pavement samples taken from the Dorval International Airport (Montreal, Canada) to clarify the role played by the deicers in asphalt deterioration, and to determine whether the damage was attributable to the physical freeze/thaw action. Only 15 freeze/thaw cycles were performed before subjecting some samples to 40 wet/dry cycles at 104°F (40°C). This research confirmed the previous finding that softening occurs during freeze/thaw and exposure to deicers causes hardening. After the freeze/thaw and wet/dry cycles, the asphalt samples in NaAc showed the greatest loss of strength and elasticity, followed by those in NaFm. Interestingly, all samples showed increased strength after the warm wet/dry cycles and all except NaFm and NaAc showed increased elasticity after the warm wet/dry cycles. However, the dry samples not exposed to freeze/thaw or wet/dry cycles had the greatest elasticity and nearly the highest strength. Overall, the Canadian studies did not indicate significant damaging effects of KAc and NaFm on asphalt pavement (Farha *et al.*, 2002; Hassan *et al.*, 2002). It should be cautioned, however, that these results were based on laboratory experiments with only two samples of asphalt pavement and the mix design for each pavement was undeterminable from the reports. In a recent study, hot-mixed asphalt samples were conditioned in NaCl, CaCl₂ and MgCl₂ and exposed to seven freeze-thaw cycles. The study found that weaker solutions of NaCl and stronger solutions of MgCl₂ and CaCl₂ are associated with higher tensile strengths of asphalt mixture (Goh *et al.*, 2011).

2.4 Cost Impacts of Anti-icing Chemicals

Kelting and Laxon recently recommended the use of anti-icing because it can decrease costs by greater than 50% compared to conventional de-icing (Kelting and Laxson, 2010).

Infrastructure damage resulting from winter highway maintenance activities is substantial. Repairing the damage caused by snow and ice control operations costs state and local agencies over \$5 billion each year. As of 2014, there were 610,749 bridges in the U.S., approximately 24 percent of which were structurally deficient (Federal Highway Administration, 2015). The estimated cost of installing corrosion protection measures in new bridges and repairing old bridges in the snowbelt states is between \$250 million and \$650 million annually (Salt and Deicing, 1991). A study estimated that 3500 to 7000 bridge decks will be damaged due to salts, and the total cost to repair 1/10 of the bridges would be between \$50 million to \$200 million per year (TRB, 1991b). Parking garages, pavements, roadside infrastructures, and non-highway objects near winter maintenance activities are also exposed to the corrosive effects of road salts. Finally, it should be noted that any repairs to the infrastructure translate to costs to the user in terms of construction costs, traffic delays and lost productivity. Indirect costs are estimated to be greater than ten times the cost of corrosion maintenance, repair and rehabilitation (Yunovich and Thompson, 2003). It is important to note that this is a generalized estimation for the nation, and the corrosion costs for Pacific Northwest Snowfighter (PNS) states and provinces could be much less, as stricter specifications are applied to winter maintenance chemicals used in these regions.

2.5 References

- "Current Deicing Practices and Alternative Deicing Materials" (2014). http://www.michigan.gov/documents/ch2-deice_51438_7.pdf, (Retrieved on February 18, 2014).
- AASHTO, A. A. o. S. H. a. T. O. (2009). "Environmental Stewardship Practices, Procedures, and Policies for Highway Construction and Maintenance." NCHRP 25-25 (04) <http://environment.transportation.org>.
- ACI Committee, A. C. I. (2004). Guide for Concrete Floor and Slab Construction, American Concrete Institute.
- Adams, E. E., R. G. Alger, J. P. Chekan, F. D. Williams and R. Valverde (1992). "Persistence of Reduced Snow to Pavement Shear-Strength for 2 Aggregate Materials Treated with CMA and NaCl." Chemical Deicers and the Environment: 481-493.
- Al-Otoom, A., A. Al-Khlaifa and A. Shawaqfeh (2007). "Crystallization technology for reducing water permeability into concrete." Industrial & engineering chemistry research 46(16): 5463-5467.
- Alger, R. G. (2005). Anti-icing coatings and methods, Google Patents.
- Alkoka, M. and K. Kandil (2002). Effectiveness of using organic by-products in decreasing the freezing point of chemical solutions. New Challenges for Winter Road Service. XIth International Winter Road Congress.
- Anonymous (2003). "Effective Temperature of Deicing Chemicals" Snow & Ice Fact #20, FY03." <http://www.saltinstitute.org/Education-Center/Snowfighterstraining/Snowfighting-training/WINOPS> (Retrieved on November 27, 2007).
- ASTM (2003). "Specification for Concrete Aggregates." ASTM Standard C33, ASTM International, West Conshohocken, PA, 2003, DOI: 10.1520/C0033-03, www.astm.org.
- Athmann, T., R. Bjornsson, P. Borrell and P. Thewlis (2014). "Geothermal Heating of Airport Runways" Saint Cloud State University, <http://emerald.ts.odu.edu/Apps/FAAUDCA.nsf/AcevesDADEFullProposal.pdf?OpenFileResource> (Retrieved on February 18, 2014).
- Axon, E. and R. Couch (1963). "Effect of insulating the underside of a bridge deck." Highway Research Record(14).
- Baroga, E. (2005). "2002-2004 Salt Pilot Project." A final report prepared for the Washington State Department of Transportation. Olympia, WA.
- Barrett, M. L. and J. G. Pigman (2001). "Evaluation of automated bridge deck anti-icing system."
- Bell, G. T., W. A. Nixon and R. D. Stowe (2006). A synthesis to improve the design and construction of Colorado's bridge anti-icing systems.
- Blackburn, R. R., K. M. Bauer, A. McElroy and J. E. Pelkey (1991). "Chemical undercutting of ice on highway pavement materials." Transportation Research Record(1304).
- Brandt, G. H. (1973). "Environmental Degradation by De-icing Chemicals and Effective Countermeasures: Potential impact of Sodium Chloride and Calcium Chloride De-icing Mixtures on Roadside Soils and Plants." Highway Research Record, Highway Research Board, National Academy of Engineering, Washington, D.C., no. 425, p. 52-65.
- Burnett, W. C. (1985). "Letter from William C. Burnett, Director, Engineering Research and Development Bureau, State of New York Department of Transportation, Albany, NY to Robert J. Nittinger, Jr., L & R Distributors, Stanhope, NJ. February 27, 1985."

- Callahan, M. R. (1990). TRR 1211(1) (1990), 12-17.
- Center for Watershed Protection (2003). "The Stormwater Manager's Resource Center, Stormwater Management Fact Sheets." <http://www.stormwatercenter.net/> Retrieved on June 20, 2008.
- CERF (2005). "Evaluation of the FreezeFree Anti-Icing System." Final Report by the Civil Engineering Research Foundation, Prepared for the U.S. Federal Highway Administration.
- Chang, C., M. Ho, G. B. Song, Y. L. Mo and H. Li (2009). "A feasibility study of self-heating concrete utilizing carbon nanofiber heating elements." *Smart Materials & Structures* 18(12).
- Chollar, B. H. and Y. P. Virmani (1988). "Effects of calcium magnesium acetate on reinforced steel concrete." *Public Roads* 51(4).
- Christillin, M., C. Ardemagni and G. Trombella (1998). THE BUTHIER VIADUCT-A DIFFERENT APPROACH TO ROAD NETWORK MAINTENANCE IN WINTER. Xth PIARC International Winter Road Congress.
- Coleman, M. (2014). "The Economics of Anti-icers." *Grounds Maintenance Putting a price on productivity*, Penton Media Inc(Retrieved on April 3, 2014).
- CTC & Associates (2011). "Snow and Ice Control at Extreme Temperatures." A synthesis report prepared for the Wisconsin Department of Transportation Bureau of Highway Operations. Madison, WI. April 2011.
- Cuelho, E., J. Harwood, M. Akin and E. Adams (2010). "Establishing best practices for removing snow and ice from California roadways." Presentation to the Winter Maintenance Committee at the 89th.
- Darwin, D., J. Browning, L. Gong and S. R. Hughes (2008). "Effects of deicers on concrete deterioration." *Aci Materials Journal* 105(6).
- Deja, J. and G. Loj (1999). Effect of cations occurring in the chloride solutions on the corrosion resistance of slag cementitious materials. Infrastructure regeneration and rehabilitation improving the quality of life through better construction. International conference.
- Derwin, D., P. Booth, P. Zaleski, W. Marsey and W. Flood Jr (2003). "SNOWFREE® heated pavement system to eliminate icy runways." *Management* 2012: 03-16.
- DeVries, R. M. and B. Hodne (2006). "Chloride Cocktail: Department in Illinois Finds Good Results Mixing Their Own Deicer/Anti-Icer." *Roads & Bridges* 44(8).
- Farha, M., Y. Hassan, A. A. El Halim, A. Razaqpur, A. El-Desouky and A. Mostafa (2002). Effects of new deicing alternatives on airfield asphalt concrete pavements. Federal Aviation Administration Technology Transfer Conference.
- Fay, L. and X. Shi (2010). "Laboratory investigation of performance and impacts of snow and ice control chemicals for winter road service." *Journal of Cold Regions Engineering* 25(3): 89-114.
- Fay, L., K. Volkening, C. Gallaway and X. Shi (2008). Performance and impacts of current deicing and anti-icing products: User perspective versus experimental data. Proc., 87th Annual Meeting of Transportation Research Board, Transportation Research Board Washington, DC.
- Federal Highway Administration (1999). "FOCUS Federal Highway Administration." Washington DC, Sept.: 6.

- Federal Highway Administration (2005). "How do Weather Events Impact Roads." http://ops.fhwa.dot.gov/Weather/ql_roadimpact.htm.
- Fischel, M. (2001). "Evaluation of selected deicers based on a review of the literature."
- Flis, J., H. Pickering and K. Osseo-Asare (1998). "Interpretation of impedance data for reinforcing steel in alkaline solution containing chlorides and acetates." *Electrochimica acta* 43(12): 1921-1929.
- Friar, S. and R. Decker (1999). "Evaluation of a fixed anti-icing spray system." *Transportation Research Record: Journal of the Transportation Research Board* 1672(1): 34-41.
- Fritzsche, C. J. (1992). "Calcium magnesium acetate deicer." *Water environment & technology* 4(1): 44-51.
- Frost-Tausalz-Widerstand, V. F., M. U. LUFTPORENKENNWERTEN, R. SELS, D. DE DEVERGLAÇAGE, V. R. E. B. A. PARAMETRES and M. A. DES PORES GROSSIERS (2006). "Frost/deicing salt resistance of concrete pavements with unsuitable air void characteristics." *Otto-Graf-Journal* 17: 45.
- Fu, L., R. Omer and C. Jiang (2012). "Field test of organic deicers as pre-wetting and anti-icing agents for winter road maintenance." *TRB 91st Annual Meeting Compendium of Papers DVD*. Paper No. 12-2283. 2012.
- Giuliani, F., F. Merusi, G. Polacco, S. Filippi and M. Paci (2012). "Effectiveness of sodium chloride-based anti-icing filler in asphalt mixtures." *Construction and Building Materials* 30: 174-179.
- Goh, S. W., M. Akin, Z. You and X. Shi (2011). "Effect of deicing solutions on the tensile strength of micro-or nano-modified asphalt mixture." *Construction and Building Materials* 25(1): 195-200.
- Goodwin, L. C. and P. Pisano (2003). "Best practices for road weather management." *Road Weather*.
- Hassan, Y., A. Abd El Halim, A. Razaqpur, W. Bekheet and M. Farha (2002). "Effects of runway deicers on pavement materials and mixes: comparison with road salt." *Journal of transportation engineering* 128(4): 385-391.
- Hassan, Y., A. A. El Halim, A. Razaqpur and M. Farha (2001). Laboratory investigation of effect of deicing chemicals on airfield asphalt concrete pavements materials. *Proceedings 2nd International Conference on Engineering Materials*.
- Hellström, G. (2007). "UTES for snow melting for airport runways in Sweden. ." Presentation at European Geothermal Energy Council conference in Malmö, Sweden. http://www.egec.org/news/egec_restmac_workshop.htm ,(Retrieved on November 27, 2007).
- Heymsfield, E., A. Osweiler, P. Selvam and M. Kuss (2014). "Developing Anti-Icing Airfield Runways Using Conductive Concrete with Renewable Energy." *Journal of Cold Regions Engineering*.
- Hiroshi, T., T. Nobuhiro and K. Nobuo (1998). Development of highway snow melting technology using natural energy. *Xth PIARC International Winter Road Congress*.
- Hondo, R., M. Satake and H. Ushiyama (1974). "Diffusion of Various Ions into Hardened Portland Cement. 28 th General Assembly of the Cement Association of Japan." Tokyo, Japan.
- Hoppe, E. J. (2000). Evaluation of Virginia's First Heated Bridge.

- Hopstock, D. M. and L. M. Zanko (2005). "Minnesota taconite as a microwave-absorbing road aggregate material for deicing and pothole patching applications."
- Ihs, A. and K. Gustafson (1997). Test and evaluation of calcium magnesium acetate-sodium chloride mixtures in sweden. Transportation Research Board Conference Proceedings.
- Janke, G. A. and W. D. Johnson Jr (1997). Deicing composition and method, Google Patents.
- Janke, G. A. and W. D. Johnson Jr (1998). Deicing composition and method, Google Patents.
- Joerger, M. D., F. C. Martinez and ODOT Research Unit (2006). "Electric Heating Of I-84IN LADD Canyon, Oregon." Final Report, SPR 304-461, Oregon Department of Transportation
http://www.oregon.gov/ODOT/td/tp_res/docs/reports/laddcanyonheatingproject.pdf
- Johnson, G. (2006). "Smart Roads Can De-ice itself: Pavement overlay Releases Chemical in Bad Weather." The Calgary Herald.
- Kahl, S. (2004). "Agricultural By-Products for Anti-Icing and De-Icing Use in Michigan." In: Transportation Research Board (ed.), Proc. 6th Intl. Symposium on Snow Removal and Ice Control Technology. Transportation Research Circular E-C063: Snow and Ice Control Technology SNOW04-009, pp. 552-555.
- Kelting, D. L. and C. L. Laxson (2010). "Review of Effects and Costs of Road De-icing with Recommendations for Winter Road Management in the Adirondack Park." Adirondack Watershed Institute, Paul Smith's College, Paul Smiths, NY, Adirondack Watershed Institute Report# AWI2010-01.
- Kennelley, K. and C. Locke Jr (1990). "Electrochemical Behavior of Steel in Calcium Magnesium Acetate." Corrosion 46(11): 888-895.
- Kennelley, K. J. (1986). "Corrosion electrochemistry of bridge structural metals in calcium magnesium acetate."
- Keranen, P. (1998). Automated bridge deicers for increased safety and decreased salt use in Minnesota. Xth PIARC International Winter Road Congress.
- Ketcham, S. A., L. D. Minsk, R. Blackburn and E. Fleege (1996). "Manual of practice for an effective anti-icing program." Virginia: FHWA.
- Kharshan, M., K. Gillette, A. Furman, R. Kean and L. Austin (2012). "Novel Corrosion Inhibitors Derived From Agricultural By-Products: Potential Applications In Water Treatment." CORROSION 2012.
- Khattak, A. J., G. Pesti and V. Kannan (2003). Guidelines for prioritizing bridge deck anti-icing system installations. Phase I and Phase II Report.
- Kiljan, J. (1989). Verglimit Evaluation (Boulder). Final Report.
- Klein-Paste, A. and J. Wählín (2013). "Wet pavement anti-icing—A physical mechanism." Cold Regions Science and Technology 96: 1-7.
- Korhonen, C. (2002). Effect of high doses of chemical admixtures on the freeze-thaw durability of portland cement concrete, DTIC Document.
- Levelton Consultants Limited (2007). Guidelines for the selection of snow and ice control materials to mitigate environmental impacts, Transportation Research Board.
- Li, W., M. Pour-Ghaz, J. Castro and J. Weiss (2011). "Water absorption and critical degree of saturation relating to freeze-thaw damage in concrete pavement joints." Journal of Materials in Civil Engineering 24(3): 299-307.

- Litvan, G. G. (1975). "Phase Transitions of Adsorbates: VI, Effect of Deicing Agents on the Freezing of Cement Paste*." *Journal of the American Ceramic Society* 58(1 - 2): 26-30.
- Locke, C. E., K. J. Kennelley, M. D. Boren and V. Luster (1987). "A study of corrosion properties of a new deicer, calcium magnesium acetate." *Transportation Research Record*(1113).
- Lohrey, E. (1992). *Field Evaluation of an Experimental Bituminous Pavement Utilizing an Ice-Retardant Additive-Verglimit. Final Report.*
- Long, H. W. (2001). *Asphaltic compositions and uses therefor, Google Patents.*
- Lu, L., L. Zhang and Y. Guo (2009). "Chemical antifreezing pavement applications: a review. *Highway Engineering and Transportation (in Chinese)*." No. 206.
- Lund, J. (2000). "Pavement Snow Melting." *GHC BULLETIN, JUNE 2000* <http://geoheat.oit.edu/bulletin/bull21-2/art4.pdf>((Retrieved on April 3, 2014)).
- Lund, J. (2014). "Pavement Snow Melting. ." *Geo-Heat Center, Oregon Institute of Technology, Klamath Falls, OR.* <http://goite.org/documents/PavementSnowMelting.PDF>(Retrieved on February 18, 2014).
- Man, M., L. Hazell and R. Smith (1990). "On-Line Measurement of Simulated Reinforcement Corrosion in Concrete Under Action of De-Icers." *Elsevier Applied Science*: 384-394.
- Marchand, J., J. Maltais, Y. Marchabée, C. Tablot and M. Pigeon (1997). "Effects of fly ash on microstructure and deicer salt scaling of concrete." *Frost Resistance of Concrete: Proceedings of the International RILEM Workshop* M. J. Setzer and R. Auberg, Eds. E & FN SPON. Essen, Germany.
- Marchand, J., E. Sellevold and M. Pigeon "The Deicer Salt Scaling Deterioration of Concrete-An Overview."
- Maupin, G. (1986). *Field investigation of verglimit.*
- McCutchon, J., A. Joseph and J. Valkenberg (1998). *Assessment of the effect of urea deicing solution on asphaltic concrete pavements. PROCEEDINGS OF THE ANNUAL CONFERENCE-CANADIAN TECHNICAL ASPHALT ASSOCIATION, POLYSCIENCE PUBLICATIONS INC.*
- McDonald, D. and W. Perenchio (1997). "Effects of salt type on concrete scaling." *Concrete International* 19(7).
- Mends, N. and P. Carter (2002). "Economic Impact of Magnesium Chloride Anti-Icing on Montana Bridges." *Canadian Society for Civil Engineering*..(Cited in NCHRP Report 577): 739-744.
- Mitchell, G. F., W. Richardson and A. Russ (2006). *Evaluation of ODOT Roadway/Weather Sensor Systems for Snow & Ice Removal Operations/RWIS Part IV: Optimization of Pretreatment or Anti-Icing Protocol.*
- Möller, S. (2007). "New Technology and New Methods in Winter Road Maintenance." *VTI Rapport Issue No. 569. Publisher: Swedish National Road and Transport Research Institute.*
- Montgomery, R. and B. Y. Yang (2003). *Biodegradable deicing composition, Google Patents.*
- Morita, K. and M. Tago (2000). *Operational characteristics of the Gaia snow-melting system in Ninohe, Iwate, Japan. Proc. World Geothermal Congress.*
- Murray, D. M. and M. R. Eigerman (1972). "A Search: New Technology for Pavement Snow and Ice Control."

- Mussato, B. T., O. K. Gepreags and G. Farnden (2004). "Relative effects of sodium chloride and magnesium chloride on reinforced concrete: State of the art." *Transportation Research Record: Journal of the Transportation Research Board* 1866(1): 59-66.
- Myhra, T. (2012). "Deicing and Anti-Icing Decisions for Runways and Ramps." Presented at FAA Alaskan Region Airports Conference, Anchorage, AK, May 8–9, 2012, http://www.faa.gov/airports/alaskan/airports_news_events/2012_conference/index.cfm?print=go.
- Naik, T. R., R. N. Kraus, B. W. Ramme and Y.-m. Chun (2005). "Deicing salt-scaling resistance: laboratory and field evaluation of concrete containing up to 70% Class C and Class F fly ash." *Journal of ASTM International* 2(7): 93-104.
- Nixon, W. (2006). "An Analysis of the Performance of the Safelane™ Overlay during winter 2005–06." A report submitted to Cargill May 2006.
- Nixon, W. (2007). "An Analysis of the Performance of the Safelane™ Surface Overlay during Winter 2006–07." A report submitted to Cargill May 2007.
- Nixon, W. A. and A. D. Williams (2001). *A Guide for Selecting Anti-Icing Chemicals, Version 1.0, IIHR Technical Report.*
- Norem, H. (2009). "Selection of Strategies for Winter Maintenance of Roads Based on Climatic Parameters." *Journal of Cold Regions Engineering* 23(4): 113-135.
- O’Keefe, K. and X. Shi (2005). "Synthesis of information on anti-icing and pre-wetting for winter highway maintenance practices in North America." Final Rep. for the Pacific Northwest Snowfighters Association and the Washington State Dept. of Transportation, Olympia, WA.
- Ohio DOT (2011). "Snow & Ice Practices." Ohio Department of Transportation, Division of Operations, Office of Maintenance Administration. March 2011.
- Pachauri, N. and B. He (2006). Value-added utilization of crude glycerol from biodiesel production: a survey of current research activities. *Proceedings of the ASABE Annual International Meeting.*
- Perchanok, M. S., D. G. Manning and J. Armstrong (1991). "Highway de-icers: Standards, practice, and research in the province of ontario."
- Pesti, G. and Y. Liu (2003). *Winter Operations-Abrasives and Salt Brine.*
- Peterson, O. (1995). "Chemical effects on cement mortar of calcium magnesium acetate as a deicing salt." *Cement and concrete research* 25(3): 617-626.
- Pigeon, M. and R. Pleau (2010). *Durability of concrete in cold climates, CRC Press.*
- Poonguzhali, A., H. Shaikh, R. Dayal and H. Khatak (2008). "A review on degradation mechanism and life estimation of civil structures." *Corrosion Reviews* 26(4): 215-294.
- Resource Concepts Inc (1992). "Survey of: Alternative Road Deicers " Technical Report, Nevada Department of Transportation and California Department of Transportation, FHWA-SA-95-040.
- Roosevelt, D. S. (1997). *A Survey of Anti-Icing Practice in Virginia.*
- Rubin, J., P. Garder, C. Morris, K. Nichols, J. Peckenham, P. McKee, A. Stern and T. Johnson (2010). "Maine Winter Roads: salt, safety, environment and cost." A report by the Margaret Chase Smith Policy Center, The University of Maine.
- Salt Institute (2008). "Salt and Highway Deicing."

- Salt, N. R. C. C. o. t. C. C. o. R. and C. M. A. f. H. Deicing (1991). Highway Deicing: Comparing Salt and Calcium Magnesium Acetate, Transportation Research Board.
- Samples, L. M. and J. A. Ramirez (1999). "Methods of Corrosion Protection and Durability of Concrete Bridge Decks Reinforced with Epoxy-Coated Bars-Phase I."
- Santagata, M. and M. Collepardi Concrete deterioration caused by exposure to calcium-magnesium acetate aqueous solutions. Proc. 2nd Int. Conf. On Concrete under Severe Conditions.
- Santagata, M. and M. Collepardi (2000). "The effect of CMA deicers on concrete properties." Cement and concrete research 30(9): 1389-1394.
- Šelih, J. (2010). "Performance of concrete exposed to freezing and thawing in different saline environments." Journal of Civil Engineering and Management 16(2): 306-311.
- Seo, Y., U. Seo, J. Eum and S. J. Lee (2011). "Development of a Geothermal Snow Melting System for Highway Overlays and Its Performance Validations." Journal of Testing and Evaluation 39(4): 592-602.
- Shi, X. (2008). Impact of airport pavement deicing products on aircraft and airfield infrastructure, Transportation Research Board.
- Shi, X., M. Akin, T. Pan, L. Fay, Y. Liu and Z. Yang (2009a). "Deicer Impacts on Pavement Materials: Introduction and Recent Developments." Open Civil Engineering Journal 3.
- Shi, X., L. Fay, C. Gallaway, K. Volkening, M. Peterson, T. Pan, A. Creighton, C. Lawlor, S. Mumma and Y. Liu (2009b). Evaluation of Alternative Anti-icing and Deicing Compounds Using Sodium Chloride and Magnesium Chloride as Baseline Deicers, Phase I, Colorado Department of Transportation, DTD Applied Research and Innovation Branch.
- Shi, X., L. Fay, M. M. Peterson and Z. Yang (2010). "Freeze-thaw damage and chemical change of a portland cement concrete in the presence of diluted deicers." Materials and structures 43(7): 933-946.
- Shi, X., L. Fay, Z. X. Yang, T. A. Nguyen and Y. J. Liu (2009c). "Corrosion of Deicers to Metals in Transportation Infrastructure: Introduction and Recent Developments." Corrosion Reviews 27(1-2): 23-52.
- Shi, X., C. Strong, R. Larson, D. Kack, E. Cuelho, N. El Ferradi, A. Seshadri, K. O'Keefe and L. Fay (2006). "Vehicle-based technologies for winter maintenance: the state of the practice." Western Transportation Institute.
- SICOP (2004). "Fixed, Automated Anti-icing Spraying Systems." Snow and Ice Pooled Fund Cooperative Program <http://www.sicop.net/FAST%20Project.pdf>(Retrieved on July 10, 2006).
- Song, S. (2009). Deicing method based on carbon/glass fiber hybrid textile, Google Patents.
- Staples, J. M., L. Gamradt, O. Stein and X. Shi (2004). Recommendations for winter traction materials management on roadways adjacent to bodies of water, Montana Department of Transportation, Research Section.
- Stowe, R. (2001). A benefit/cost analysis of intelligent transportation system applications for winter maintenance. Transportation Research Board 80th Annual Meeting.
- Stuart, K. and W. Mogawer (1991). Laboratory Evaluation of Verglimit and Plusride. Final Report.
- Sumsion, E. S. and W. S. Guthrie (2013). Physical and Chemical Effects of Deicers on Concrete Pavement: Literature Review.

- Sutter, L. and S. Dakota (2008). The deleterious chemical effects of concentrated deicing solutions on Portland cement concrete, South Dakota Department of Transportation.
- Switzenbaum, M. S., S. Veltman, D. Mericas, B. Wagoner and T. Schoenberg (2001). "Best management practices for airport deicing stormwater." *Chemosphere* 43(8): 1051-1062.
- Takeichi, K., I. Sato, F. Hara and C. Yamamoto (2001). "Performance of various antifreezing pavements by field test." *Advances and Issues in Snow-Removal and Ice-Control Technology*(1741): 114-123.
- Taylor, P., J. Verkade, K. Gopalaakrishnan, K. Wadhwa and S. Kim (2010). "Development of an Improved Agricultural-based Deicing Product." Institute for Transportation, Iowa State University.
- Thompson, J. and B. He (2006). "Characterization of crude glycerol from biodiesel production from multiple feedstocks." *Applied Engineering in Agriculture* 22(2): 261.
- Transportation Association of Canada (2003). "Synthesis of Best Practices – Road Salt Management." <http://www.tac-atc.ca/english/pdf/pavement.PDF>.
- TRB (1991a). "Highway Deicing: Comparing Salt and Calcium Magnesium Acetate " Special Report 235 National Research Council Washington, D.C., 1991.
- TRB (1991b). "Highway Deicing: Summary of Cost and Use Issues." Special Report 235 National Research Council Washington, D.C., 1991.
- Trost, S. E., F. J. Heng and E. Cussler (1987). "Chemistry of deicing roads: Breaking the bond between ice and road." *Journal of transportation engineering* 113(1): 15-26.
- Tuan, C. (2004). "Conductive Concrete for Bridge Deck Deicing and Anti-icing University of Nebraska." Nebraska Department of Roads Project No. SPR-PL-1(037) P512 July 2004.
- Tuan, C. Y. (2008). Implementation of Conductive Concrete for Deicing (Roca Bridge).
- Turgeon, C. (1989). Evaluation of Verglimit (A De-Icing Additive in Plant Mixed Bituminous Surface). Final Report.
- Ushirode, W., J. Hinatsu and F. Foulkes (1992). "Voltammetric behaviour of iron in cement Part IV: Effect of acetate and urea additions." *Journal of applied Electrochemistry* 22(3): 224-229.
- Wang, K., D. E. Nelsen and W. A. Nixon (2006). "Damaging effects of deicing chemicals on concrete materials." *Cement and Concrete Composites* 28(2): 173-188.
- Ward, B. (2002). Evaluation of a fixed anti-icing spray technology (FAST) system. Proceedings of the 81st Annual Meeting of the Transportation Research Board, Washington, DC.
- Warrington, P. D. and C. Phelan (1998). ROADSALT AND WINTER MAINTENANCE FOR BRITISH COLUMBIA MUNICIPALITIES, BEST MANAGEMENT PRACTICES TO PROTECT WATER QUALITY.
- Wasstrom, R. (2007). "Before the Storm: Knowing How and When to Apply Salt and Other Chemicals Makes Crews More Effective Once the Snow Flies." *Public Works* 138(11).
- Wee, T., A. K. Suryavanshi and S. Tin (2000). "Evaluation of rapid chloride permeability test (RCPT) results for concrete containing mineral admixtures." *Aci Materials Journal* 97(2).
- Wieringa, J. (2010). "North American Winters in Europe: Focus on High Performance!" *Industry Match, Groningen – The Netherlands - 2010*.
- Williams, D. (2003). "Past and current practices of winter maintenance at the Montana Department of Transportation (MDT)." White Paper.

- Wisconsin Transportation Information Center (1996). "Using Salt and Sand for Winter Road Maintenance." Wisconsin Transportation Bulletin No. 6.
- Wyant, D. C. (1998). "Final report: exploring ways to prevent bonding of ice to pavement." Virginia Transport Research Council, Charlottesville, VA.
- Yang, Q., S. Zhang and X. Wu (2002). "Deicer-scaling resistance of phosphate cement-based bind for rapid repair of concrete." *Cement Concr. Res.* 2(1): 165-168.
- Yang, T., Z. J. Yang, M. Singla, G. B. Song and Q. Li (2012). "Experimental Study on Carbon Fiber Tape-Based Deicing Technology." *Journal of Cold Regions Engineering* 26(2): 55-70.
- Yasukawa, K. (2007). "Direct Use of Geothermal Energy in Japan, Institute for Geo-Resources and Environment." National Institute of Advanced Industrial Science and Technology The 12th Annual Eastern Snow Expo, 2007.
- Yehia, S. and C. Y. Tuan (1999). "Conductive concrete overlay for bridge deck deicing." *Aci Materials Journal* 96(3): 382-390.
- Yehia, S., C. Y. Tuan, D. Ferdon and D. Chen (2000). "Conductive concrete overlay for bridge deck deicing: Mixture proportioning, optimization, and properties." *Aci Materials Journal* 97(2): 172-181.
- Yehia, S. and Y. Tuan (1998). "Bridge Deck Deicing, Proc. Crossroads 2000 – 1998 Transportation Conference." Iowa State University. Ames, IA.
- Yehia, S. A. and C. Y. Tuan (1998). "Bridge deck deicing."
- Yunovich, M. and N. G. Thompson (2003). "Corrosion of highway bridges: Economic impact and control methodologies." *Concrete International* 25(1).
- Zenewitz, J. A. (1977). Survey of alternatives to the use of chlorides for highway deicing.
- Zhang, H. (2009). "Research on the Antifreezing Asphalt Mixture by Crumb Rubber Modified." Master's thesis - Dissertation Chang'an University: U418.441.
- Zhang, H., S. Han and H. Liu (2008). "A summary of asphalt concrete pavement for deicing and snow melting technology." *Helongjiang Jiaotong Keji (in Chinese)* 3: 8-9.
- Zhang, J., D. Das and R. Peterson (2009). "Selection of effective and efficient snow removal and ice control technologies for cold-region bridges." *Journal of Civil, Environmental, and Architectural Engineering* 3(1): 1-14.
- Zhou, X.-m., Z. J. Yang, C. Chang and G. Song (2011). "Numerical assessment of electric roadway deicing system utilizing emerging carbon nanofiber paper." *Journal of Cold Regions Engineering* 26(1): 1-15.

CHAPTER 3. SURVEY RESULTS FROM STATE DOTS

The research team developed a survey to learn the snow and ice control environmental best management practices of winter maintenance agencies.

The survey was distributed in September 2014 through the online tool Survey Monkey, and was open for responses for two weeks. The purpose of this survey was to gather information from winter maintenance professionals at state, provincial and local transportation agencies on their experience, challenges, lessons learned, and environmental concerns regarding winter snow and ice control practices. The survey consisted of 19 questions. Detailed information about response percentages, response counts and individual answers to each question is provided below.

Q1: Please provide your contact information.

There were 12 responses to this question, with 1 respondent skipping this question. Survey respondents were mainly “Highway maintenance manager” (25.0%) and “Highway maintenance supervisor II” (25%). There were also a few other representatives having the title of “Highway maintenance worker IV” (16.7%), “Assistant district engineer” (16.7%), “Highway maintenance worker II” (8.3%) and “Highway maintenance supervisor I” (8.3%). Specific response counts and response percentages for each title type are presented in Table 3- 1.

Table 3- 1 Number of responses for each title type

Title Type	Response Percent	Response Count
Highway maintenance worker II	8.3%	1
Highway maintenance worker IV	16.7%	2
Highway maintenance manager	25.0%	3
Highway maintenance supervisor I	8.3%	1
Highway maintenance supervisor II	25.0%	3
Assistant district engineer	16.7%	2
	<i>Answered question</i>	12
	<i>Skipped question</i>	1

Q2. Please indicate the district you belong to

A total of 13 responses were received from 3 Districts in Nevada, of which only one respondent from District 1 provided specific city information as “Glendale.” Detailed responses are shown in Table 3- 2.

Table 3- 2 Number of responses for district distribution.

Answer choices	Response Percent	Response Count
District 1 - (southern Nevada, with headquarters in Las Vegas, and a major maintenance station in Tonopah)	61.54%	8
District 2 - (northwest Nevada, with headquarters in Sparks)	15.38%	2
District 3 - (northeast Nevada, with headquarters in Elko, and major maintenance stations in Winnemucca and Ely)	23.08%	3
	<i>Answered question</i>	13

Q3. Do you use any of the following anti-icing technologies for snow and ice control for winter maintenance activities? (Note that many of these deal with physical or chemical modification of the pavement surface such that it would be easier to break the bond of snow/ice to pavement).

There were 10 responses collected for this question, with 3 respondents skipping this question and 1 respondent selecting the applied anti-icing product “Ice slicer” in the “Other” option list. The survey results suggest that few highway winter maintenance agencies in Nevada State use the listed anti-icing technologies, implying that traditional anti-icing treatments are probably still widely used across Nevada (e.g., chemical applications). This also suggests that NDOT may need to focus additional efforts on research and testing of anti-icing alternatives. Detailed responses are shown in Table 3- 3.

Table 3- 3 Responses on the application of anti-icing technologies

Answer options	Yes	No	Don't know	Response Count
Rough surfaces and physical bending of pavements	0	9	1	10
High friction anti-icing polymer overlays	0	10	0	10
Asphalt pavement with anti-icing additives	0	9	1	10
Heated pavement technologies (Geothermal thermal heating, Electrical heating, Alternative heating via Solar, Wind, Microwave, or Infrared)	0	10	0	10
Fixed Automated Spray Technology (FAST)	1	8	1	10
<i>Answered question</i>				10
<i>Skipped question</i>				3

Q4. If you use "Rough surfaces and physical bending of pavements". Please provide the following information.

This is a follow-up question to Q3. Based on above summary of Q3, no respondents indicated that they currently used "Rough surfaces and physical bending of pavements" in practice. Therefore, there were no responses to Q4.

Q5. If you use "High friction anti-icing polymer overlays". Please provide the following information.

According to the results of Q3, no respondents indicated that they use "High friction anti-icing polymer overlays." Therefore, there were no responses to Q5.

Q6. If you use "Asphalt pavement with anti-icing additives". Please provide the following information.

According to the results of Q3, no respondents indicated that they use "Asphalt pavement with anti-icing additives." Therefore, there were no responses to Q6.

Q7. If you use "Heated pavement technologies (Geothermal thermal heating, Electrical heating, Alternative heating via Solar, Wind, Microwave or Infrared)". Please provide the following information.

According to the results of Q3, no respondents indicated that they use “Heated Pavement Technologies.” Therefore, there were no responses to Q7.

Q8. If you use "Fixed Automated Spray Technology (FAST)". Please provide the following information.

Only one respondent from “District 2 - (northwest Nevada, with headquarters in Sparks)” provided information on the use of "Fixed Automated Spray Technology (FAST)." The respondent replied that the system was from Boshung, but additional information about the initial installation cost, annual maintenance and operations costs, service life, and salvage value of this FAST system was not specified.

Q9. What chemicals you are using for anti-icing operations for winter maintenance activities?

Nine respondents replied to this question, and 4 respondents skipped it. Six respondents gave answers regarding salt brine (NaCl), with 4 marking “Yes” and 2 marking “No”. Nine respondents also gave replies on the use of liquid Magnesium Chloride (MgCl₂), with 4 answering yes, but over half (n=5) answering “No.” For the use of liquid potassium acetate (KAc), 2 marked “Yes” and 5 marked “No.” None of the respondents indicated current usage of liquid Calcium Chloride (CaCl₂) or liquid Calcium Magnesium Acetate (CMA). Detailed responses are presented in Figure 3- 1.

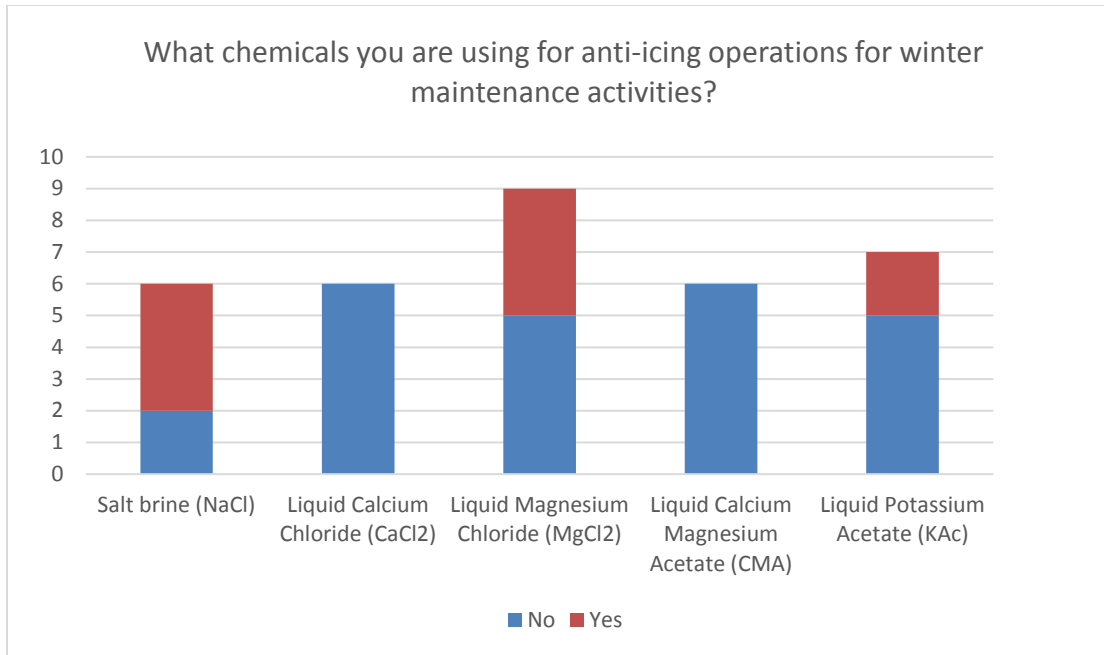


Figure 3- 1 Survey results about the training conditions of agency staff

Q10. Please provide the following for the chemicals used for anti-icing operations?

Only 4 respondents provided complete or partial answers to this question. Specific information from respondents is provided in Table 3- 4.

Table 3- 4 Responses on the chemicals used for anti-icing operations

Title	District	Chemical name(s)	Cost per gallon	Typical application rates (gallons/lanemile)	Estimated total usage per winter season (gallons)
Highway Maintenance Manager	District 1		0.05	150 gallons/lanemile	50,000
Highway Maintenance Manager	District 2	Liquid Potassium Acetate	10	Not sure	16,035
Highway Maintenance Supervisor II	District 1	Salt			

Title	District	Chemical name(s)	Cost per gallon	Typical application rates (gallons/lane-mile)	Estimated total usage per winter season (gallons)
Highway Maintenance Supervisor II	District 2	Salt Brine		50 gallon/lane mile	60,000

Q11. What is your main consideration in choosing anti-icing technologies and/or chemicals for winter maintenance activities?

Seven responses were collected for this question. “Anti-icing performance” was the most common response for the main consideration in choosing anti-icing technologies and/or chemicals for winter maintenance activities (n=7), followed by the “purchase cost” (n=5). “Risk to asphalt pavements,” “Risk to motor vehicles,” and “Risk to the natural environment” were also cited as in the selection of anti-icing technologies and/or chemicals. However, “Risk to steel bridges” and “Risk to concrete pavement and bridge decks” were not identified as major concerns for choosing anti-icing technologies and/or chemicals. Response distribution is provided in Figure 3- 2.

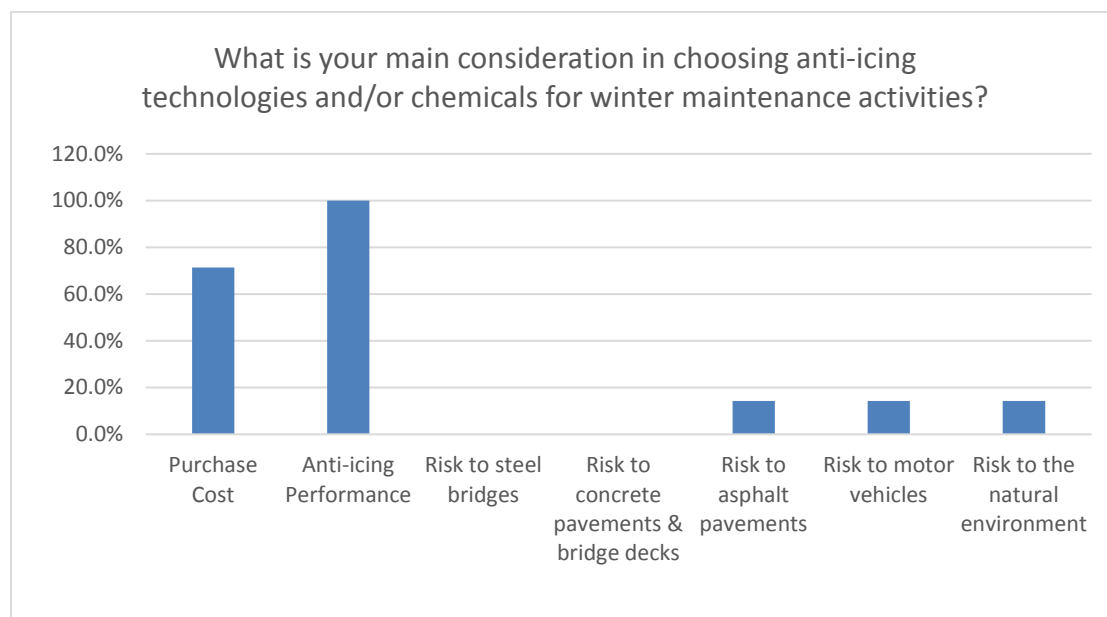


Figure 3- 2 Main considerations of NDOT highway winter maintenance agencies in choosing anti-icing technologies and/or chemicals.

Q12. Please estimate cost savings for your agency's snow and ice control program due to the implementation of anti-icing technologies or chemicals for winter maintenance activities?

Six responses were collected for this question. Respondents estimated cost savings ranging from zero to over 30% as a result of implementing anti-icing technologies or chemicals. Detailed responses are provided in Table 3- 5.

Table 3- 5 Agency’s responses on estimated cost savings as a result of implementing anti-icing technologies or chemicals.

Title	District	Response	Comment
Highway Maintenance Manager	District 1		Unknown at this time because we have just been doing this for 2-3 years
Highway Maintenance Manager	District 2	More than 30%	
Assistant District Engineer	District 3	10%	
Assistant District Engineer	District 3	No cost reduction	
Highway Maintenance Supervisor II	District 1	10%	
Highway Maintenance Supervisor II	District 2	25%	

Q13. Have the practices of anti-icing improved the level of service (or safety and mobility)?

A total of 7 agencies responded to this question, and all of them confirmed the positive effect of anti-icing treatment in improving the level of service (or safety and mobility), which suggests a trend toward increased use of anti-icing strategies in winter maintenance practices.

Q14. What is the typical weather maintenance period in your district?

There were 7 responses to this question. The results showed that the maintenance period can vary even within a district. In District 2, for example, the final month of the maintenance period could be as early as March or as late as June. Generally the starting month of maintenance period is October or November, and the ending month is more dependent on the specific maintenance area. Detailed responses are listed in Table 3- 6.

Table 3- 6 Responses on the typical weather maintenance period.

Title	District	Starting month	Ending month
Highway Maintenance Supervisor I	District 1	January	January
Highway Maintenance Manager	District 1	November	May
Highway Maintenance Manager	District 2	October	June
Assistant District Engineer	District 3	October	May
Assistant District Engineer	District 3	October	April
Highway Maintenance Supervisor II	District 1	October	March
Highway Maintenance Supervisor II	District 2	November	March

Q15. Please comment on the typical road weather scenarios for winter highway maintenance in your district and your main challenges with the use of chemicals for snow and ice control.

There were only 3 responses to this question. Full comments are documented in Table 3-7.

Table 3- 7 Comments on the typical road weather scenarios for winter highway maintenance.

Title	District	Comment
Highway Maintenance Supervisor I	District 1	Little to no snow and ice in our area.
Highway Maintenance Manager	District 2	Right use and correct application at the right time.
Assistant District Engineer	District 3	We have a lot of miles to cover so we stick to salt/sand mix. Chemicals and salt are often diluted out before we get back. Fortunately, we get a large temp increase during the day, and often some sun. If we fall behind, the desert catches us up in a day or two. Mountain grades are a problem. Super elevations on steep grades are compounded problems. Shaded areas in mountainous terrain is a big problem. A shaded area on a steep grade and in a curve is my biggest problem spot on I-80.

Q16. In your opinion, does anti-icing operations pose any significant risk to the durability of highway infrastructure?

Six respondents replied to this question, of whom 5 provided negative answers and one replied “Yes.” Detailed responses and additional comments are shown in Table 3- 8.

Table 3- 8 Responses on the significant risk of anti-icing operations to the durability of highway infrastructure.

Title	District	Response	Comment
Highway Maintenance Manager	District 1	No	
Highway Maintenance Manager	District 2	No	Not if used responsibly.
Assistant District Engineer	District 3	Yes	Use of any salt product reduces durability infrastructure.
Assistant District Engineer	District 3	No	
Highway Maintenance Supervisor II	District 1	No	
Highway Maintenance Supervisor II	District 2	No	

Q17. What are the maintenance and replacement costs associated with infrastructure damage due to anti-icing operations?

Only 2 responses from District 2 and 3 were collected for this question. Detailed responses and comments are presented in Table 3- 9.

Table 3- 9 Responses on the maintenance and replacement costs associated with infrastructure damage due to anti-icing operations.

Title	District	Response
Highway Maintenance Manager	District 2	Not sure
Assistant District Engineer	District 3	Reduction of maintenance operation equipment life, Bridge structure damage and loss of design life, and damage to ITS equipment in the area of the road.

Q18. Has your agency conducted any study to evaluate or mitigate the risk of anti-icing chemicals to infrastructure? If so, Email Me Documents

There were 4 agencies that responded to this question, but none of them knew about any agency studies to evaluate or mitigate the risk of anti-icing chemicals to infrastructure. A summary of responses is shown in Table 3- 10.

Table 3- 10 Existence of agency studies to evaluate or mitigate the risk of anti-icing chemicals to infrastructure

Title	District	Response
Highway Maintenance Manager	District 1	Unknown
Highway Maintenance Manager	District 2	Not that I know of
Assistant District Engineer	District 3	Not that I am aware of
Assistant District Engineer	District 3	Don't know

Q19. Please share your insights on the use of anti-icing strategies for snow/ice control (best practices, cost-effective technologies or products, limitations, future developments, etc.). THANKS!

There were only 3 agencies from District 2 and 3 that shared their insights on the application of anti-icing strategies for winter snow and ice control. Details are presented in Table 3- 11.

Table 3- 11 Insights on the use of anti-icing strategies for snow and ice control.

Title	District	Response
Highway Maintenance Manager	District 2	Training is the ultimate most important aspect of anti-icing, next is providing the most advance application equipment available.
Assistant District Engineer	District 3	You need to weight the use of any salt product with the benefit that it creates on the road to improve driving conditions. Anti-icing (pre-Storm) if done properly can reduce the amount of salt products need for de-icing (during the storm).
Assistant District Engineer	District 3	From what I've seen, concrete surface delamination that are blamed on salt damage are usually caused by cement finishers using too much water. If salt or chemicals add to Alkali Silica Reaction then it would be a problem for us. I don't know if there is a relationship.

CHAPTER 4. FIELD PERFORMANCE OF CORING CONCRETE SAMPLES

4.1 Introduction

Unlike laboratory testing in which the environmental conditions are well designed and precisely controlled, the deterioration of concrete infrastructure in the field due to exposure to deicers and highly variable environmental conditions is dependent on the following factors: weather, environment, traffic conditions, and infrastructure configuration. Deicers may be applied directly to a concrete bridge deck or roadway, but other nearby concrete elements such as rails, barriers, and columns may be vulnerable due to splash. Consequently, not all bridges or concrete components (e.g., decks, beams/crossbeams, diaphragms, abutments, piers and piles) are expected to have the same likelihood of damage or rate of deterioration. Although the laboratory studies using concentrated solutions to accelerate testing have demonstrated that deicing chemicals have the potential to damage concrete, past research has claimed that the field cores extracted from sites in Colorado, Idaho, Iowa, Montana, and South Dakota did not exhibit damage conclusively attributable to deicers (Sutter et al, 2008).

As a result, without an agreement of laboratory and field data of the potential damage induced by deicers to concrete infrastructure, there is no widely accepted strategy for protecting the existing concrete infrastructure. Deicers are widely used in many places in accordance with guidelines, established by organizations like the Pacific Northwest Snow Fighters Association, to maintain the safety and productivity of roadways during the winter season. A need has been identified to evaluate appropriate practices and products for snow and ice control which also preserve the integrity and durability of concrete infrastructure in the presence of deicer chemicals. Further investigation is needed to explain the mechanisms that cause damage to the cementitious materials exposed to chemical attack in the field environment (Farnam, 2015).

In this chapter, the field cores from NDOT concrete bridge decks were used to demonstrate the deterioration of the concrete from exposure to deicing chemicals. Mechanical properties of collected samples were tested to evaluate the engineering performance of the concrete bridge pavements at these sites. A secondary investigation looking at the concrete microstructure was used to evaluate the service status of these bridge decks as well.

4.2 Methodology

4.2.1 Field Sampling

Coring samples from the field sites were collected by NDOT and shipped to the WTI CSIL for laboratory testing. Locations for the coring were situated throughout the length of the test sites at various distances from the bridge pavements. Field bridge decks were examined for possible concrete coring to support this investigation. Three sites in the State of Nevada, namely the *Galena*

Creek Bridge Structure B-1948 (indicated as Creek in the following sections), Steamboat Hills Bridge Structure B-521 (indicated as Hills in the following sections), and Galena Forest Bridge Structure B-2521 (indicated as Forest in the following sections), were selected as the potential candidates as typical concrete pavements that were exposed to deicer attacks. The concrete coring and part of the data collection were conducted by the staff of the Nevada Department of Transportation (NDOT). Note that these pavements on each bridge were exposed to significantly different deicer types, frequency of usage and application rates, and climatic conditions. By design, this helps to shed light on the effects of each deicer type and other factors on the durability of concrete pavements in different environments. For the state of Nevada, the coring occurred in randomly selected locations and avoided locations with severe cracking so as to ensure reasonable structural integrity of core specimens. For the vast majority of the deck core samples, no significant deterioration was visible other than surface scaling. In other words, there were generally no signs of significant longitudinal, transverse, or diagonal cracking and no evidence of visible precipitates where core samples were collected.

4.2.2. Compressive Strength

The compressive strength of the cored concrete cylinders was determined following the standard test method ASTM C39-2014 for Compressive Strength of Cylindrical Concrete Specimens. Before testing, the cored concrete cylinders were surface-ground on both ends to ensure a uniform surface finish (and thus a uniformly distributed compressive load). The flattened cylinders were then placed in a hydraulic Material Testing System (MTS Model 880) equipped with two spherical bearing blocks with hardened surfaces. A compressive load of about 80-120 pounds per second was applied manually until the concrete core sample failed. The ultimate compressive strength was then calculated by dividing the load (lbs/sec) at failure by the cross-sectional area resisting the load. The test results are shown as the average of three cores taken from the same bridge deck.

4.2.3. Splitting Tensile Strength

The splitting tensile strength is very important with respect to cracking, shear capacity, anchorage capacity, and durability for concrete. The splitting tensile strength of the concrete cylinders cored from the above mentioned three sites was determined using the ASTM C496-2011 for Splitting Tensile Strength of Cylindrical Concrete Specimens test method. This method was performed to evaluate the shear resistance provided by concrete.

The test method consisted of applying a diametrical compressive force manually along the longitudinal axis of the cylindrical concrete cores at a rate of 50-80 pounds per second until the concrete core sample failed. Two thin pieces of plywood with thickness of about 2mm were placed along the longitudinal axis of the concrete cylinder to evenly distribute the compressive load.

Figure 4-1 shows the setup of the splitting tensile strength test. The load was applied manually until the concrete core failed (typically splitting in half), and the maximum load at the failure was recorded and used to calculate the splitting tensile strength as follows (Equation 1).

$$STS \text{ (psi)} = \frac{P \cdot C}{\pi \cdot L \cdot D} \quad (1)$$

where:

P = Load at failure (lb)

C = Estimated length of contact on the top and bottom (for un-scaled specimens, C = 2; but significantly scaled specimens would feature lower contact areas)

L = Length of specimen (in.)

D = Diameter of specimen (in.)

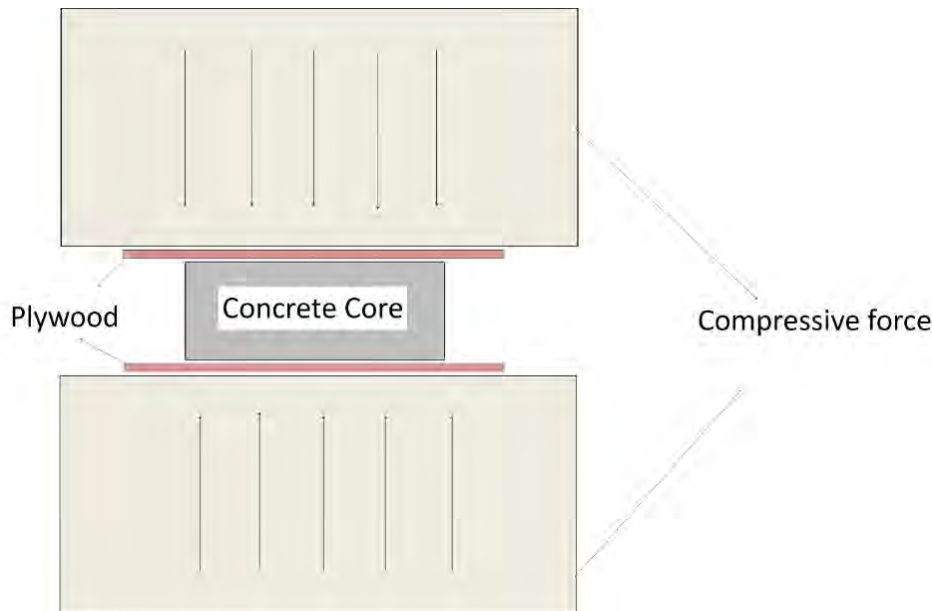


Figure 4- 1 The setup of the splitting tensile strength test

4.2.4 Microstructure Analysis

Scanning electron microscopy (SEM) was used to analyze the microstructures of the samples cored from three sites. SEM was mainly applied to demonstrate the morphology of the cement paste at the interfaces between two aggregates. The fracture surface morphology of lab prepared samples was performed on an FEI-Quanta 200F scanning electron microscope. SEM was conducted under an accelerating voltage of typically 20 kV. SEM was coupled with an energy dispersive spectroscopy (EDS) analyzer. For EDS, a micro-analytical unit was employed to detect

the small variations in trace element content, using an accelerating voltage of typically 15-20 kV and a scan time of 60 seconds per sampling area.

4.3 Mechanical Properties

4.3.1 Compressive Strength

The results of the compressive strength tests are shown in Figure 4-2. The samples cored from site Steamboat Hills Bridge Structure B-521 had the lowest compressive strength, while the Galena Forest Bridge Structures B-2521 samples show the highest, with average values of 2906 ± 619 psi and 3339 ± 508 psi, respectively. The samples cored from Galena Creek Bridge Structure B-1948 show a value of 3114 ± 379 psi.

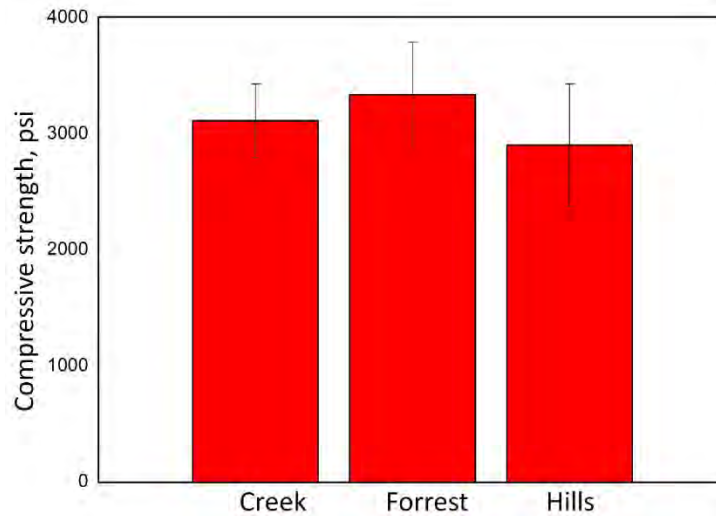


Figure 4- 2 Compressive strengths of cored concrete samples from the bridge decks of Creek, Forest, and Hills

4.3.2 Splitting Tensile Strength

The results of the splitting tensile strength tests are shown in Figure 4-3.. The samples cored from Creek site exhibit the lowest splitting tensile strength, while the Forest samples show the highest, with average values of 433 ± 71 psi and 552 ± 37 psi, respectively. The samples cored from Hills show an average value of 489 ± 58 psi.

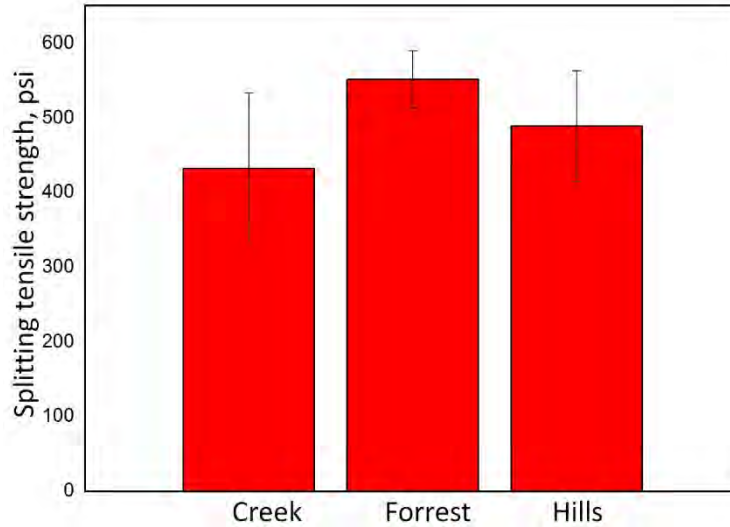


Figure 4- 3 Splitting tensile strengths of cored concrete samples from the bridge decks of Creek, Forest, and Hills.

As demonstrated by the compressive and splitting tensile strengths, these concrete samples cannot be evaluated as satisfied conditions when compared with the normal designed compressive or splitting tensile strengths. Like all porous materials, the mechanical properties of concrete are largely governed by the macro pores (with a size of centimeters to millimeters) of the samples. The combined results of the compressive strength and splitting tensile strength testing results show a loss of the mechanical strength. We hypothesized the loss of mechanical strength resulted from the microstructure changes within the samples without showing obvious deterioration. Microstructure analysis of the core samples is reported in the following section.

4.4 Microstructure Analysis

4.4.1 SEM Analysis

Like all solid materials, the overall performance of concrete is largely determined by its microstructures. Therefore, the microstructure of the concrete samples was analyzed to elucidate the mechanisms behind the degradation in performance. In this section, scanning electron microscopy (SEM) was used to analyze the microstructure of the samples cored from three sites. The goal of the SEM analysis was to demonstrate the morphology of the cement paste at the interface between two aggregates.

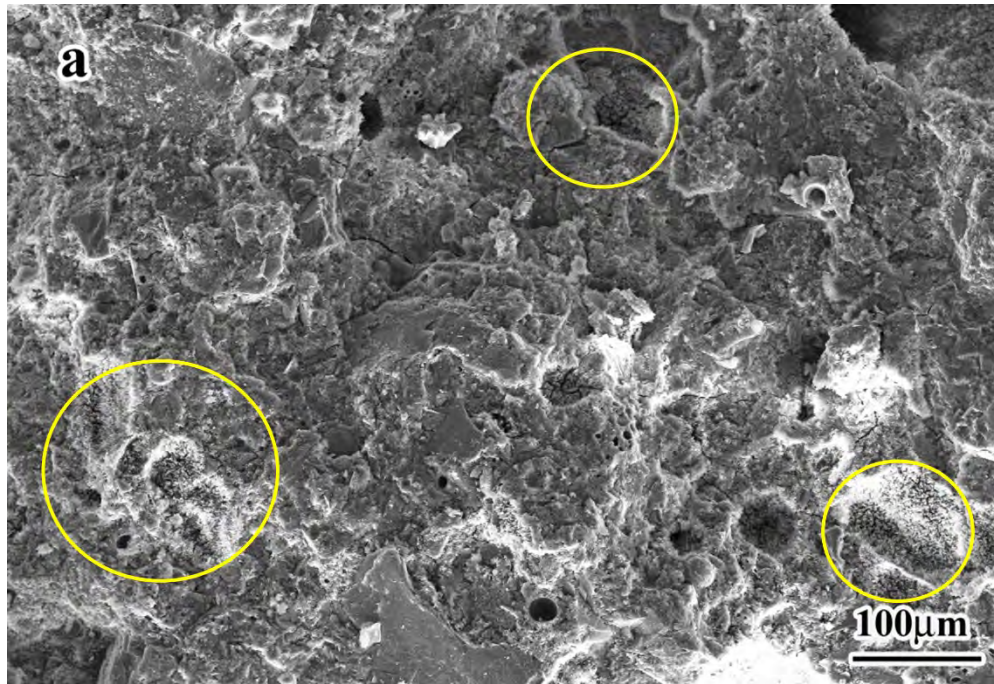
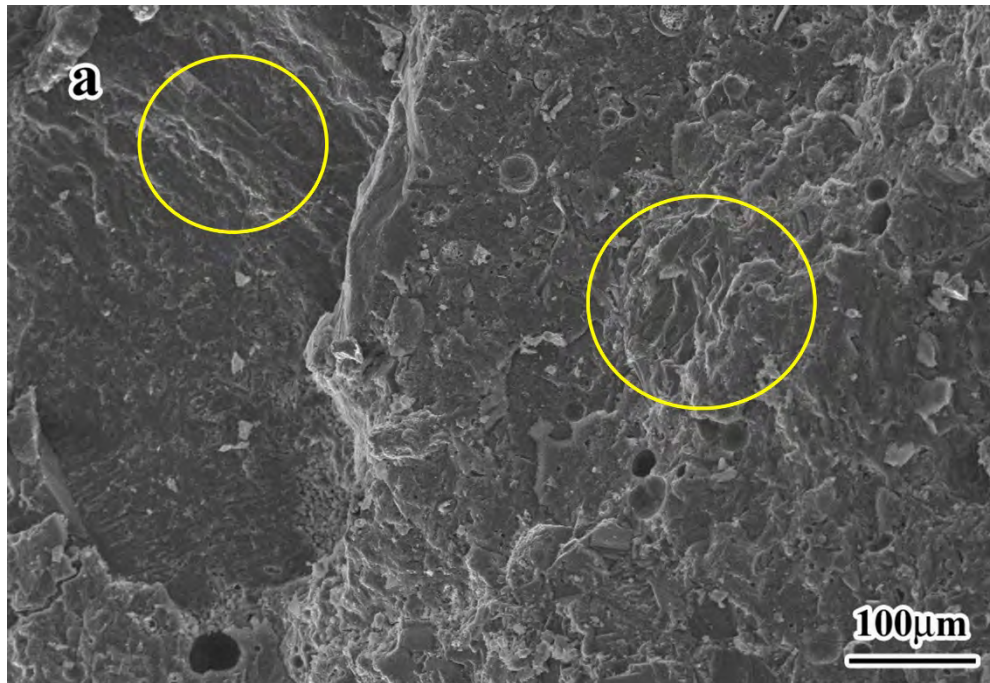


Figure 4- 4 SEM fracture surface morphologies of the samples cored from the Creek site with a) low and b) high magnification.

As can be seen in the low magnification image Figure 4- 4a, a large quantity of pores can be observed in the cement paste. In addition, the fracture surface shows limited intact C-S-H phases, and many small sized “bumpy phases” can be detected (the areas in yellow circles). Furthermore, in the high magnification image (Figure 4- 4b), some sticky precipitate phases can be observed, and the quantity of the amorphous binder phase is far less than normal cement paste. A small number of crystal particles were embedded in the sticky phase, and some of the homogenous amorphous binder phase has become stripped in randomly orientated directions (shown as the red circle areas in Figure 4- 4b). The degradation of the concrete mostly resulted from the production of these crystal precipitates in the C-S-H binder phase, and this is the reason why these samples show the lowest mechanical properties.

Figure 4- 5 a) and b) show the low and high magnification SEM fracture surface morphologies of the samples cored from the Forest site, respectively. As can be seen in the low magnification image Figure 4- 5a, the quantity of the pores in the cement paste of the Forest sample is less than that from the samples of the Creek site. In the high magnification image (Figure 4- 5b), in comparison with the Creek sample, some layered structure C-S-H phases can be observed, and the surfaces of the pores are smoother than those from the Creek site. Similar to the Creek samples, some sticky precipitate phases can also be observed, and crystal particles embedded in the sticky phase can be detected as well (as shown in the red circle in the high magnification image).



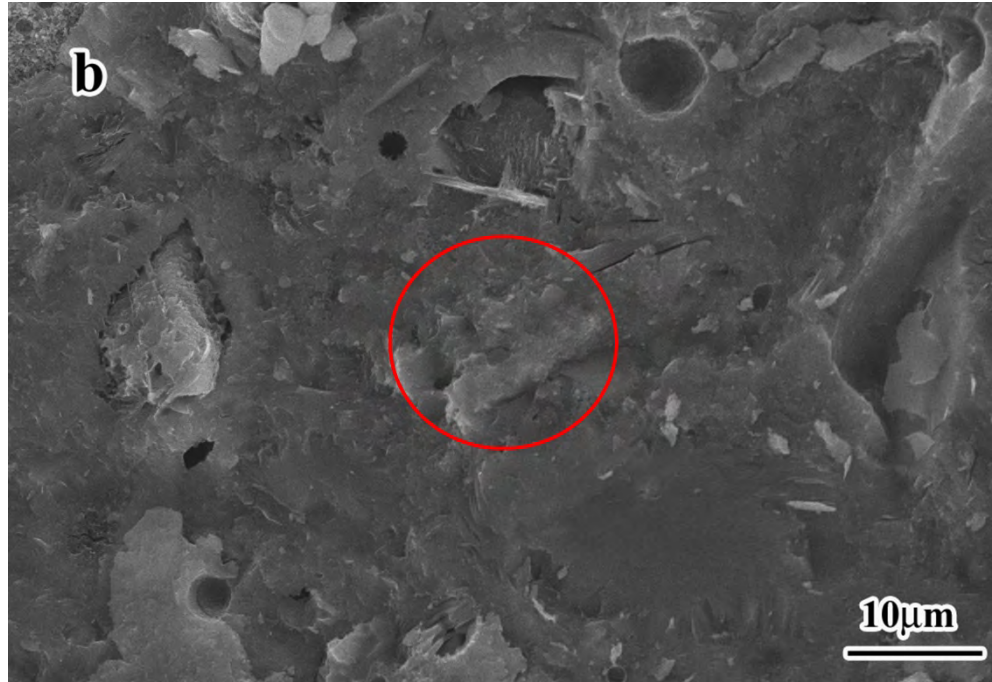


Figure 4- 5 SEM fracture surface morphologies of the samples cored from the Forest site with a) low and b) high magnification.

Figure 4- 6a) and b) show the low and high magnification SEM fracture surface morphologies of the samples cored from the Hills site, respectively. In the low magnification image (Figure 4- 6a), the surface shows relatively low pore content, and the layered C-S-H phase can be observed. In the high magnification image, however, some needle shaped precipitates, which are embedded in the sticky phases (shown as the red circle in Figure 4- 6b), can be observed, although the content is relatively low. As demonstrated in Figure 4- 6b, the diameters of the needle shaped precipitates are about 100 nm, and the surfaces of some needles are smooth while others are not.

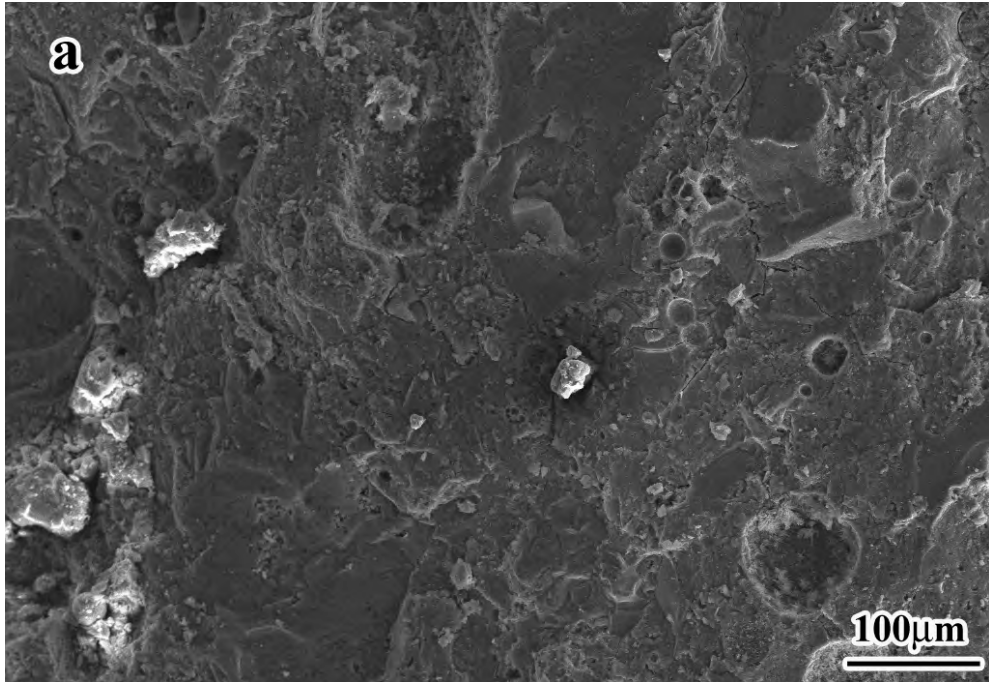


Figure 4- 6 SEM fracture surface morphologies of the samples cored from the Hills site with a) low and b) high magnification.

4.4.2 SEM/EDS Analysis

Figure 4- 7, Figure 4- 8, and Figure 4- 9 show the scanning electron microscopy/energy dispersive spectroscopy (SEM/EDS) analysis results of cored concrete samples from the three bridge decks - Creek, Forest, and Hills. As seen in these three figures, the chloride (Cl⁻) content of the Creek site has the highest value and the Forest site has the lowest with value of 0.41 at.% and 0.04 at.%, respectively. The Hills site samples have a Cl⁻ content 0.13 at.%. On the contrary, the calcium (Ca²⁺) content of the samples from the Forest site has the highest value, while the Creek site has the lowest with values of 14.33 at.% and 10. 46 at%, respectively. The Hills site samples have a Ca²⁺ content of 12.96 at.%. In addition, the silicon (Si) content of the samples from the three sites are 5.81 at.%, 6.10 at.%, and 6.17 at.%, the magnesium (Mg) content are 0.45 at.%, 0.63 at.%, and 0.88 at.%, and the sodium (Na) contents are 0.49 at.%, 0.64 at.%, and 0.67 at.%, corresponding to Creek, Forest, and Hills. The details of the chemical content of the concrete samples are listed in Table 4-1.

Table 4-1 The chemical contents of filed cored samples

Elements content, at.%	Creek	Forest	Hills
Cl	0.41	0.04	0.13
Ca	10. 46	14.33	12.96
Si	5.81	6.10	6.17
Mg	0.45	0.63	0.88
Na	0.49	0.64	0.67

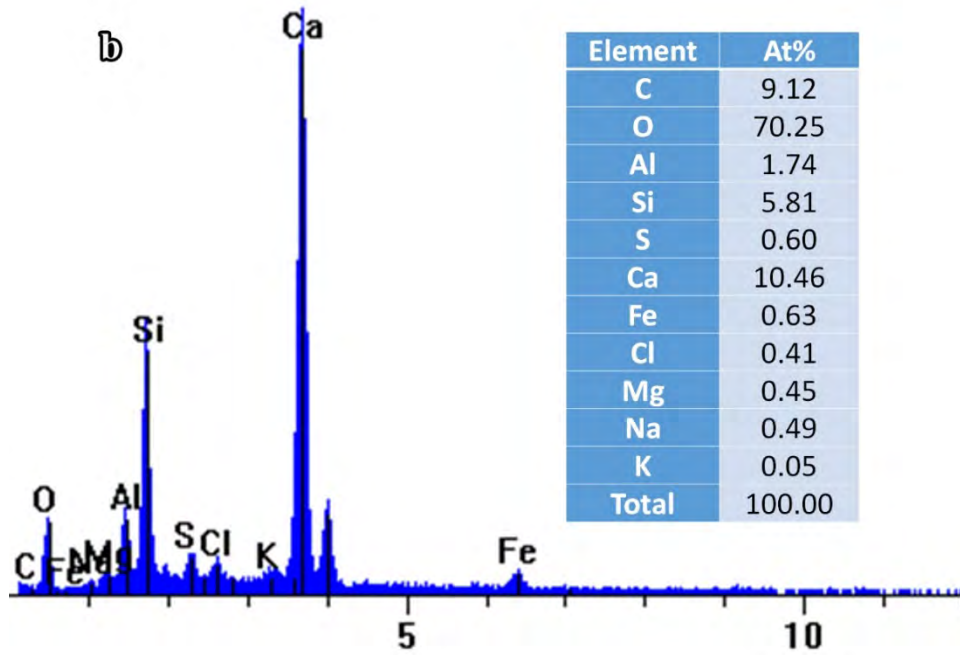
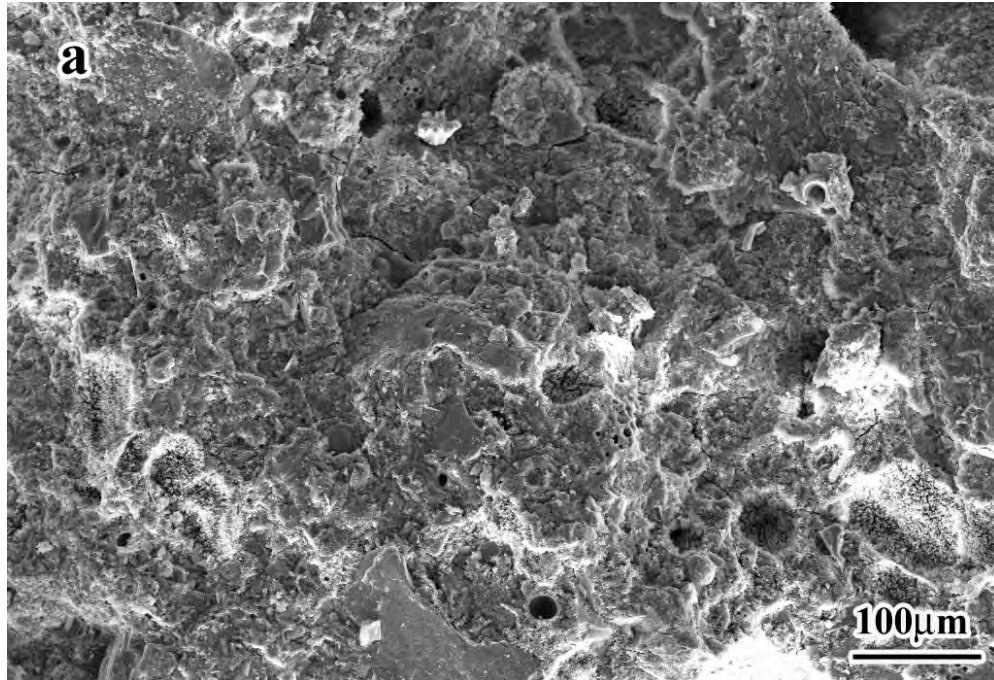


Figure 4- 7 SEM/EDS of the fracture surface of the samples cored from the Creek site with a) SEM image and b) corresponding EDS results.

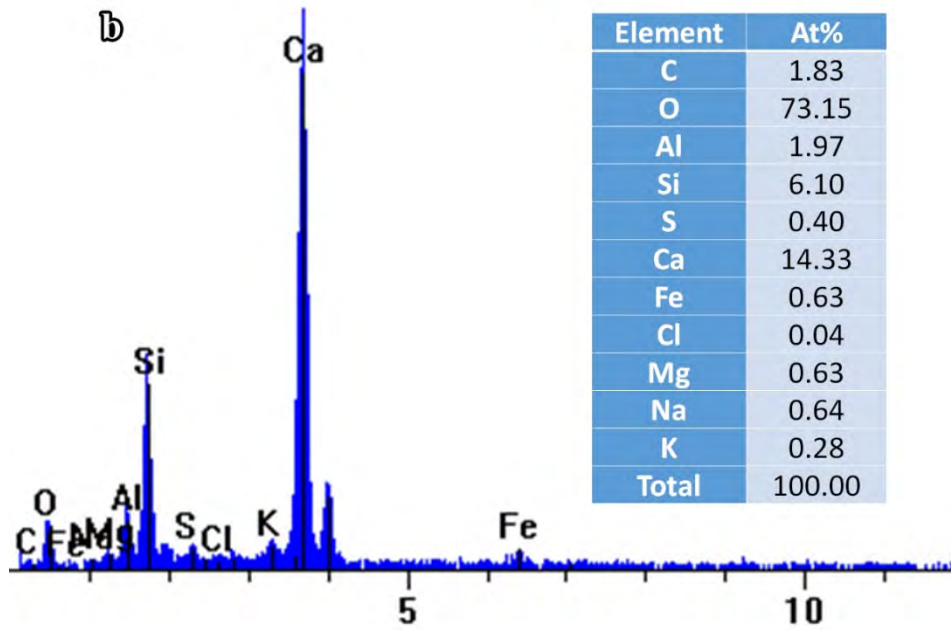
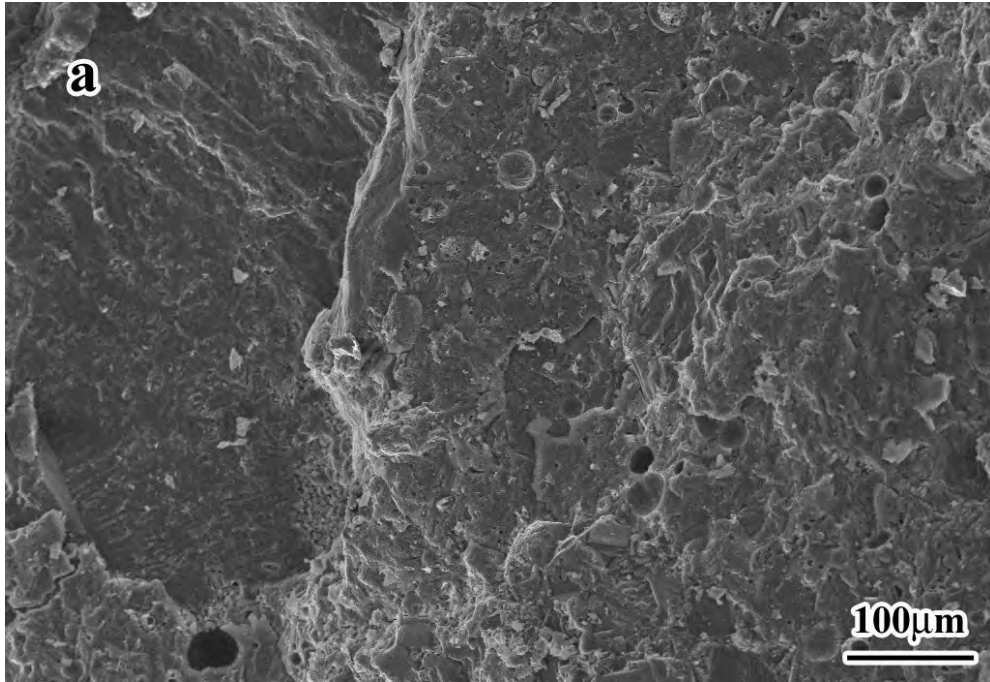


Figure 4- 8 SEM/EDS of the fracture surface of the samples cored from the Forest site with a) SEM image and b) corresponding EDS results.

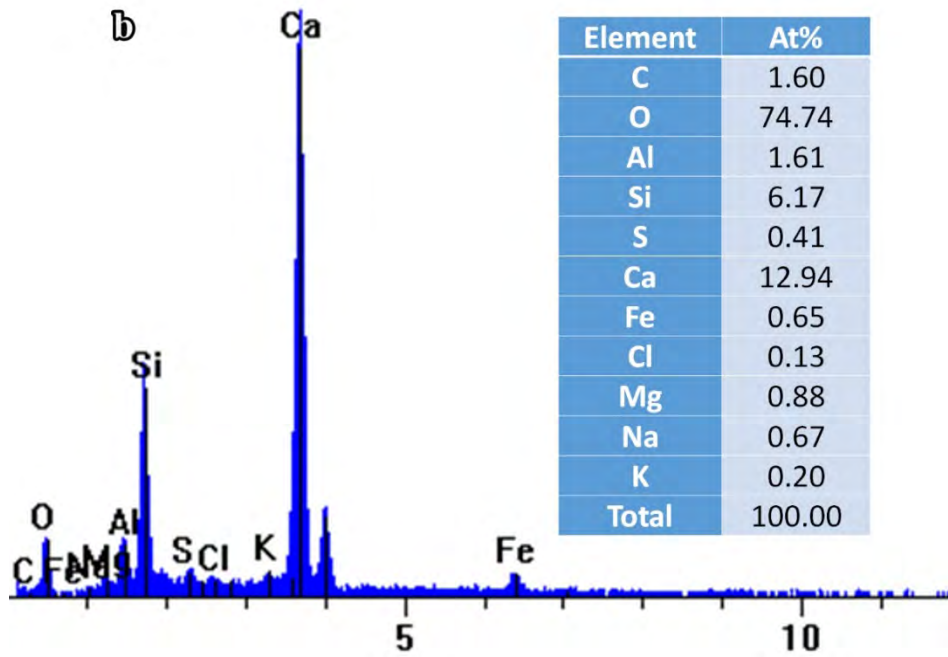
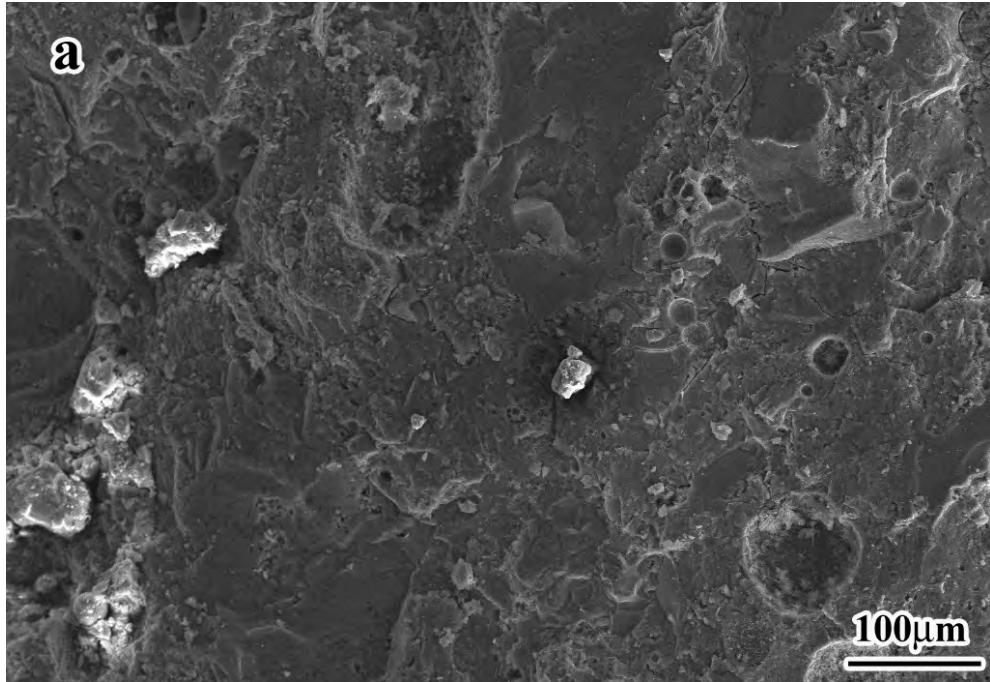


Figure 4- 9 SEM/EDS of the fracture surface of the samples cored from the Hills site with a) SEM image and b) corresponding EDS results.

4.5 Key Findings

The samples cored from the Forest site show the highest compressive strength, while the Hills shows the lowest. However, unlike the compressive strength, the samples cored from the Creek site exhibit the lowest splitting tensile strength, while the Forest samples show the highest.

The SEM/EDS analysis results confirm the leaching of Ca^{2+} out of the cement paste, which is likely caused by the chemical reaction of MgCl_2 with Ca-rich cementitious phases. The SEM analysis demonstrates that a large quantity of pores and many small sized “bumpy phases” can be observed in the cement paste of samples cored from the Creek site. A small number of crystal particles were embedded in the sticky phase. The quantity of the pores in the cement paste of the Forest sample is relatively less than that those from the Creek site. By comparing with the Creek site sample, some layered structure C-S-H phases can be observed in the samples from the Forest site, and the surfaces of the pores are smoother than those from the Creek site. The fracture surface of the Hills sample shows relatively low pore content, and the layered C-S-H phase can be observed. Some needle shaped precipitates, with relatively low content, can be detected in the sticky phases. These may be the major reasons for the reduction of the mechanical strength of the concrete samples cored from these sites.

4.6 References

- Sutter, L. and S. Dakota (2008). The deleterious chemical effects of concentrated deicing solutions on Portland cement concrete, South Dakota Department of Transportation.
- Farnam, Y., Dick, S., Wiese, A., Davis, J., Bentz, D., & Weiss, J. (2015). The influence of calcium chloride deicing salt on phase changes and damage development in cementitious materials. *Cement and Concrete Composites*, 64, 1-15.

CHAPTER 5. LABORATORY INVESTIGATION

Although the impacts of deicers on concrete infrastructure have been investigated for decades, there is still no agreement on the negative effects of deicers on the performance and durability of concrete materials. In fact, concrete materials exposed to deicing chemicals show both physical and chemical deterioration. The physical mechanism of attack, which is mainly caused by freeze/thaw cycles, can lead to the scaling, map cracking, or paste disintegration of Portland cement concrete (Sutter, 2008). Chemical deterioration of concrete caused by deicers may occur through reactions with cement paste and/or aggregates and thus reduce concrete integrity and strength (Neville 1995, Sutter, 2008, Shi, 2008, Shi et al. 2009b). This, in turn, may foster the ingress of moisture, oxygen and aggressive agents (e.g., chloride anions) onto the rebar and dowel bar surfaces and promote their corrosion in concrete (Yu et al. 2010, Shi et al. 2011, 2012b, Liu and Shi 2012).

Accumulative studies have been conducted in the laboratory setting, often in an accelerated manner, which reported the physicochemical deterioration of concrete as a function of deicer type and test protocol (Sutter et al. 2008, Shi et al. 2010a, 2011, Fay and Shi 2011). These results illustrate the complexity of concrete durability and suggest that there is more than one mechanism at work. More investigation is needed to explain the mechanisms that damage cementitious materials exposed to deicing chemicals (Farnam, 2015).

For comparison purposes concrete samples were fabricated and exposed to the combined effect of F/T cycles and eight types of deicers, including NaCl, KCl, KAc, KFm, MgCl₂, CaCl₂, CaAc₂, and CaFm₂, under well-controlled laboratory conditions; the results of which were compared with data collected from the field core samples reported in Chapter 4.

5.1 Materials and Methods

5.1.1 Deicing Capability Test of Various Deicers

The deicing capability of the eight types of deicers, including NaCl, KCl, KAc, KFm, MgCl₂, CaCl₂, CaAc₂, and CaFm₂, were evaluated based on the SHRP H-205.1 and H-205.2 test methods for solid and liquid deicing products. In this testing procedure, a 1/8-in. (3.175-mm) thick layer of ice is frozen in a flat Plexiglas[®] dish, and the surface is leveled by partial melting and refreezing with the dish on a level surface. The test specimen is placed in a temperature-regulated enclosure and allowed to equilibrate to the test temperature. The solid or liquid deicer is spread over the surface of the ice. At specified time intervals, melted ice or brine is decanted to the edge of the dish, removed, measured via a syringe, and returned to the test specimen. The normal elapsed time period for the test is 60 min. A minimum of four incremental time intervals is employed to obtain data on rates of ice melting.

5.1.2 Corrosion Resistance Tests of Metals Exposed to Various Deicers

Three types of metal coupons, including stainless steel, plain steel, and Galvanized steel, were used in this test. The coupons used were 1/2" (approximately 1.38 in. outer diameter, 0.56 in. inner diameter, and 0.11 in. thickness) flat steel washers with an approximate density of 7.85 grams per cubic centimeter. Three coupons are used in each chemical product solution, for the deionized water and sodium chloride (NaCl) control standards. Coupons must meet ASTM F 436, Type 1, with a Rockwell Hardness of C 38-45. Each coupon used in the test procedure must be subjected to SOP for accurate test results.

Please note that removal of incidental flash rusting prior to weighing is not necessary. Also, galvanized coupons are not allowed to be used even after removing the zinc with acid. Hot dipped galvanization creates a Fe-Zn metallurgical surface bond that changes the characteristics of the steel.

The outer diameter, inner diameter, and the thickness of each coupon are measured twice at 90 degrees from each initial reading. The average for each measurement is calculated. These averages are used to calculate the surface area of each coupon.

ASTM D 1193 Type II deionized water is used to prepare each solution, blank, and control standard. Reagent grade sodium chloride was used to prepare the salt standard. A 3% solution of NaCl was prepared by weight, using the reagent grade salt and deionized water (Weight/Volume). For liquid chemical products, three parts liquid chemical product (as received) is mixed with 97 parts deionized water to produce the test solution (Volume/Volume). If the chemical product is a dry product, then the 3% solution is made by weight (Weight/Volume).

The Corrosion Testing Machine (Ad-Tek, Inc.) was used to perform the corrosion tests. Approximately 275 milliliters (actual volume determined by the surface area of test coupons) of each solution as mixed is poured into a 500 milliliter Erlenmeyer flask. Each flask is equipped with a fitted rubber stopper that has a 3-4 millimeter diameter hole drilled through it to allow a line to run through the stopper. One end of the line is attached to a vertically actuated bar, and the other end of the line is attached to a plastic frame made to hold coupons inside the flask. Three prepared coupons are attached to each plastic frame. The vertically actuated bar is controlled by a digital timer that lowers the bar for 10 minutes then raises the bar up for 50 minutes, but keeps the coupons inside of the flask for the duration of the test. This allows the coupons to be exposed to the test solution 10 minutes of each hour. The corrosion test is run for 72 hours. The solution is not agitated during the corrosion test. Corrosion tests are conducted at room temperature.

The coupons were removed from the solution after 72 hours, and cleaned with running tap water to remove any loosely adherent corrosion products. The coupons were then placed in cleaning acid: concentrated hydrochloric acid (HCl) containing 50 grams/liter SnCl₂ (stannous

chloride) and 20 grams/liter SbCl_3 (antimony trichloride). The two salts are added to the HCl to stop the reaction of the HCl with the steel once the corrosion product is removed. After 15 minutes the coupons are removed from the cleaning acid and successively rinsed with tap water, deionized water, and finally placed onto a paper towel to allow for drying. After 24 hours of drying, each coupon is weighed to a constant weight to the ten-thousandth gram.

The weight loss of each coupon is determined by subtracting the final weight from the original weight. The corrosion rate for each coupon is expressed as millimeter penetration per year (MPY) by the following formula where the density for steel is 7.85 g/cm^3 :

$$\text{MPY} = \frac{534 \times [(\text{final weight (g)}) - (\text{initial weight (g)})]}{(\text{area (cm}^2\text{)}) \times (\text{duration (hrs)}) \times (\text{metal density (g/cm}^3\text{)})}$$

The final MPY value for each solution is determined by calculating an average of the three individual coupons. Average MPY from this point forward will be referred to as only MPY of the solution being tested. A standard deviation of 3 or lower on the MPY is typically acceptable.

5.1.3 Preparation of Concrete Specimens

The concrete mix design followed the standard ASTM C 672-91. An ASTM specification C150-07 Type I/II low-alkali Portland cement (Holcim-Trident Plant, Three Forks, MT) was used in this study. The fine aggregates used were clean, natural silica sand, classified as SP (i.e., sand Poorly Graded per the United Soil Classification System). The mix designs had a water-to-cement ratio (w/c) of 0.40. An air entraining agent was added to the water prior to mixing. The concrete was mixed per ASTM C192 standard. After sufficient mixing, the concrete mix was placed into polyvinyl chloride piping molds to form cylinders of D2"×H4" (D 51 mm × H 102 mm), D3"×H6" (D 76 mm × H 142 mm), or D4"×H8" (D 102 mm × H 203 mm) per ASTM C192 standard. Temperature and air test per ASTM C231 standard were conducted on the wet mix to ensure the quality of the mix. After mixing, the fresh mixture was cast into molds. In the first 24 hr of molding, the concrete specimens were placed on a rigid surface and stored at room temperature. Next, the specimens were de-molded and cured in a moist cure room at room temperature and relative humidity (RH) of 95% for 27 days. Once fully-cured, the concrete specimens were air-dried for 24 h at $23 \pm 1.7^\circ\text{C}$ (73.4°F), RH 45–55% and weighed, before being used for testing.

5.1.4 Freeze-thaw Cycling in the Presence of Deicers

The impacts of the deicers on concrete were assessed by conducting freeze-thaw (F/T) tests of concrete samples in the presence of diluted deicers (with concentration of 3 wt.%). The test evaluates the combined effects of deicers and freeze-thaw cycling on the structural integrity of specimens of poorly air-entrained concrete. The dosage of air entraining agent was MicroAir™ at 0.006% by weight of cement, designed to achieve less than 6% air content typically seen in air-

entrained concrete. Depending on the statistical design of the experiments, 3, 7 or 15 exposure cycles were used to simulate the temperature and wet/dry cycles experienced by field concrete in an accelerated manner. Each cycle consisted of 48 hours of fully immersing the concrete specimens in the diluted deicer solutions at $-27\pm 5^{\circ}\text{F}$, RH $50\pm 5\%$ followed by 24 hours of thawing and 12 hours of exposing the concrete specimens in dry air at room temperature ($73.4 \pm 3^{\circ}\text{F}$, RH $25\pm 5\%$). For the deicer exposure, each concrete specimen was placed in a Ziploc bag containing sufficient deicer to avoid water evaporation. The average freezing rate was approximately $0.05^{\circ}\text{C}/\text{min}$ during the first 5 hours and then approximately $0.05^{\circ}\text{C}/\text{min}$ during the subsequent 25 hours. The average warming rate was observed to be approximately $0.01^{\circ}\text{C}/\text{min}$. After exposure cycles, the test specimens were individually rinsed under running tap water and hand-crumbed to remove any scaled-off material during the freeze/thaw cycling. The specimens were air-dried for 24 h at $23 \pm 1.7^{\circ}\text{C}$ (73.4°F), RH 45–55%. After drying, test specimens were weighed and the final weights recorded.

5.1.5 Testing Mechanical Properties of Concrete Specimens

Subsequent to the F/T and wet/dry (W/D cycling), the concrete specimens were tested for weight loss as well as compressive strength and splitting tensile strength. The compressive strength of the concrete cylinders was determined using ASTM C39 (Standard Test Method for Compressive Strength of Cylindrical Concrete Specimens). The splitting tensile strength of the concrete cylinders was determined using ASTM C496 (Standard Test Method for Splitting Tensile Strength of Cylindrical Concrete Specimens). To minimize the potential variables (e.g., operator and time of the day) on the measured results, the order of preparing and testing the concrete specimens was randomized.

5.1.6 Microscopic Characterization

The fracture surface morphology of lab prepared samples was performed on an FEI-Quanta 200F scanning electron microscope. SEM was conducted under an accelerating voltage of typically 20 kV. SEM was coupled with an energy-dispersive X-ray spectroscopy (EDS) analyzer. For EDS, a micro-analytical unit was employed to detect the small variations in trace element content, using an accelerating voltage of typically 15-20 kV and a scan time of 60 seconds per sampling area. The X-ray diffraction pattern (XRD) was obtained on a Rigaku D/max-rA X-ray diffractometer with Cu $K\alpha$ radiation ($\lambda = 1.5406 \text{ \AA}$).

The white precipitates, which will be demonstrated in details in the later section, were filtered, then put in an oven of 230°F (110°C) for 24 h to remove water. Once dry, the white precipitates were dispersed in ethanol by ultrasonic treatment and then a small drop of the dispersions was transferred to a holey carbon film supported on a copper grid for the transmission

electron microscopy (TEM) observation. The TEM images were taken out on a Phillips Tecnai 20 microscopy with an accelerating voltage of 200 kV.

5.2 Results and Discussion

5.2.1 Deicing Capability of Various Deicers

Table 5- 1 lists the volume of the melted ice exposed to various deicer solutions at different time periods. As can be seen in this table, with the increasing freezing time (from 10 min to 60 min) at -25 °F (-32 °C), CaCl₂ has the highest de-icing capability, with the volume of melted solution increasing from 2.0 to 3.2 mL, while MgCl₂ has the smallest amount of melted solution at f 0.2 mL after 60 minutes.

Table 5- 1 Lab testing results of the deicing capabilities of various deicers

Time \ Deicers	NaCl	KCl	KAc	KFm	MgCl ₂	CaCl ₂	CaAc ₂	CaFm ₂
10 min	0.0	0.2	0.2	0.2	0.0	2.0	1.8	0.0
20 min	0.2	0.4	0.4	0.6	0.0	3.0	2.0	0.0
30 min	0.3	0.8	0.9	0.8	0.0	3.1	2.1	0.2
45 min	0.4	1.0	1.3	1.0	0.0	3.2	2.2	0.4
60 min	0.8	1.2	1.4	1.4	0.2	3.2	2.3	0.4

5.2.2 The corrosion rate of metals due to exposure to deicers

Figure 5- 1 shows the corrosion rates of stainless steel due to exposure to various deicers. As can be seen in this figure, the corrosion rates of the stainless steel with exposure to various deicers are not very high; in the range of 0.0±0.2, with the exception of CaFm₂, which had a relatively high corrosion rate of 1.12 MPY.

Figure 5- 2 shows the corrosion rates of plain steel with exposure to various deicers. As can be seen in this figure, unlike the stainless steel, the corrosion rates of the plain steel with exposure to various deicers are considerably different. All chloride salts have relatively high corrosion rates ranging from 30 to 48 MPY, while KAc and CaAc₂ have relatively low corrosion rates about -2.0 MPY. CaFm₂ keeps a relatively high corrosion rate about 30 MPY.

Figure 5- 3 shows the corrosion rates of galvanized steel with exposure to various deicers. As can be seen in this table, the corrosion rates of the galvanized steel with exposure to various deicers are all relatively high, ranging from 15 to 47 MPY.

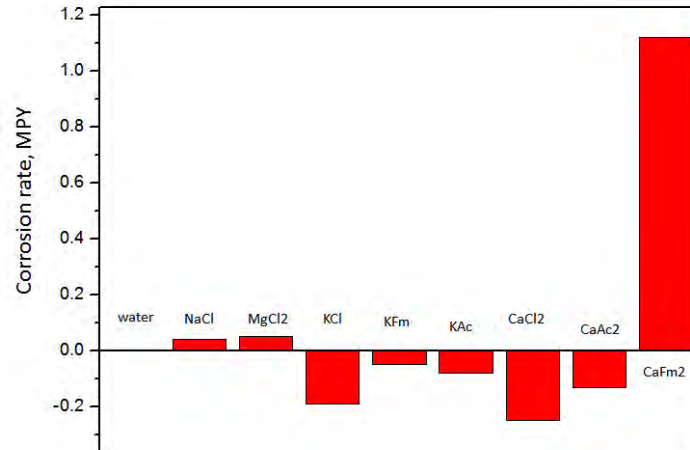


Figure 5- 1 The corrosion rates of stainless steel with exposure to various deicers.

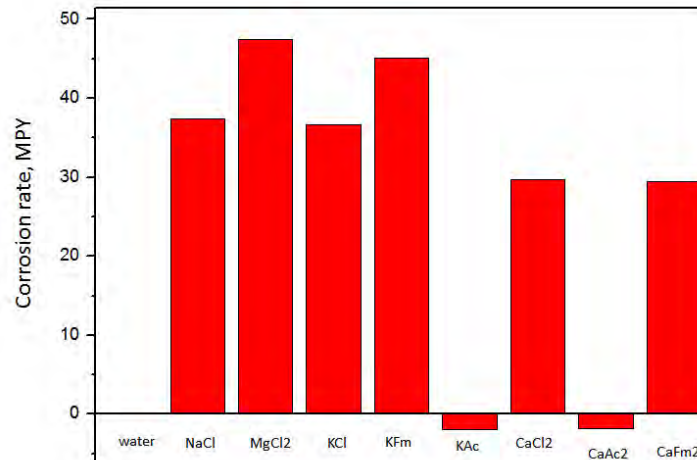


Figure 5- 2 The corrosion rates of plain steel with exposure to various deicers.

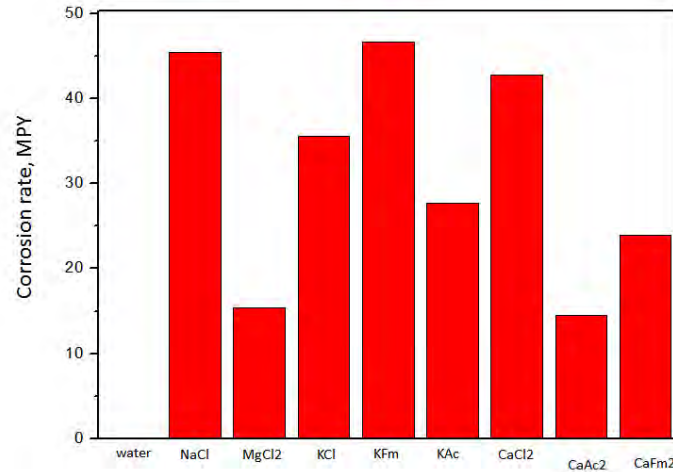
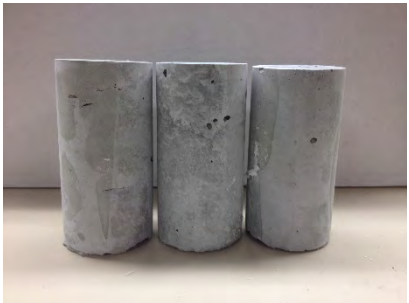







Figure 5- 3 The corrosion rates of galvanized steel with exposure to various deicers.

5.2.3 Mass Loss of Concrete Samples Exposed to Deicer Solutions and F/T Cycling

Figure 5- 4 illustrates the damage caused to laboratory-fabricated concrete cylinders exposed to the eight types of deicer solutions with concentration of 3 wt.% after 3, 7, and 15 F/T cycles, respectively. As can be seen in this figure, all concrete samples exposed to alkali based deicer solutions (KCl, NaCl, KAc, and KFm) exhibit severe surface distress after 7 F/T cycles, while the samples exposed to alkali earth based deicer solutions (CaCl₂, MgCl₂, CaAc₂ and CaFm₂) show little surface distress.

Deicers	3 F/T cycles	7 F/T cycles	15 F/T cycles
Water			
MgCl ₂			

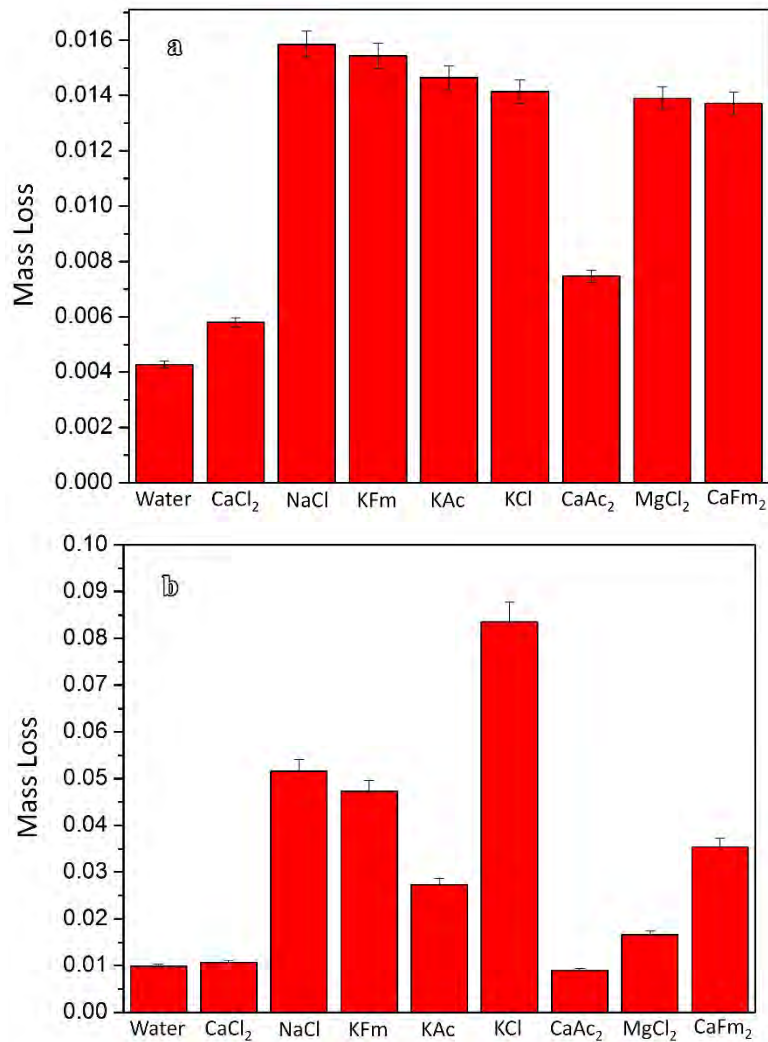
CaCl ₂			
CaAc ₂			
CaFm ₂			

NaCl			
KCl			
KAc			



Figure 5- 4 The external morphologies of laboratory-fabricated concrete cylinders exposed to various deicer solutions after 3, 7, and 15 F/T and W/D cycles.

Figure 5- 5 shows the mass loss of concrete samples exposed to F/T and W/D cycles in 3 wt.% deicer solutions. As can be seen in this figure, the mass loss of the concrete samples is not obvious after 3 cycles. The mass loss for KCl, CaCl₂, NaCl, KAc, KFm, CaAc₂, CaFm₂, and MgCl₂ reaches 0.014, 0.006, 0.016, 0.015, 0.015, 0.007, 0.014, and 0.016, respectively. However, after 7 F/T and W/D cycles, the mass loss of concrete samples becomes more variable (Figure 5- 5b). KCl shows the highest mass loss with value of 0.08, and CaCl₂ has the lowest mass loss with value of 0.01. NaCl, KAc, KFm, CaAc₂, CaFm₂, MgCl₂ have mass loss of 0.052, 0.027, 0.047, 0.008, 0.04, and 0.016, respectively. After 15 F/T and W/D cycles, the mass loss of the concrete samples shows a dramatic difference (Figure 5- 5c). KCl shows the highest mass loss with value of 0.106, and CaCl₂ has the lowest with value of 0.01. NaCl, KAc, KFm, CaAc₂, CaFm₂, MgCl₂ have mass loss of 0.063, 0.055, 0.064, 0.012, 0.053, and 0.012, respectively. The details of the mass loss of concrete samples exposed to various deicers along with F/T cycles are listed in Table 5- 2.



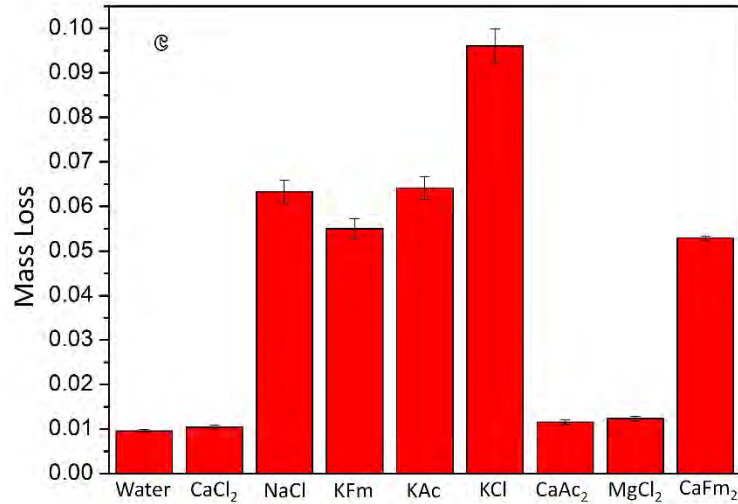


Figure 5- 5 The mass loss of concrete samples exposed to F/T and W/D cycles in various deicer solutions a) after 3 F/T cycles, b) after 7 F/T cycles, and c) after 15 F/T cycles.

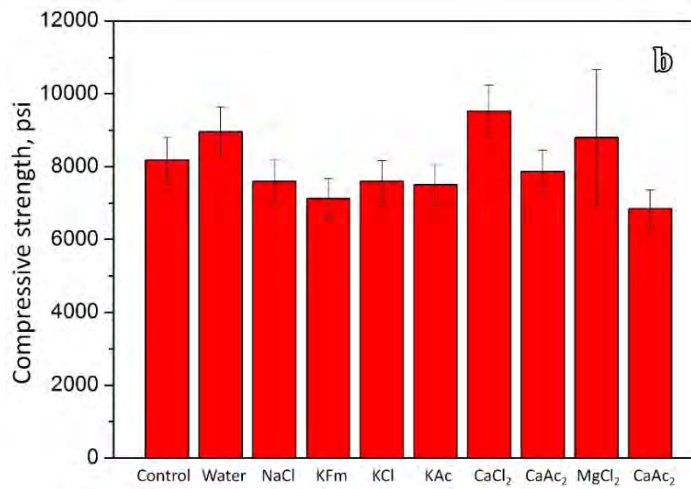
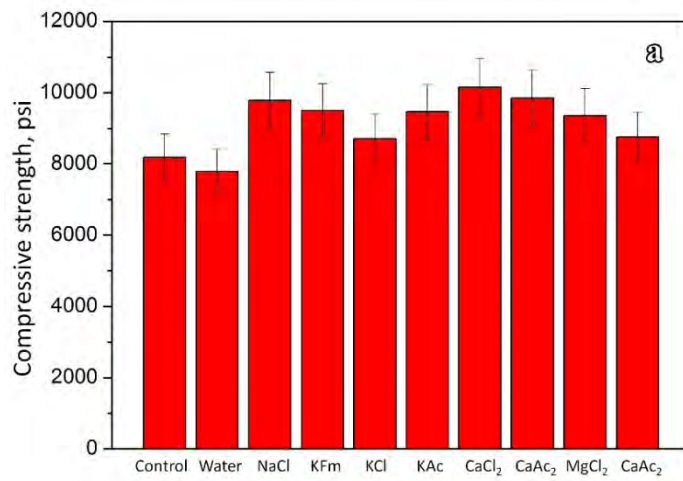
Table 5- 2 Mass loss of concrete exposed to various deicers along with F/T cycles

	Water	NaCl	KCl	CaCl ₂	MgCl ₂	KAc	KFm	CaAc ₂	CaFm ₂
3 cycles	0.0042	0.016	0.014	0.006	0.016	0.015	0.015	0.007	0.014
7 cycles	0.01	0.052	0.08	0.01	0.016	0.027	0.047	0.008	0.04
15 cycles	0.01	0.063	0.106	0.01	0.012	0.055	0.064	0.012	0.053

5.2.4 Mechanical Properties

Figure 5-6 shows the compressive strength of concrete samples exposed to 3, 7, and 15 F/T and W/D cycles in 3 wt.% deicer solutions. The compressive strength loss of the concrete samples exposed to deicer solutions with 3 F/T and W/D cycles are not considerably different, which agrees well with the limited amount of damage observed in Figure 5- 6a). The compressive strength of concrete samples exposed to water, KCl, CaCl₂, NaCl, KAc, KFm, CaAc₂, CaFm₂, and MgCl₂, were 7788, 8703, 10149, 9784, 9170, 9177, 9527, 9645, and 9686 psi, respectively. After 7 F/T and W/D cycles, the compressive strength of the concrete samples starts to show slightly different performances. The compressive strength of concrete samples exposed to water, KCl, CaCl₂, NaCl, KAc, KFm, CaAc₂, CaFm₂, and MgCl₂ were 8957, 7590, 9516, 7595, 7495, 7132, 7861, 6844, and 8802, respectively. After 15 F/T and W/D cycles, the compressive strength of the concrete samples shows considerably different values. The compressive strength of concrete samples exposed to KCl sharply decreased, and KAc shows similar results. The compressive strength of concrete samples exposed to KCl is only 3439 psi, and those exposed to KAc is 5866 psi. KFm, CaAc₂,

NaCl, CaFm₂, MgCl₂, CaCl₂, and water were 6059, 6270, 7114, 8298, 9591, 9449, and 8479, respectively. The details of the compressive strengths of concrete samples exposed to various deicers along with F/T cycles are listed in Table 5- 3.



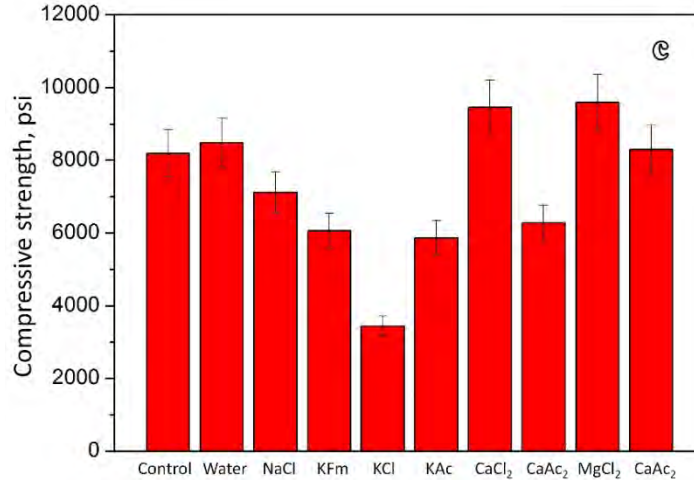


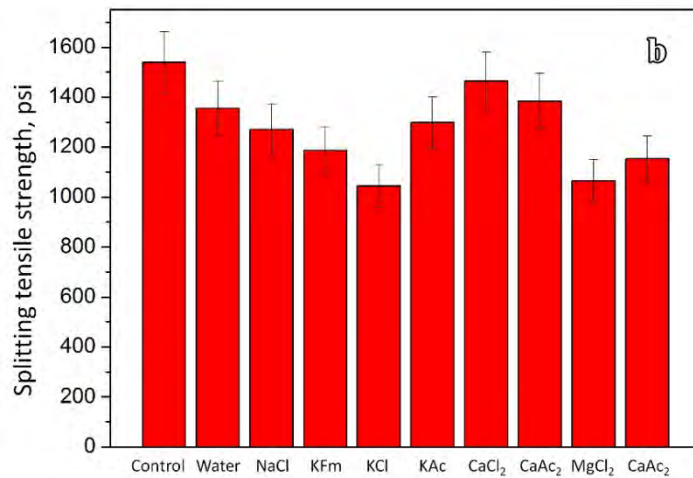
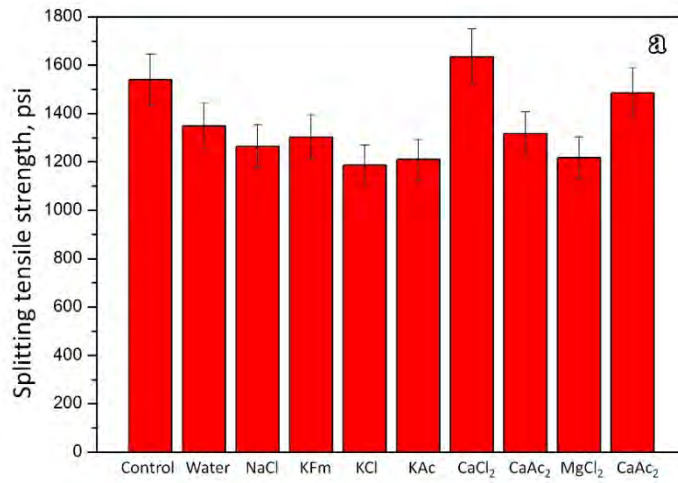
Figure 5- 6 Compressive strength of concrete samples exposed to various deicers with a) 3, b) 7, and c) 15 F/T cycles.

Table 5- 3 Compressive strength (psi) of concrete samples exposed to various deicer solutions along with F/T cycles

	Water	NaCl	KCl	CaCl ₂	MgCl ₂	KAc	KFm	CaAc ₂	CaFm ₂
3 cycles	7788	9784	8703	10149	9686	9170	9177	9527	9645
7 cycles	8957	7595	7590	9516	8802	7495	7132	7861	6844
15 cycles	8479	7114	3439	9449	9591	5866	6059	6270	8298

Figure 5- 7 shows the splitting strength of concrete samples exposed to 3, 7, and 15 F/T and W/D cycles in 3 wt.% deicer solutions. As demonstrated in Figure 5- 7 a), similar to the compressive strength performances, the splitting tensile strengths of the concrete samples exposed to deicer solutions with 3 F/T and W/D cycles are not considerably different. The splitting tensile strengths of concrete samples exposed to water, KCl, CaCl₂, NaCl, KAc, KFm, CaAc₂, CaFm₂, and MgCl₂ were 1348, 1186, 1635, 1264, 1210, 1303, 1316, 1486, and 1217 psi, respectively. After 7 F/T and W/D cycles, the splitting tensile strengths of the concrete samples start to show obvious differences. The splitting tensile strength of concrete samples exposed to water for KCl, CaCl₂, NaCl, KAc, KFm, CaAc₂, CaFm₂, and MgCl₂ are 1354, 1044, 1463, 1270, 1298, 1187, 1384, 1153, and 1064 psi, respectively. After 15 F/T and W/D cycles, the splitting tensile strengths of the concrete samples show considerably different values. The splitting tensile strength of concrete samples exposed to MgCl₂ sharply decreased, while KCl and KAc show a large reduction in splitting tensile strength. The splitting tensile strength of concrete samples exposed to MgCl₂ is only 708 psi, and those exposed to KCl and KAc are 984 and 1193 psi. The splitting tensile strength

of concrete samples exposed to KFm, CaAc₂, NaCl, CaFm₂, CaCl₂, and water are 1221, 1243, 1180, 1299, 1479, and 1211 psi, respectively. The details of the compressive strengths of concrete samples exposed to various deicers along with F/T cycles are listed in Table 5- 4.



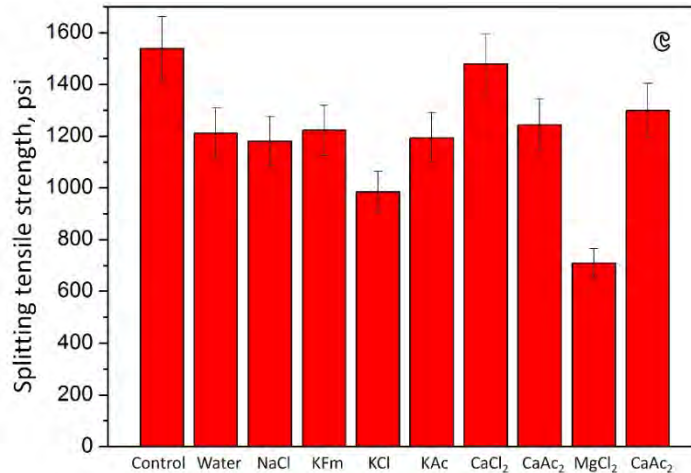


Figure 5- 7 Splitting tensile strength of concrete samples exposed to various deicers with a) 3, b) 7, and c) 15 F/T cycles

Table 5- 4 Splitting tensile strength (psi) of concrete samples exposed to various deicer solutions along with F/T cycles

	Water	NaCl	KCl	CaCl ₂	MgCl ₂	KAc	KFm	CaAc ₂	CaFm ₂
3 cycles	1348	1264	1186	1635	1217	1210	1303	1316	1486
7 cycles	1354	1270	1044	1463	1064	1298	1187	1384	1153
15 cycles	1211	1180	984	1479	708	1193	1221	1243	1299

5.3 Microstructure Analysis

5.3.1 SEM Analysis

Figure 5- 8 shows the low and high magnification SEM images of the concrete samples after 15 F/T and W/D cycles in water. As can be seen in this figure, the C-S-H phase is well maintained and no crystal precipitates can be detected from either the low nor from the high magnification images.

Figure 5- 9 shows the low and high magnification SEM images of the concrete samples after 15 F/T and W/D cycles in NaCl. Unlike the microstructure of the samples in water, the fracture surface of the NaCl sample is not flat and shows many needle shaped precipitates that are nanometers in diameter. These nano sized needle shape precipitates are randomly distributed in the hydration products without any orientations.

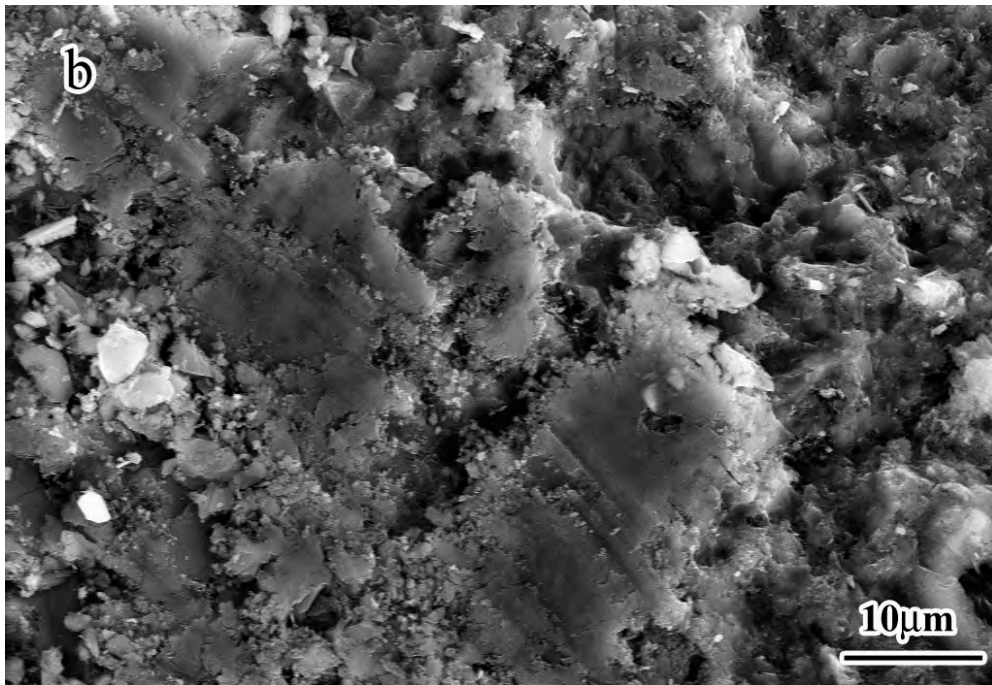
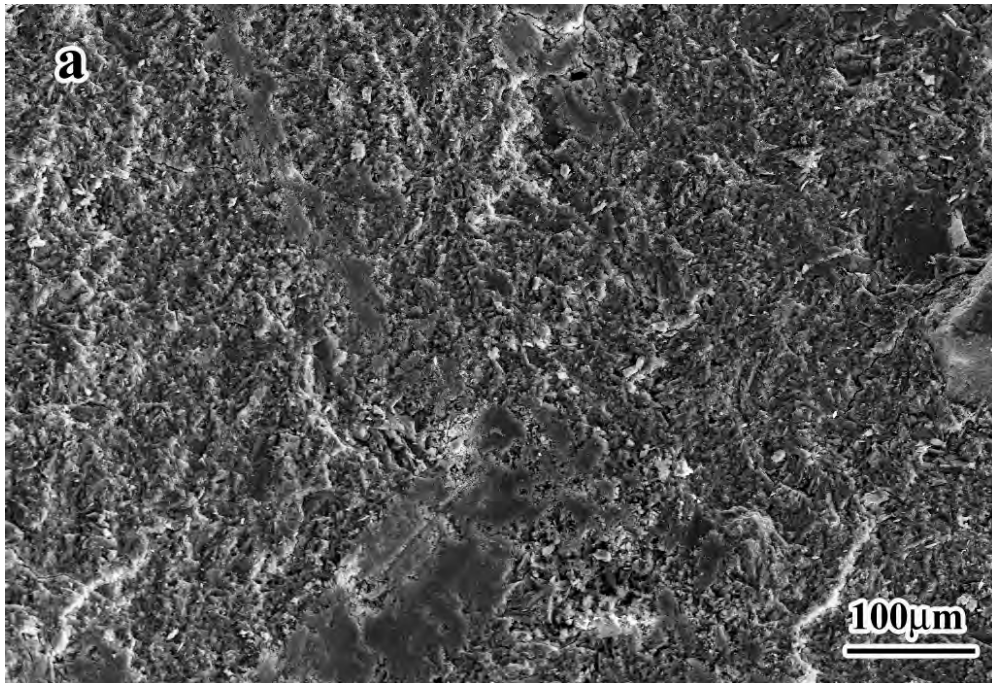


Figure 5- 8 SEM images of the concrete samples after 15 F/T and W/D cycles in water with a) low and b) high magnification.

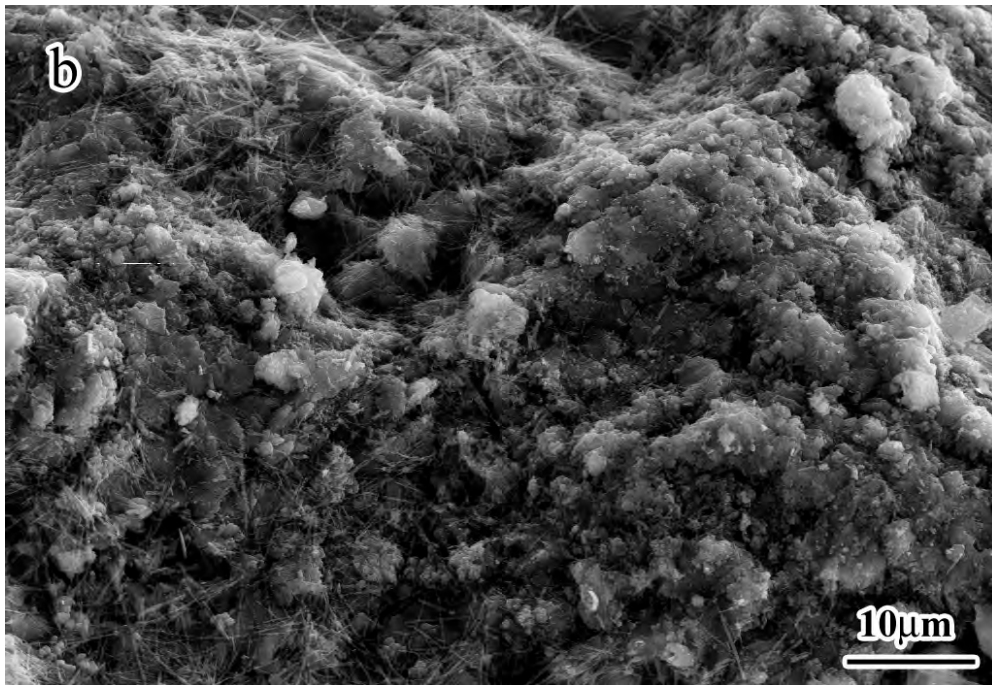
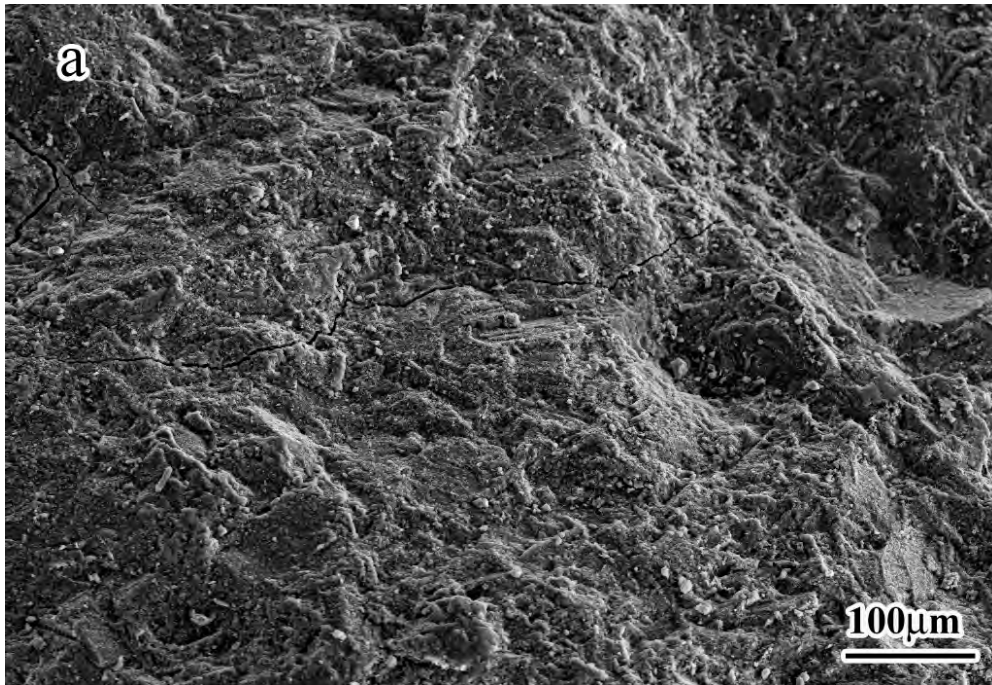


Figure 5- 9 SEM images of the concrete samples after 15 F/T and W/D cycles in NaCl solution with a) low and b) high magnification.

As demonstrated in Figure 5- 10 and Figure 5- 11, the concrete samples exposed to $MgCl_2$ solution are composed of different microstructures than those exposed to water and $NaCl$. One typical microstructure observed in the $MgCl_2$ exposed samples is the large quantity of plate-like precipitates, which are randomly distributed in the cement paste matrix, shown as Figure 5- 10 a). As shown in the high magnification image Figure 5- 10 b), the precipitates are mostly composed of plate-like crystals without specific orientations. Another typical microstructure, demonstrated in Figure 5- 11, is the highly porous microstructure and absence of high density cement hydrates. It can be seen from the high magnification image that the microstructure of the high density C-S-H phase was no longer a dense lamellar structure but a penetrable porous structure. This deleterious microstructure corresponds very well with the low splitting tensile strength of the samples.

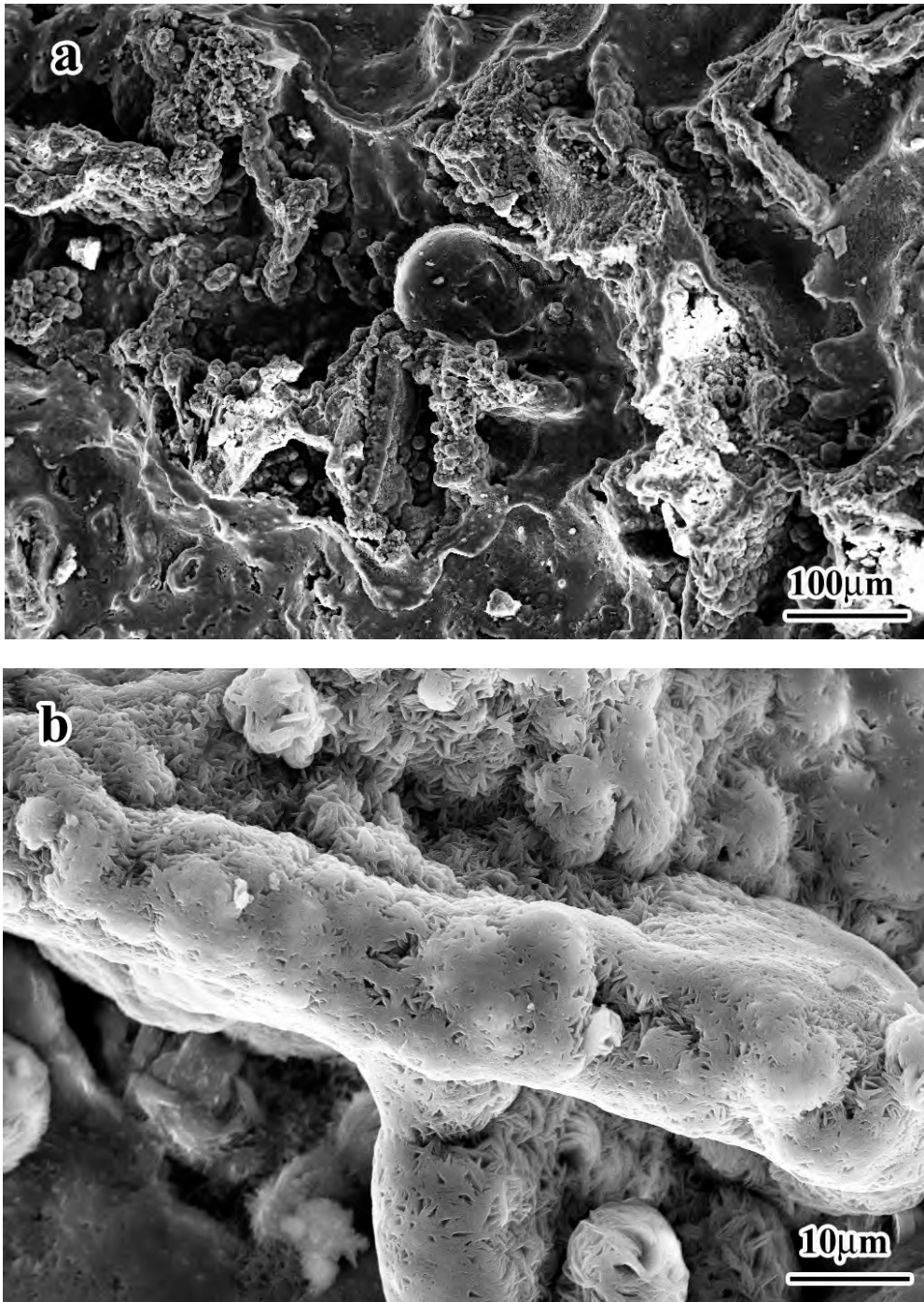


Figure 5- 10 The SEM images of the concrete samples after 15 F/T and W/D cycles in MgCl₂ solution with a) low and b) high magnification.

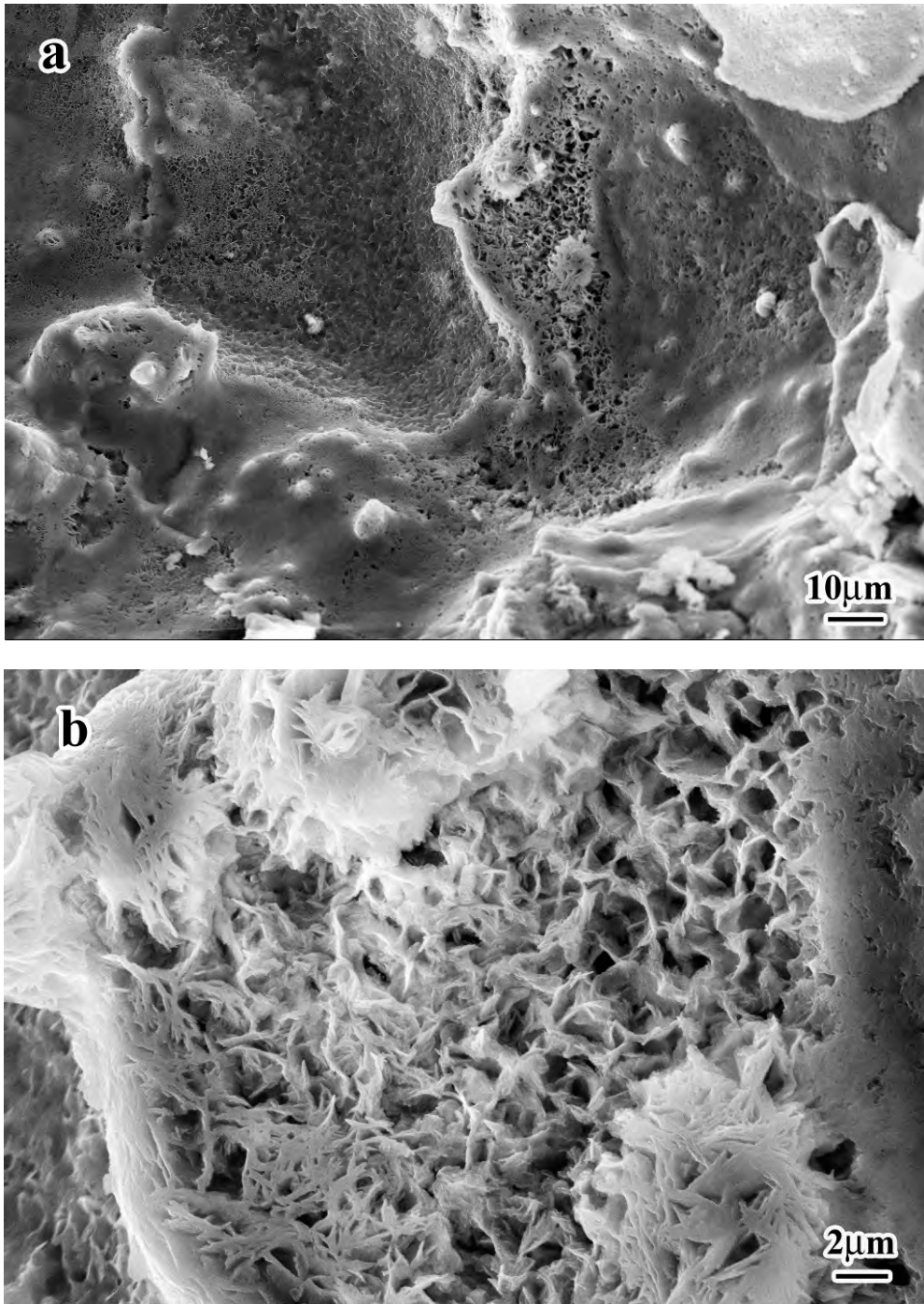


Figure 5- 11 The SEM images of the concrete samples after 15 F/T and W/D cycles in MgCl₂ solution with a) low and b) high magnification.

Figure 5- 12 shows the low and high magnification SEM images of the concrete samples after 15 F/T and W/D cycles in KFm solution. Similar to those samples with exposure to $MgCl_2$ solution, the deterioration of the high density C-S-H binder phase can be detected. In addition, as demonstrated in the high magnification image (Figure 5- 12 b), many flower petal shaped structures have been formed. The layered structure of the C-S-H binder phase has deteriorated and a highly porous structure has formed. Some sticky phase can be observed around the pores and embedded in the petal shaped phases (shown as the red areas in Figure 5- 12 b).

Figure 5- 13 shows the microstructure of the sample after 15 F/T and W/D cycles with exposure to KAc solution. Similar to the microstructure of the samples with exposure to $MgCl_2$ and NaCl, the fracture surfaces are not smooth, and small sized bumpy phase can be detected on the fracture surfaces. However, different from the microstructures of the samples exposed to water, NaCl, and $MgCl_2$, the KAc samples have rod shaped crystals, rather than plate-like precipitates, which can be observed at the fracture surface of the cement paste. From the high magnification observation shown in Figure 5- 13 b) it can be observed that the precipitate phases are composed of needle-shaped crystal bundles about 1 μm in diameter. Formation of these precipitates can lead to the volume expansion of the concrete and thus result in a reduction of the mechanical strength. The precipitation process and the chemical analysis of these precipitates should be further investigated in future studies.

Different from alkali based deicers or $MgCl_2$, the effects of the Ca based deicers on the microstructure show that most of the C-S-H binder phase remains, as demonstrated in Figure 5- 14 and Figure 5-15, which are the fracture surface images of concrete samples exposed to $CaCl_2$ and $CaAc_2$ solutions, respectively. Although the increasing porosity can be found in these two samples (as demonstrated in the low magnification images (Figure 5-14 a) and Figure 5-15 a)), the layered and flat C-S-H phase are the main components of the cement paste (as shown in the high magnification images (Figure 5-14 b and Figure 5-15 b)).

Similar to the microstructure of the sample exposed to NaCl solution, the fracture surface of the sample exposed to $CaFm_2$ shows a bumpy morphology (Figure 5-16). Many small sized precipitates are embedded in the binder phase. As demonstrated in the high magnification image (Figure 5-16 b), many needle shaped precipitates with diameters of nanometers can be clearly observed. These nano sized needle shape precipitates are randomly distributed in the hydration products without any orientations.

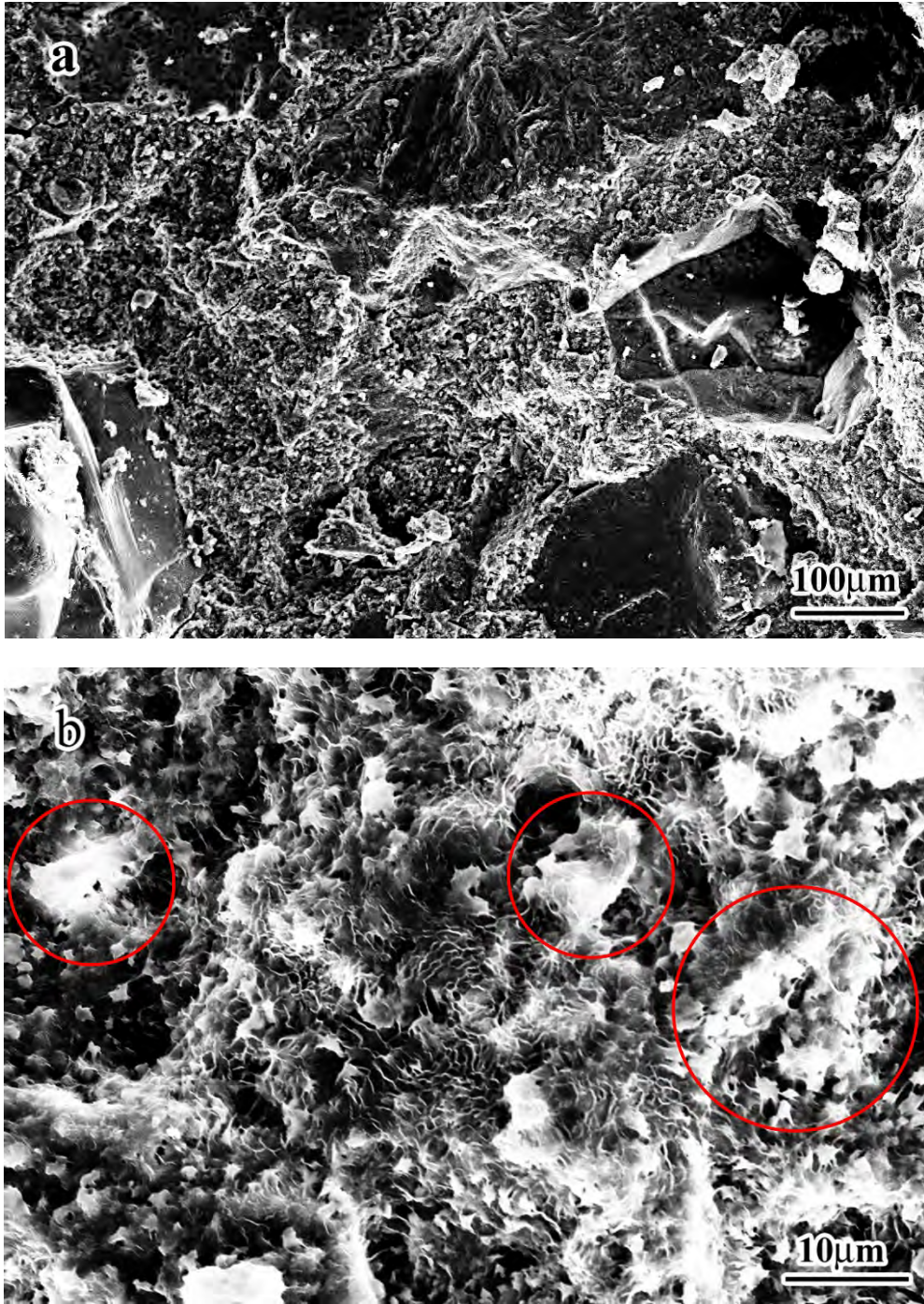


Figure 5- 12 The SEM images of the concrete samples after 15 F/T and W/D cycles in KFm solution with a) low and b) high magnification.

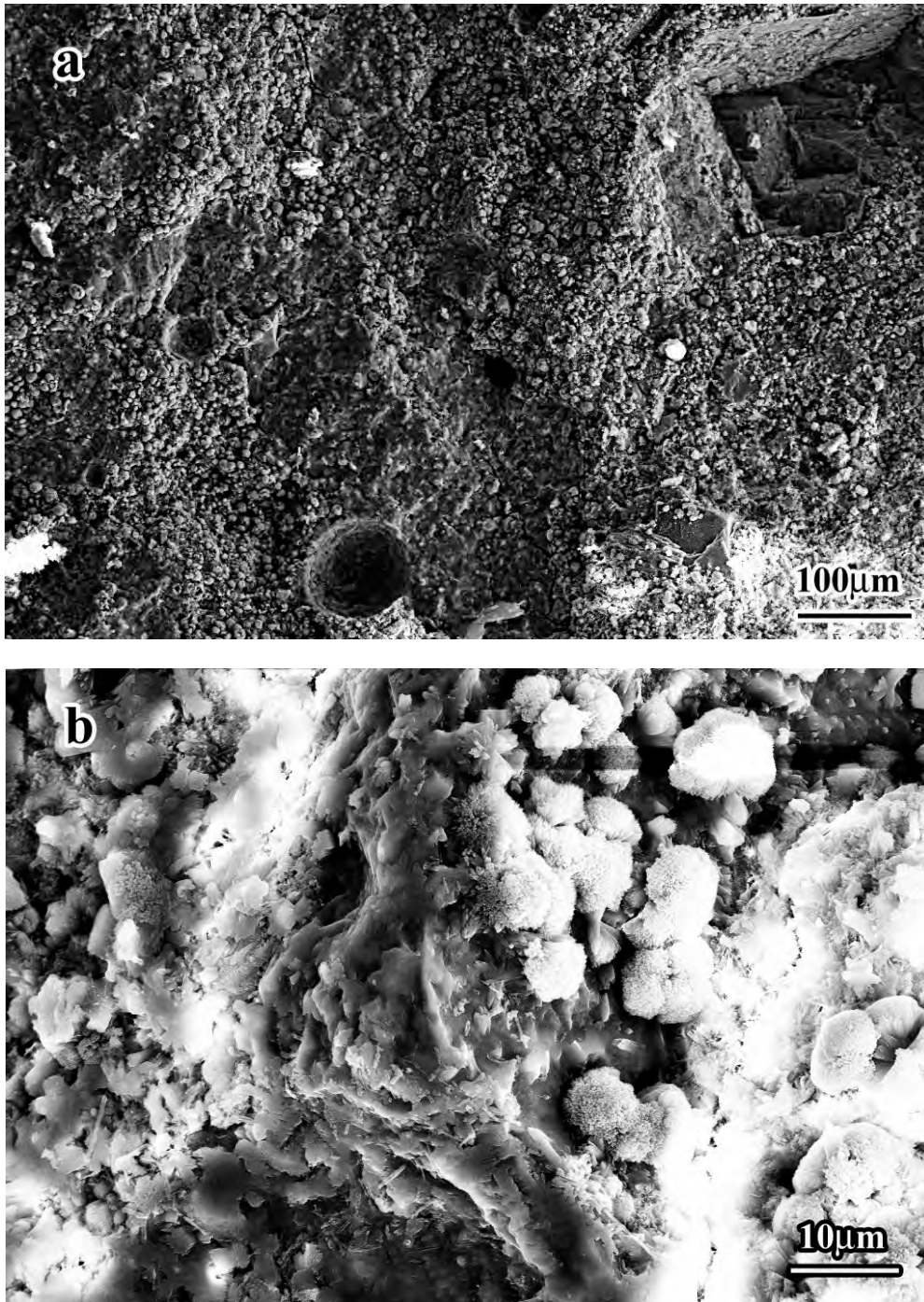


Figure 5- 13 The SEM images of the concrete samples after 15 F/T and W/D cycles in KAc solution with a) low and b) high magnification.

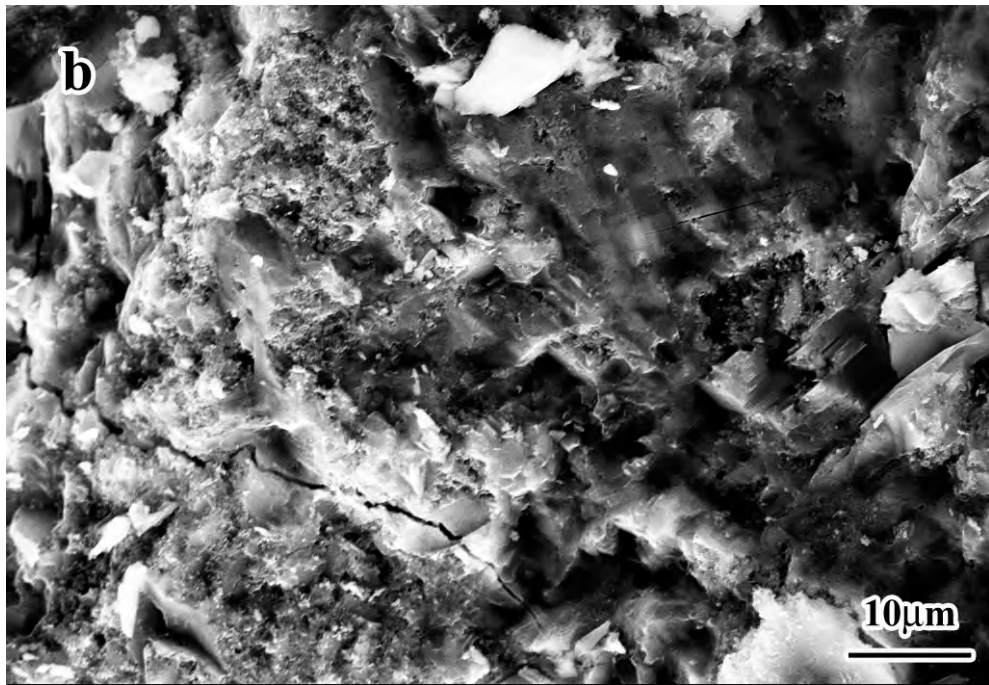
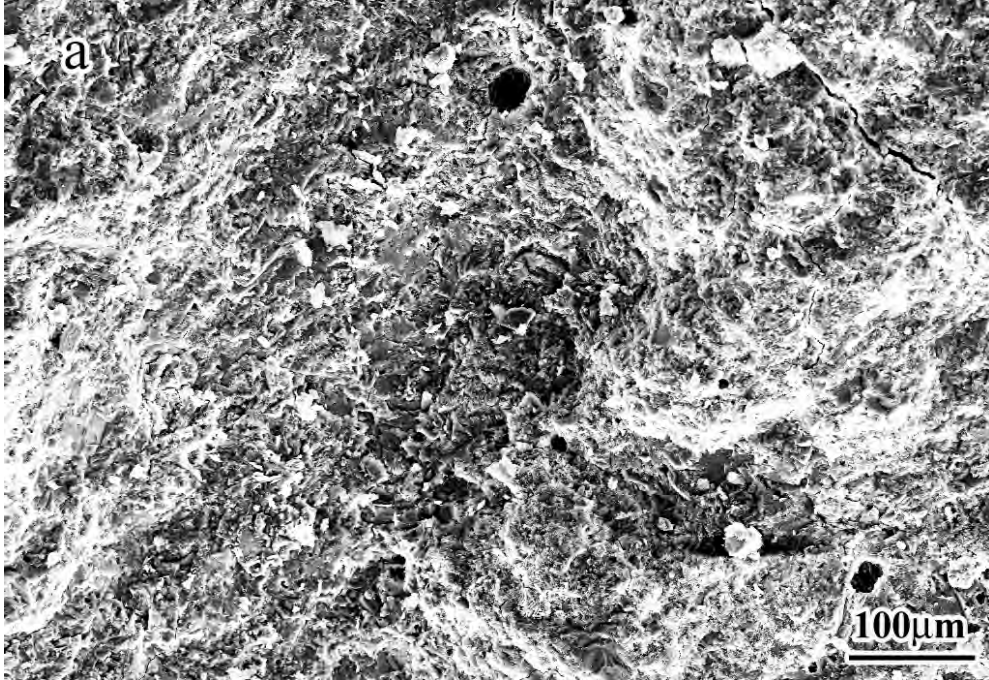


Figure 5- 14 The SEM images of the concrete samples after 15 F/T and W/D cycles in CaCl₂ solution.

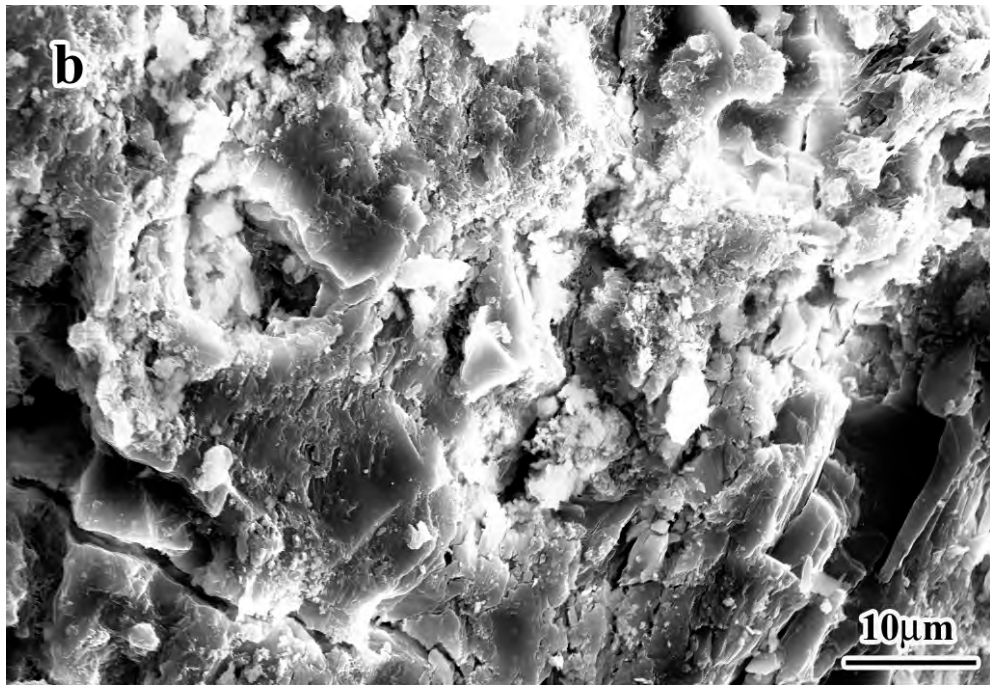
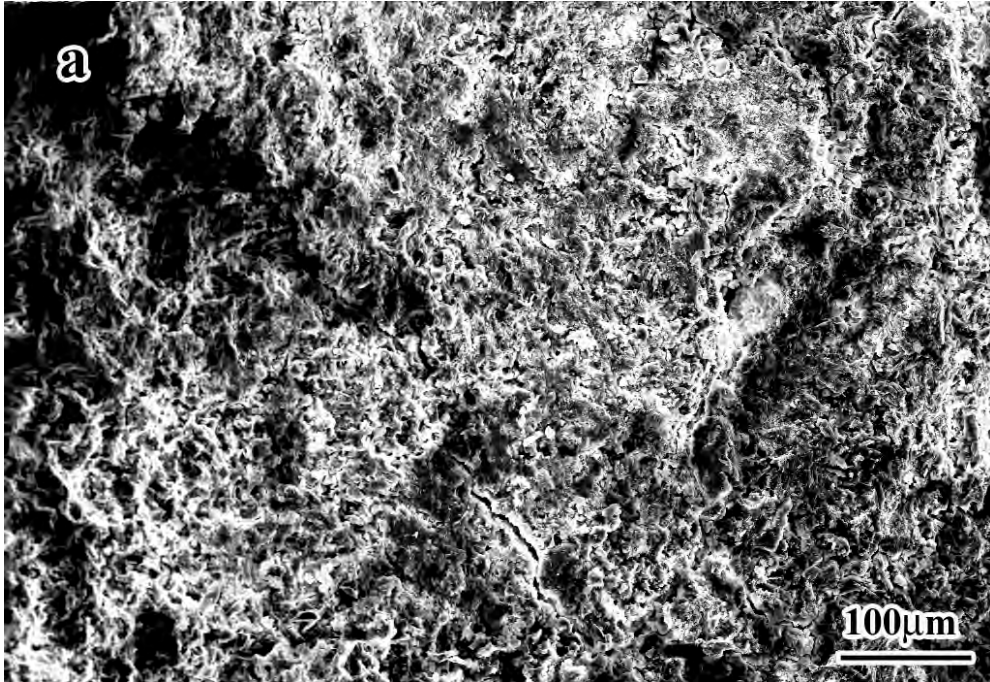


Figure 5- 15 The SEM images of the concrete samples after 15 F/T and W/D cycles in CaAc2 solution with a) low and b) high magnification.

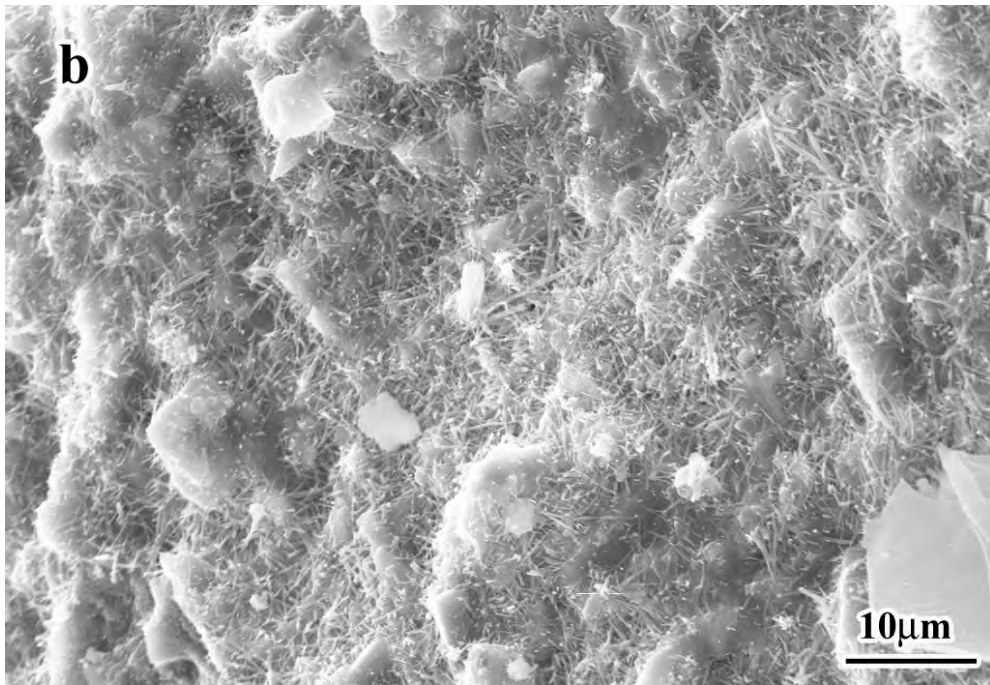
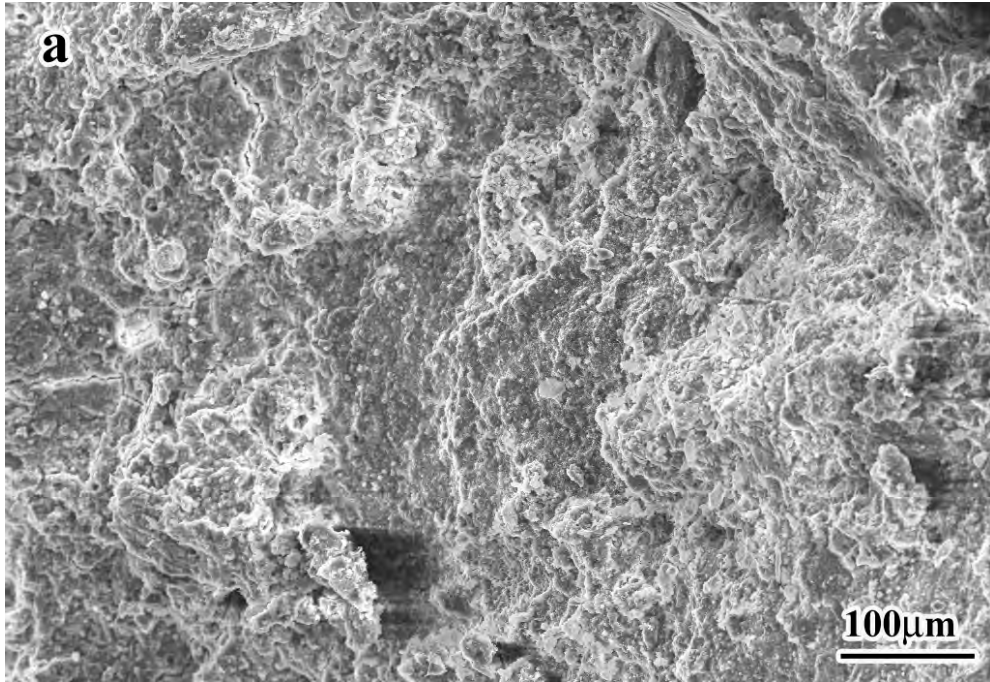


Figure 5- 16 The SEM images of the concrete samples after 15 F/T and W/D cycles in CaFm2 solution with a) low and b) high magnification.

5.3.2 SEM/EDS Analysis

Figure 5-17 to Figure 5-26 present the SEM/EDS analysis results of the concrete samples with exposure to 15 F/T and W/D cycles along with water and deicer solutions of NaCl, MgCl₂, KAc, KFm, CaCl₂, CaAc₂, and CaFm₂, respectively. Figure 5-17 shows the SEM/EDS results for the water sample that experienced 15 F/T cycles. It can be seen from Figure 5-17 b), which shows the elements distribution corresponding to the fracture surface image shown in Figure 5-17 a), that the Ca content is about 15 at.% and Si content about 3 at.%. Not surprisingly, no impurity elements can be detected. The elements distribution results corresponding to the low and high magnification fracture surface image are shown in Figure 5-18 and Figure 5-19 for the NaCl sample that experienced 15 F/T cycles. As demonstrated in these figures, the Ca content is about 12 at.%, which is considerably lower than the samples exposed to water. Furthermore, large amounts of Na, about 1 at.%, and Cl, about 0.3 at.%, can be detected in the nano sized needle shaped precipitates, as shown in Figure 5-19.

Figure 5-20, Figure 5-21, and Figure 5-22 present the SEM/EDS analysis results of samples exposed to MgCl₂ solution for 15 F/T cycles. In this sample, the Mg content was as high as 12 at.% corresponding to the two typical fracture surface images. In addition, as can be seen from the high magnification SEM/EDS results, the plate like precipitates are composed of high Mg and Cl, about 22 at.% and 0.7 at.%, respectively. The Ca and Si content is as low as 1 at.% and 0.1 at.%, respectively. The results strongly support the assumption that the reaction occurs between the Mg and the C-S-H phase.

Figure 5-23 to Figure 5-26 show the low and high magnification SEM/EDS results of the concrete samples with exposure to KAc and KFm after 15 F/T cycles, respectively. As can be seen from the low magnification EDS results, about 0.3 at.% K can be detected in the samples with exposure to both KAc and KFm solutions. The Ca content, however, is different in these two samples. The sample exposed to KAc solution has a higher Ca content than the one exposed to KFm solution, which are 12.3 at.% and 8.6 at.%, respectively. The high magnification SEM/EDS results of the crystal bundles show that these bundles are composed mainly from Ca, Si, and O (Figure 5-24 and Figure 5-26). More investigation is necessary to further demonstrate the details of these crystals.

Figure 5-27 to Figure 5- 29 present the SEM/EDS analysis results of Ca based deicers, including CaCl₂, CaAc₂, and CaFm₂. As demonstrated in Figure 5-27 and Figure 5-28, the Ca content is well retained in the samples exposed to CaCl₂ and CaAc₂ solution with a value of about 14 at.%, which is similar to the samples exposed to water. Not surprisingly, small amounts of Cl can be detected in the sample with exposure to CaCl₂, with a value of 0.13 at.%. The SEM/EDS results of the sample exposed to CaFm₂, however, show surprisingly less Ca, as shown in Figure 5-29. The high magnification SEM/EDS results of the sample exposed to CaFm₂, as shown in

Figure 5- 29, demonstrate that the nano-sized needle shaped precipitates are composed mainly from Ca and Si. The reaction mechanism is worthy of further systematic investigation.

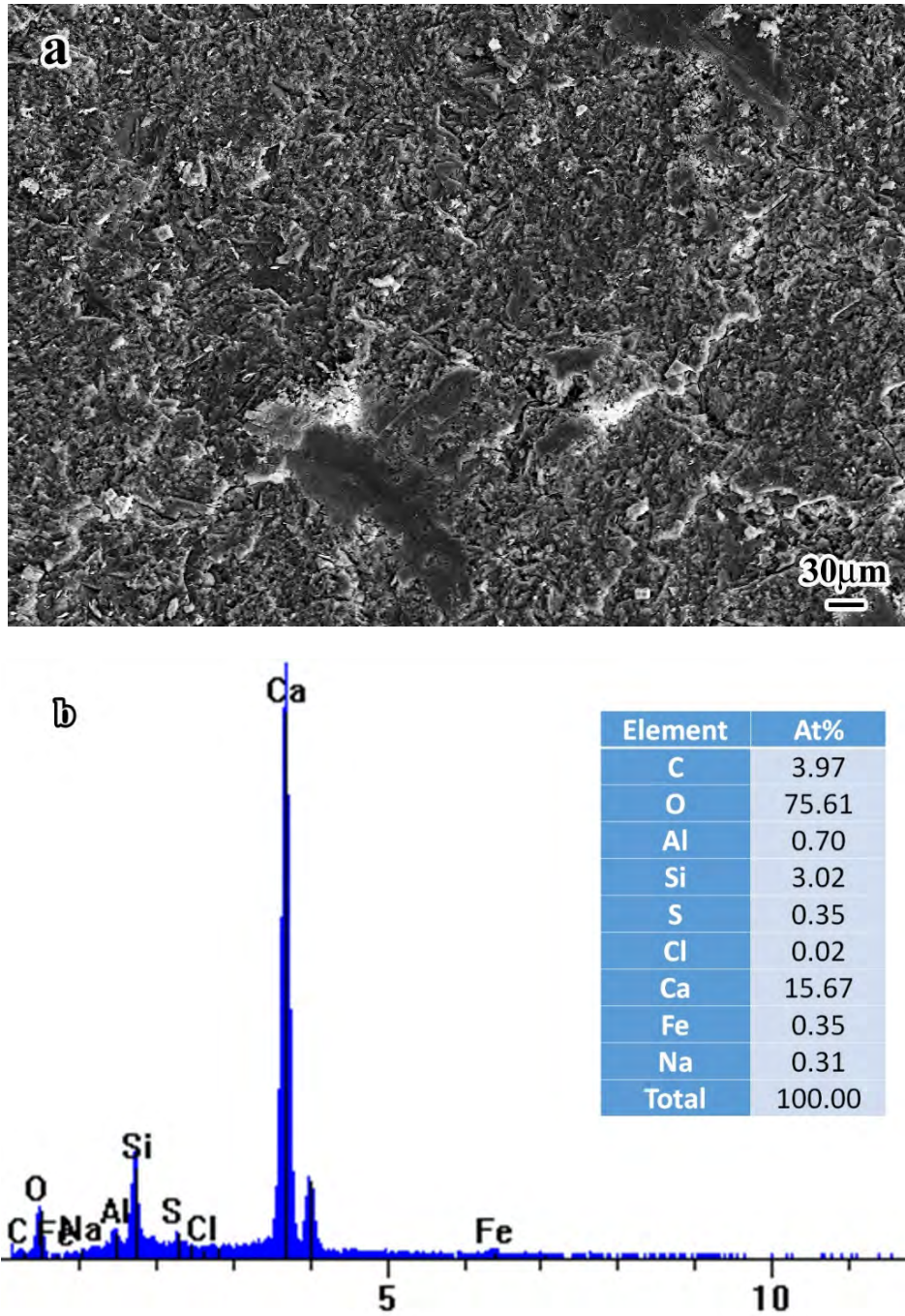


Figure 5- 17 The SEM/EDS result of the concrete samples after 15 F/T and W/D cycles in water with a) SEM image and b) corresponding EDS element distribution results.

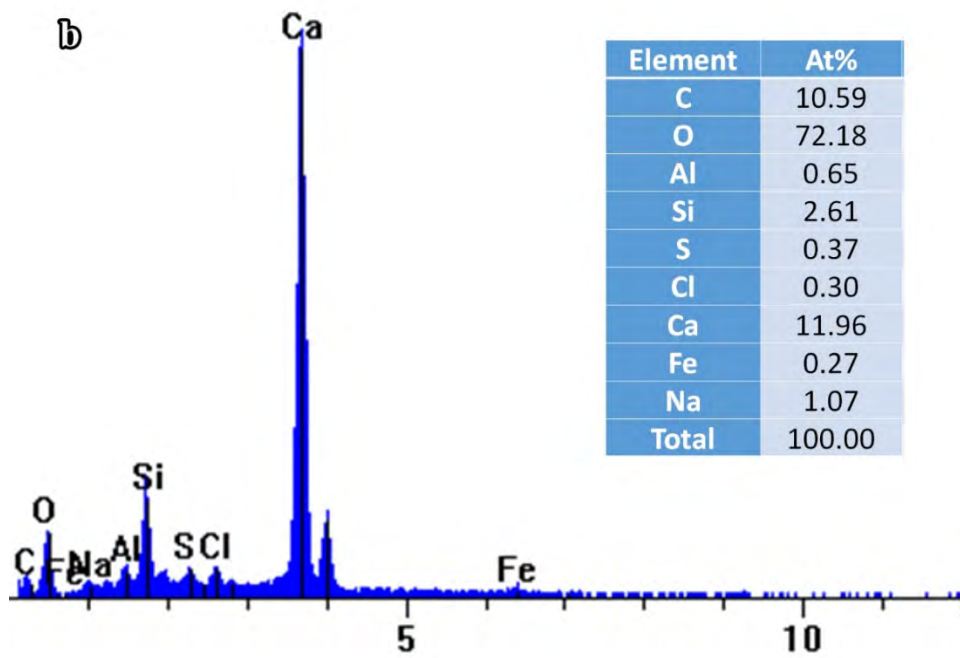
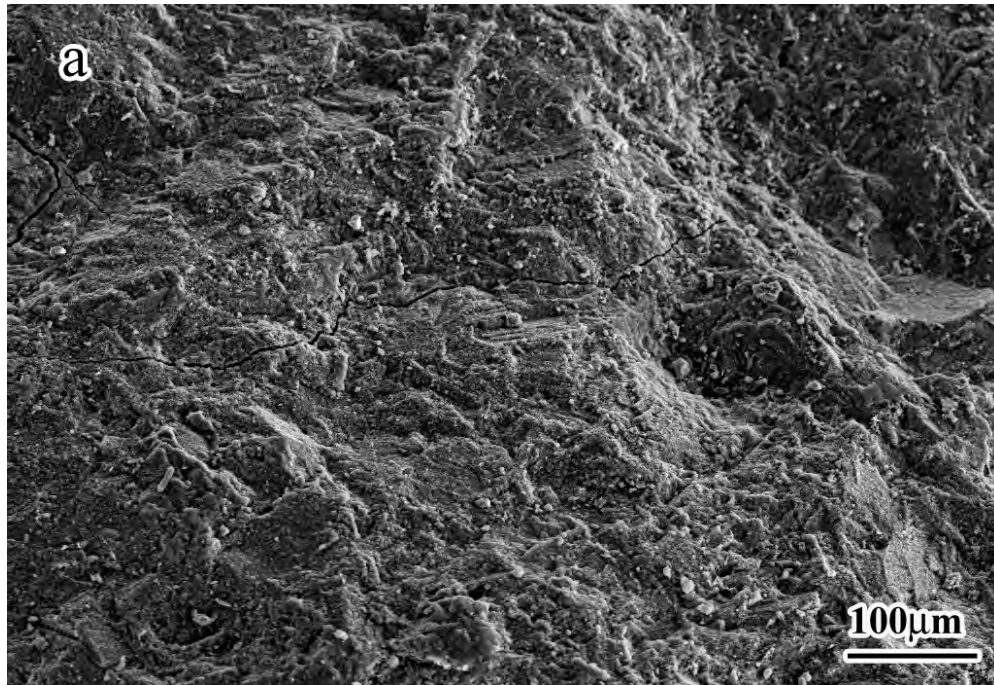


Figure 5- 18 The SEM/EDS result of the concrete samples after 15 F/T and W/D cycles in NaCl with a) SEM image and b) corresponding EDS element distribution results.

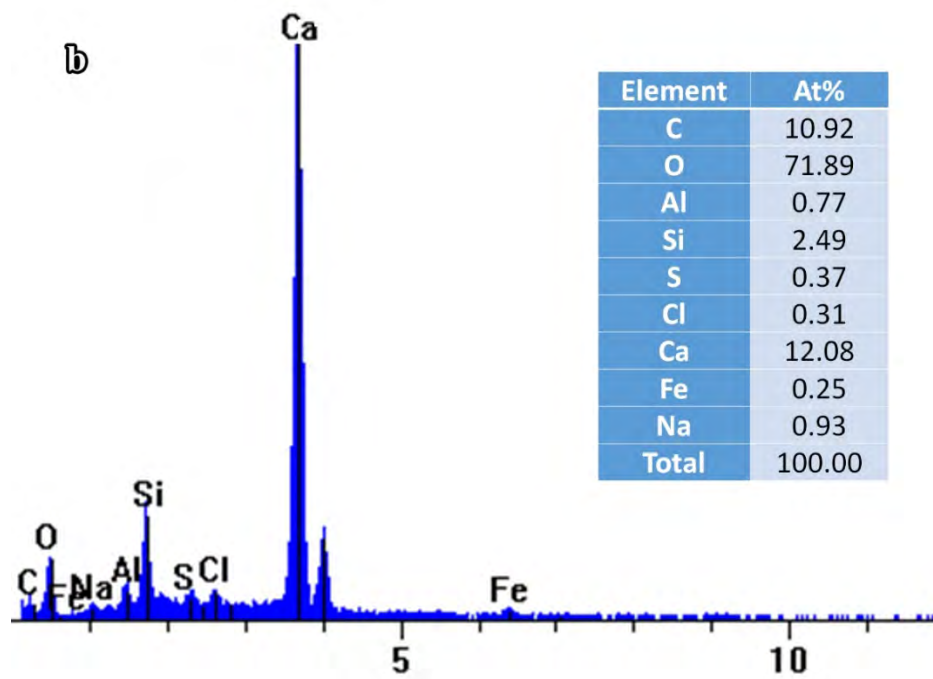


Figure 5- 19 The SEM/EDS result of the concrete samples after 15 F/T and W/D cycles in NaCl with a) high magnification SEM image and b) corresponding EDS element distribution results. *NOTE: The SEM image is a little bit out of focus due to the device limitation on magnification.*

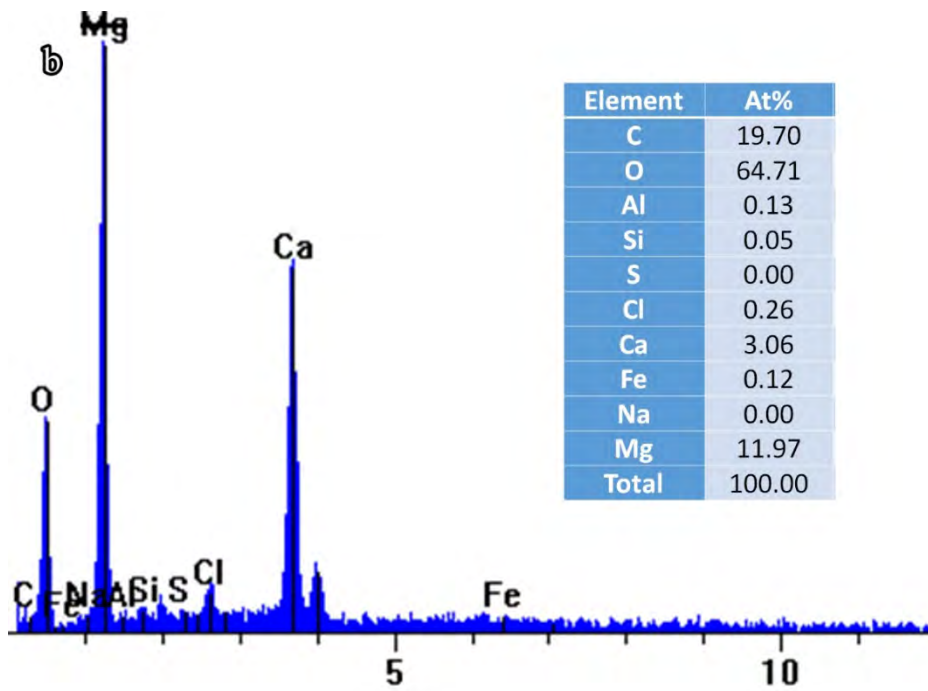
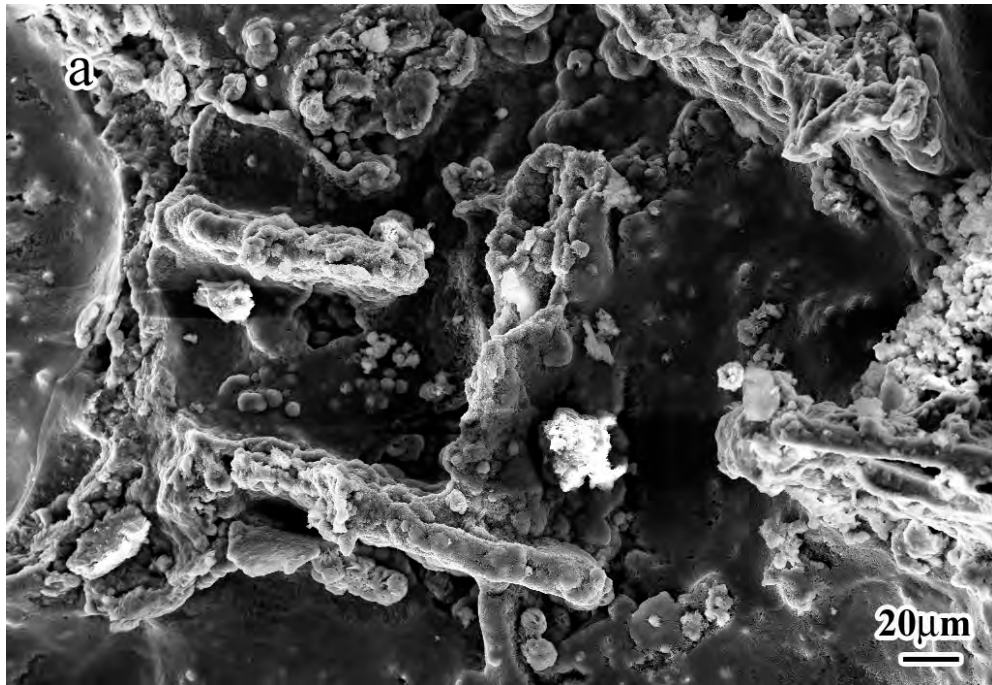


Figure 5- 20 The SEM/EDS result of the concrete samples after 15 F/T and W/D cycles in MgCl₂ with a) SEM image and b) corresponding EDS element distribution results.

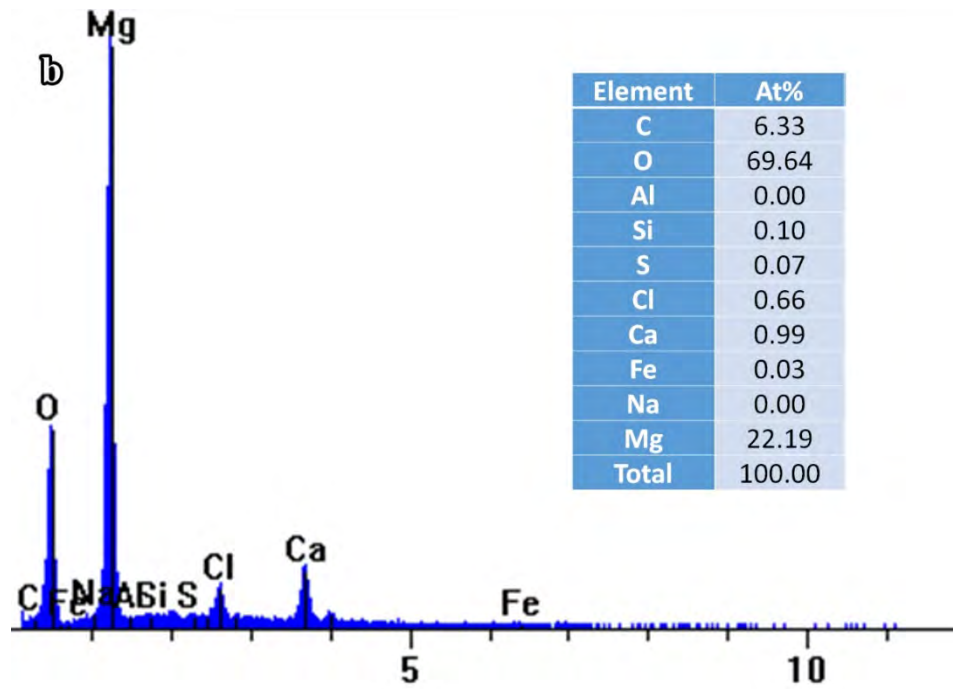
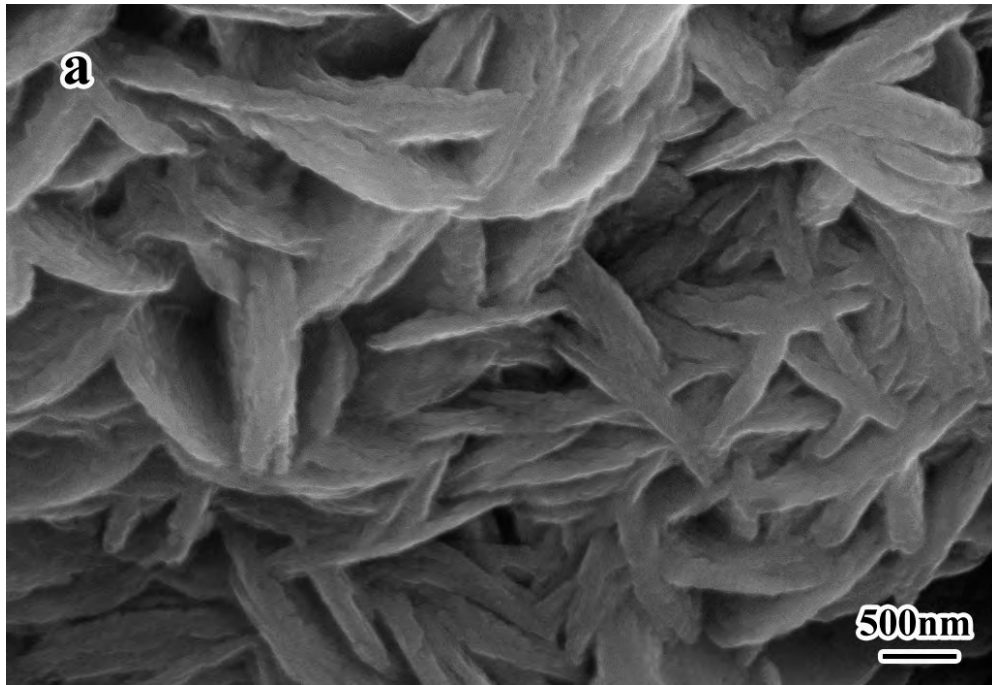


Figure 5- 21 The SEM/EDS result of the concrete samples after 15 F/T and W/D cycles in $MgCl_2$ with a) high magnification SEM image and b) corresponding EDS element distribution results.

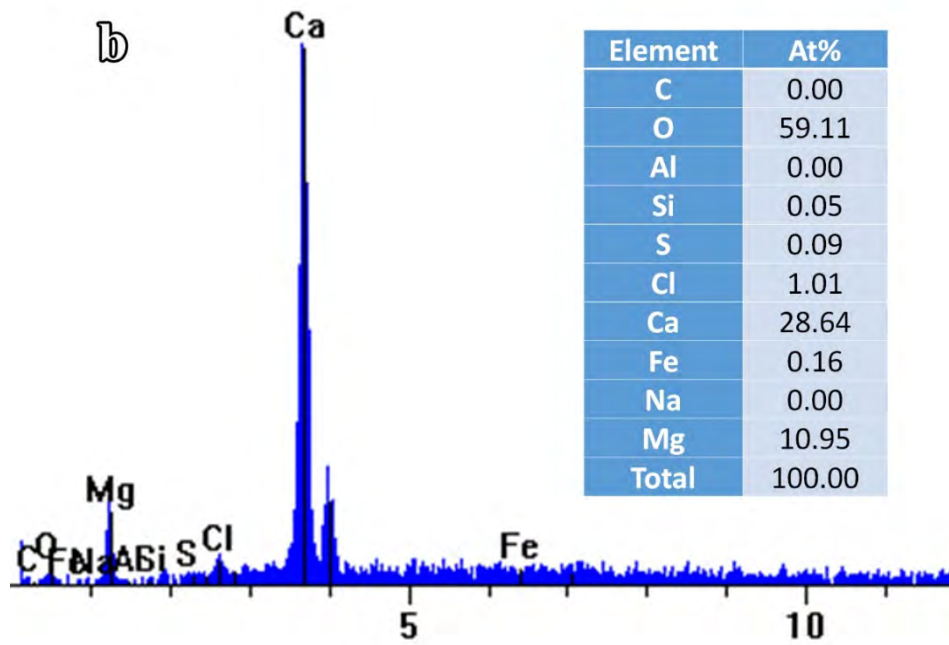
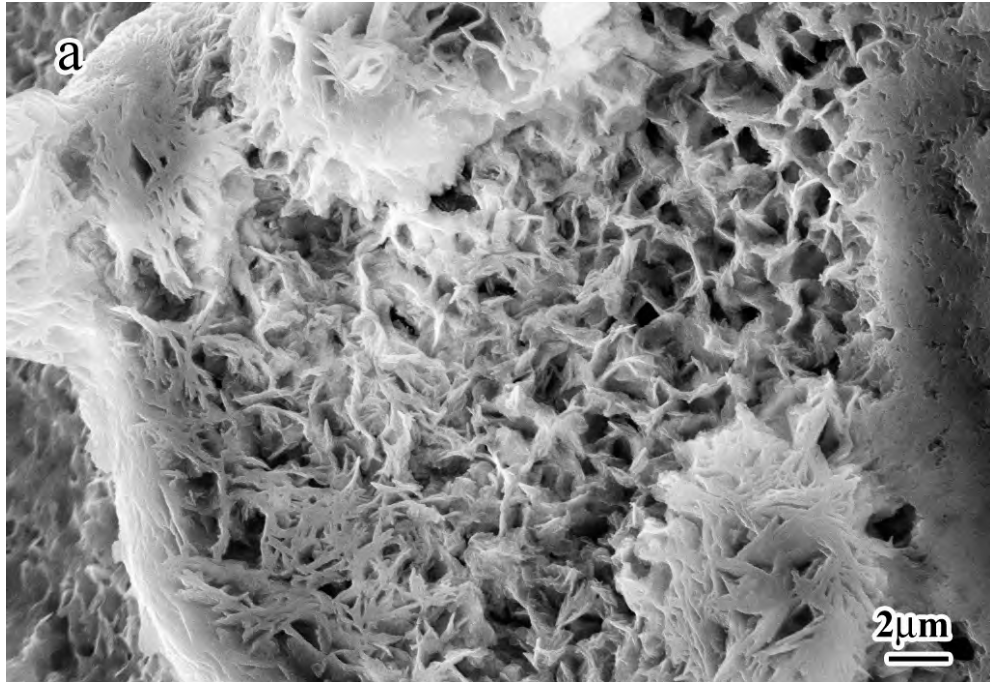


Figure 5- 22 The SEM/EDS result of the concrete samples after 15 F/T and W/D cycles in MgCl₂ with a) SEM image and b) corresponding EDS element distribution results.

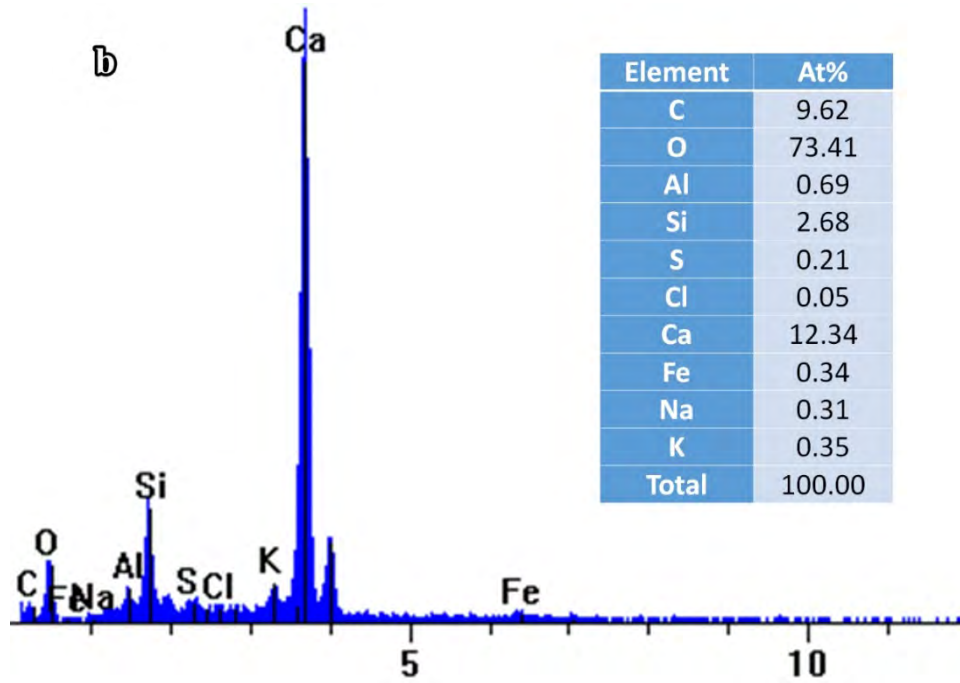
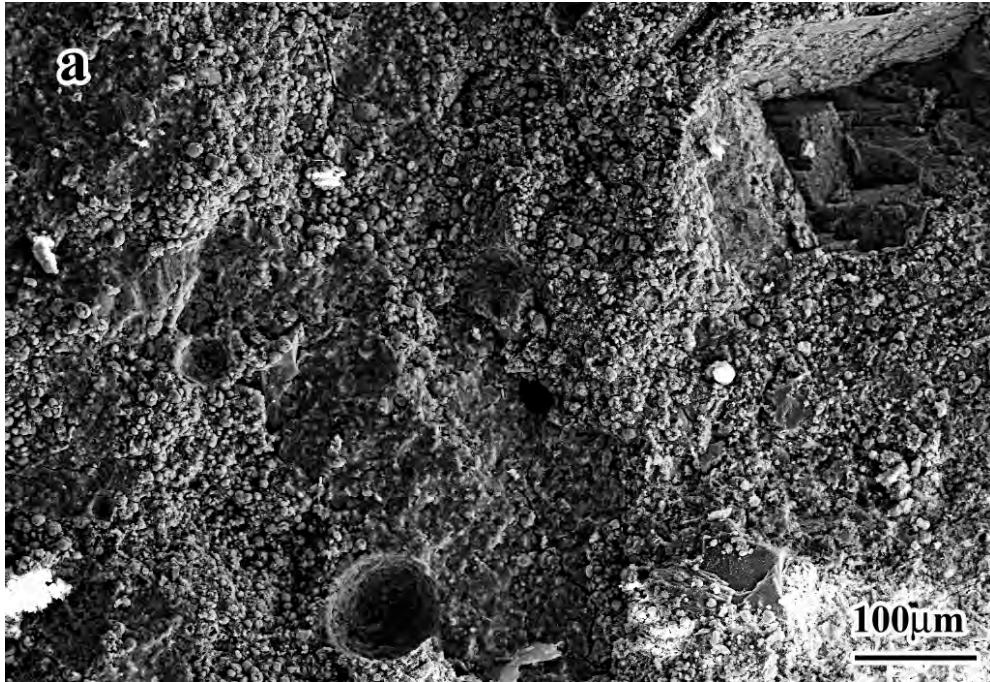


Figure 5- 23 The SEM/EDS result of the concrete samples after 15 F/T and W/D cycles in KAc with a) SEM image and b) corresponding EDS element distribution results.

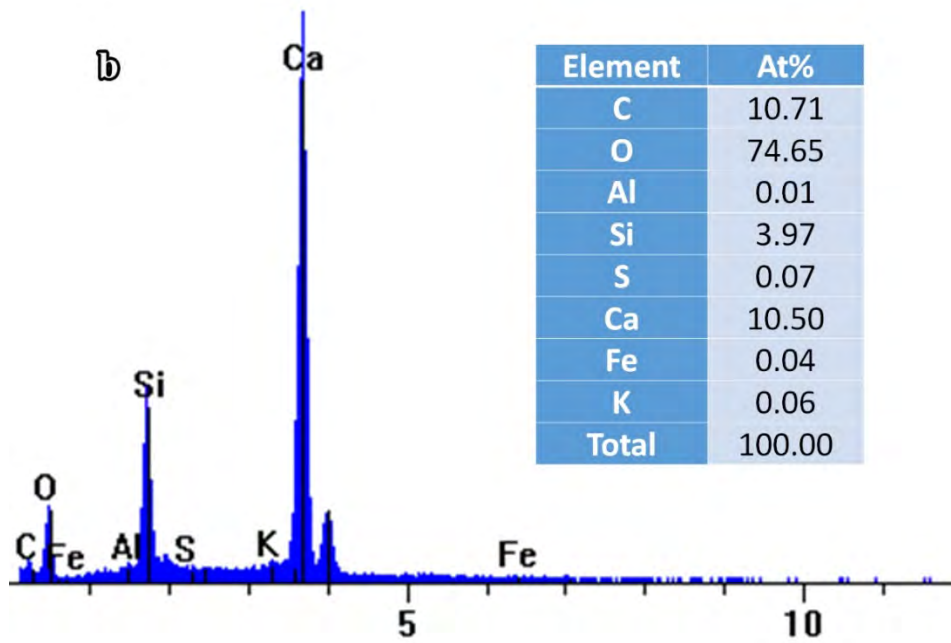
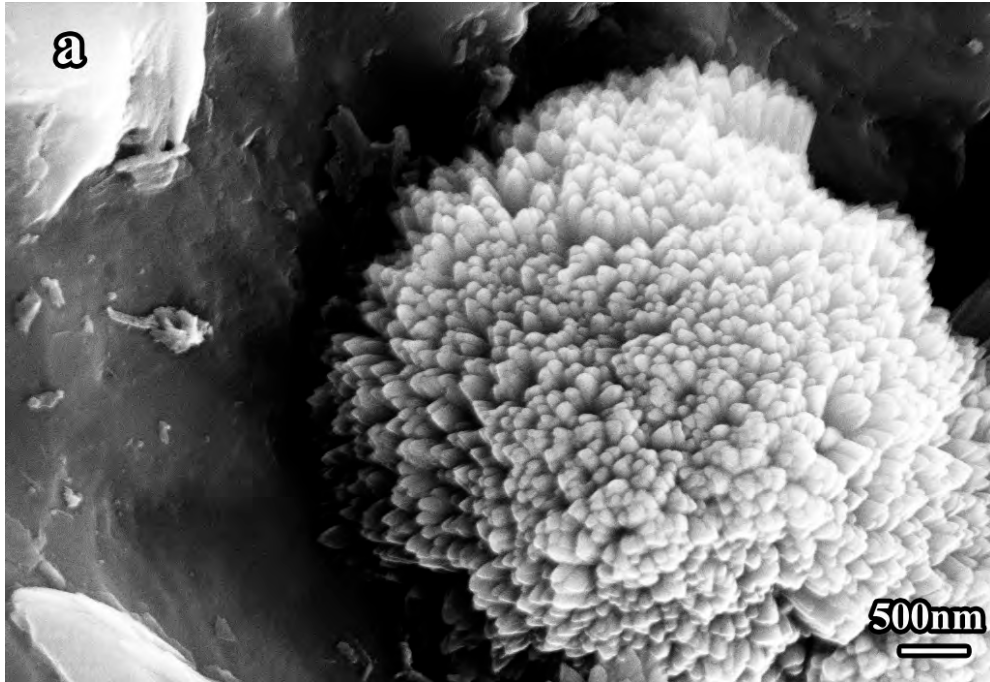


Figure 5- 24 The SEM/EDS result of the concrete samples after 15 F/T and W/D cycles in KAc with a) high magnification SEM image and b) corresponding EDS element distribution results.

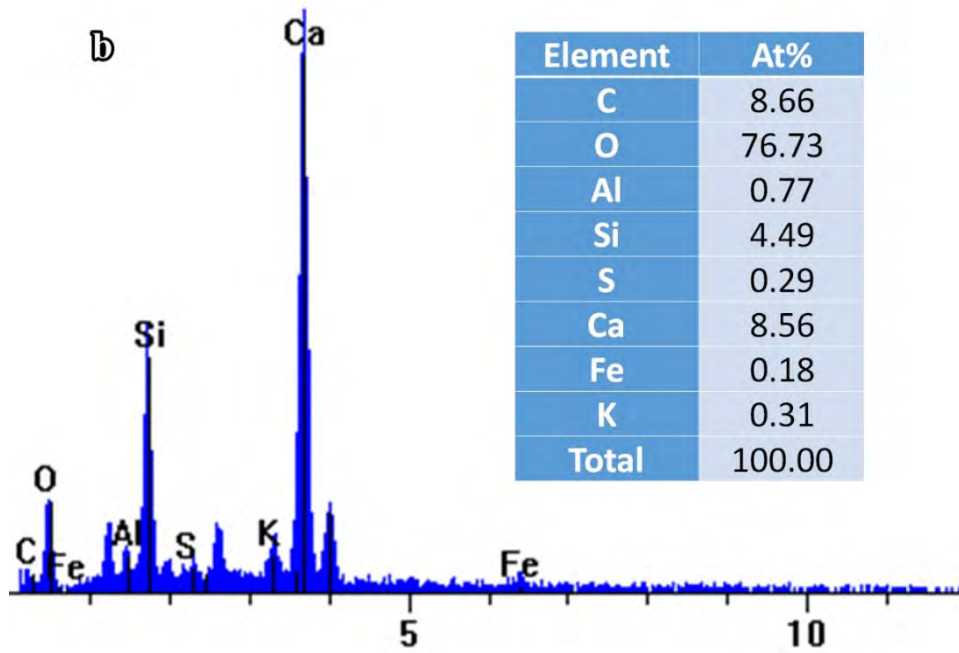
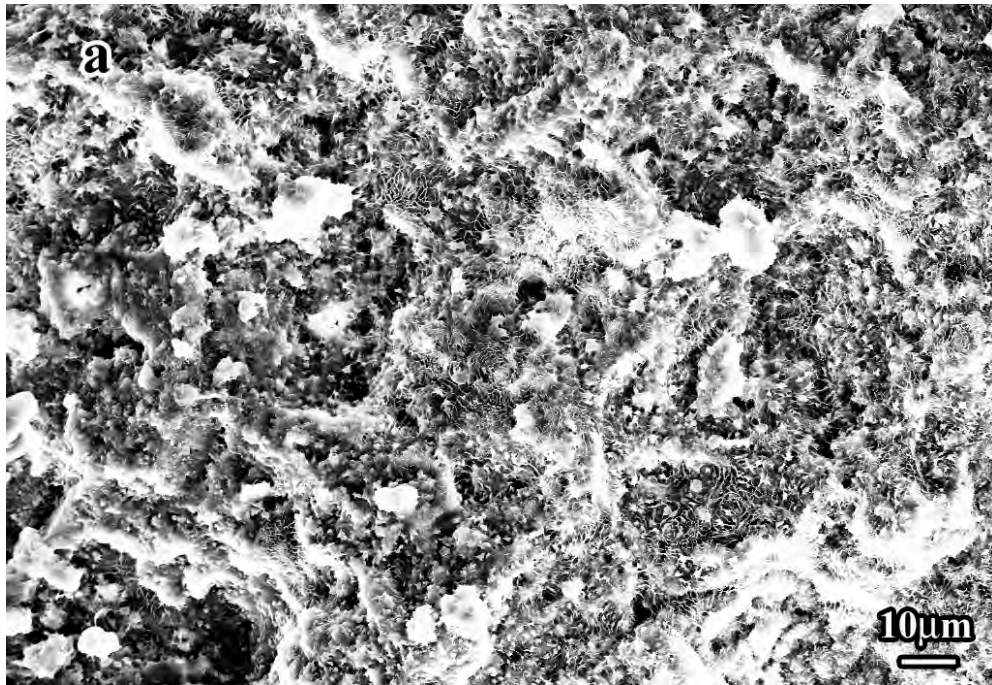


Figure 5- 25 The SEM/EDS result of the concrete samples after 15 F/T and W/D cycles in Kfm with a) SEM image and b) corresponding EDS element distribution results.

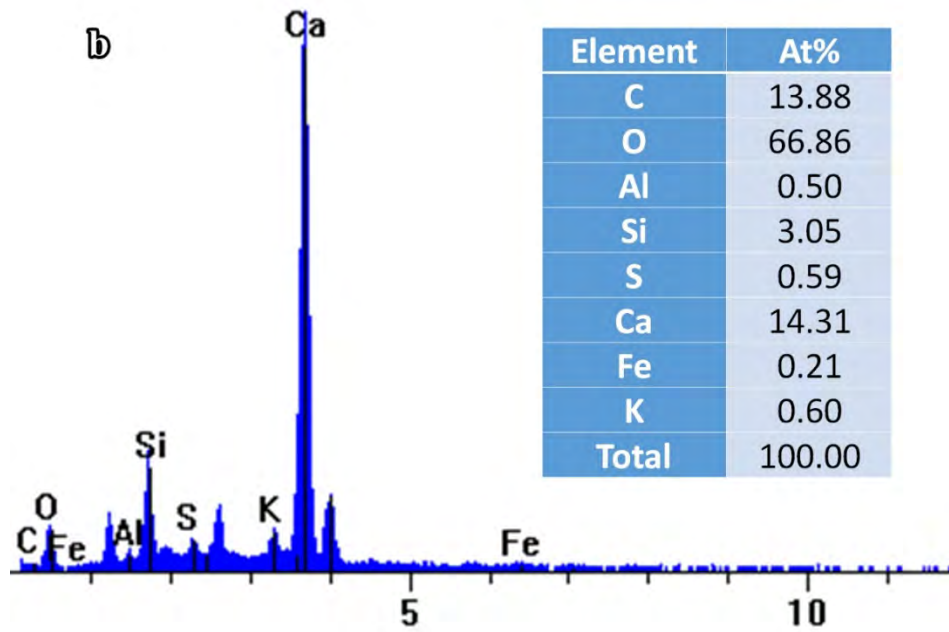
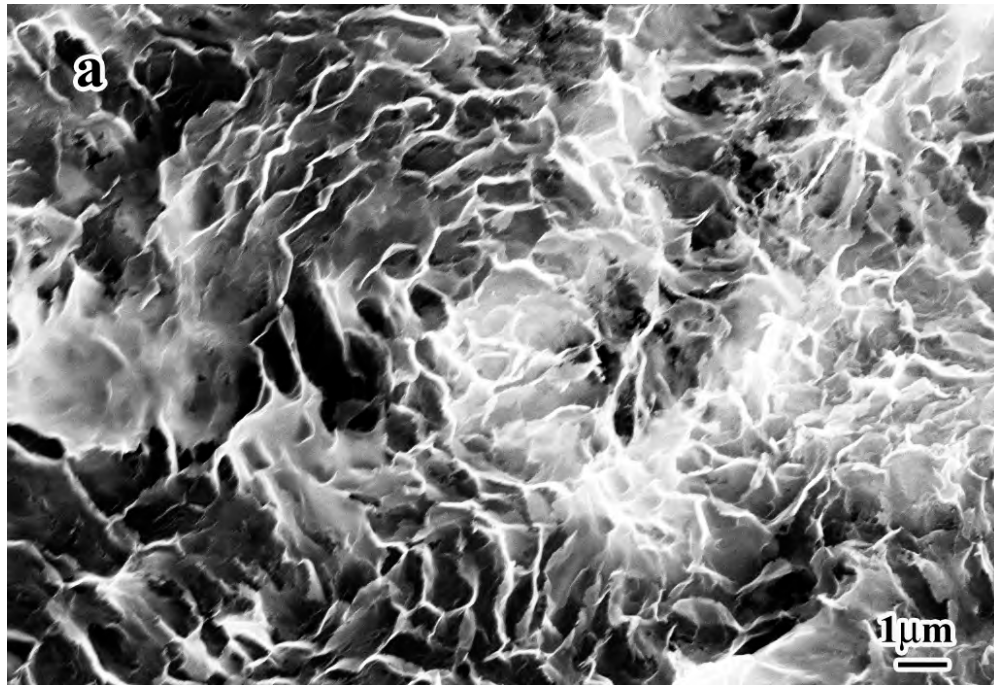


Figure 5- 26 The SEM/EDS result of the concrete samples after 15 F/T and W/D cycles in Kfm with a) high magnification SEM image and b) corresponding EDS element distribution results.

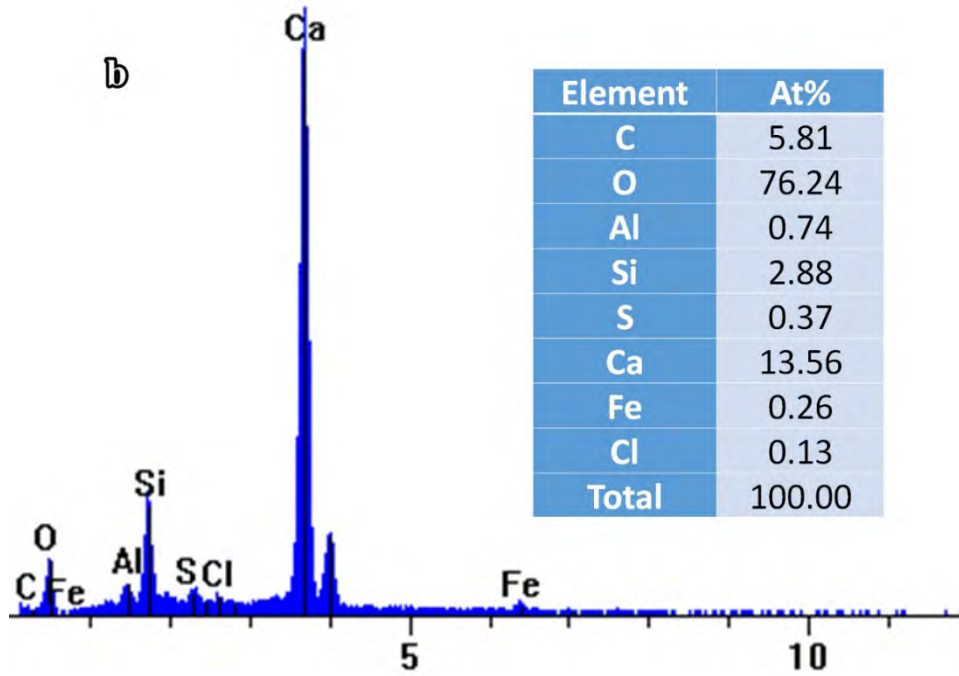
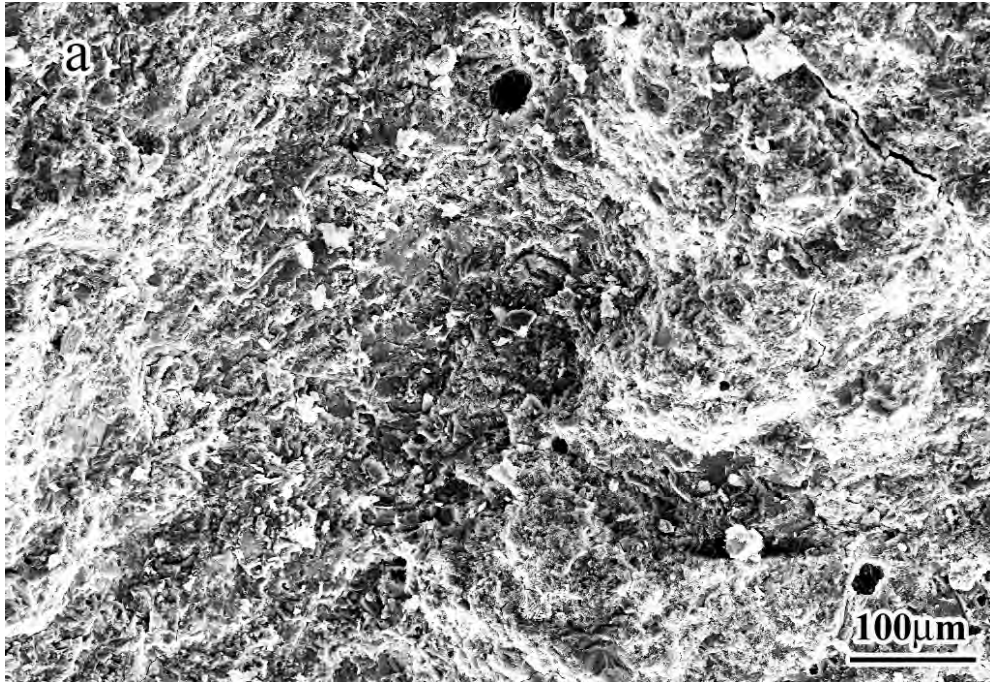


Figure 5- 27 The SEM/EDS result of the concrete samples after 15 F/T and W/D cycles in CaCl_2 with a) SEM image and b) corresponding EDS element distribution results.

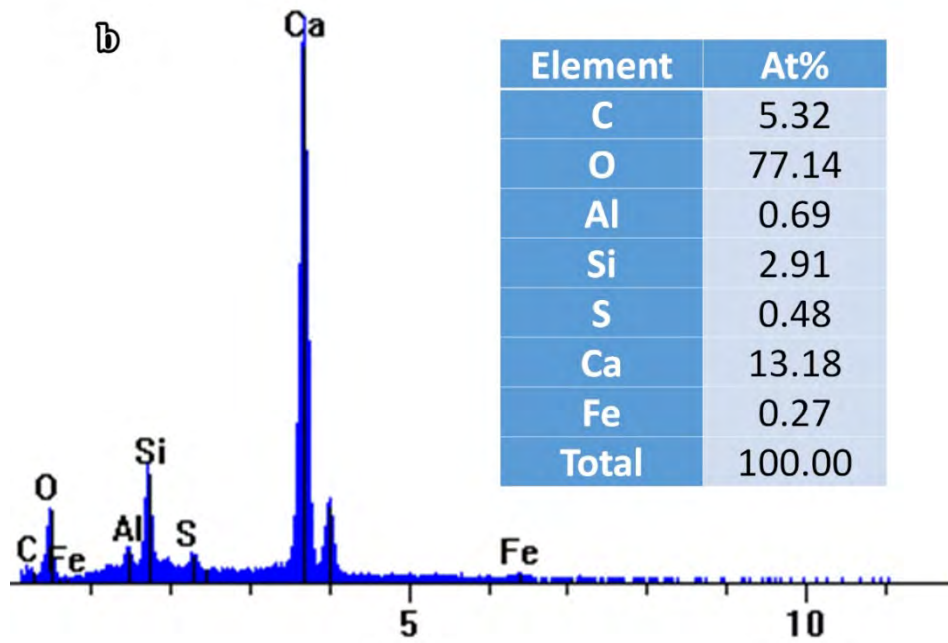
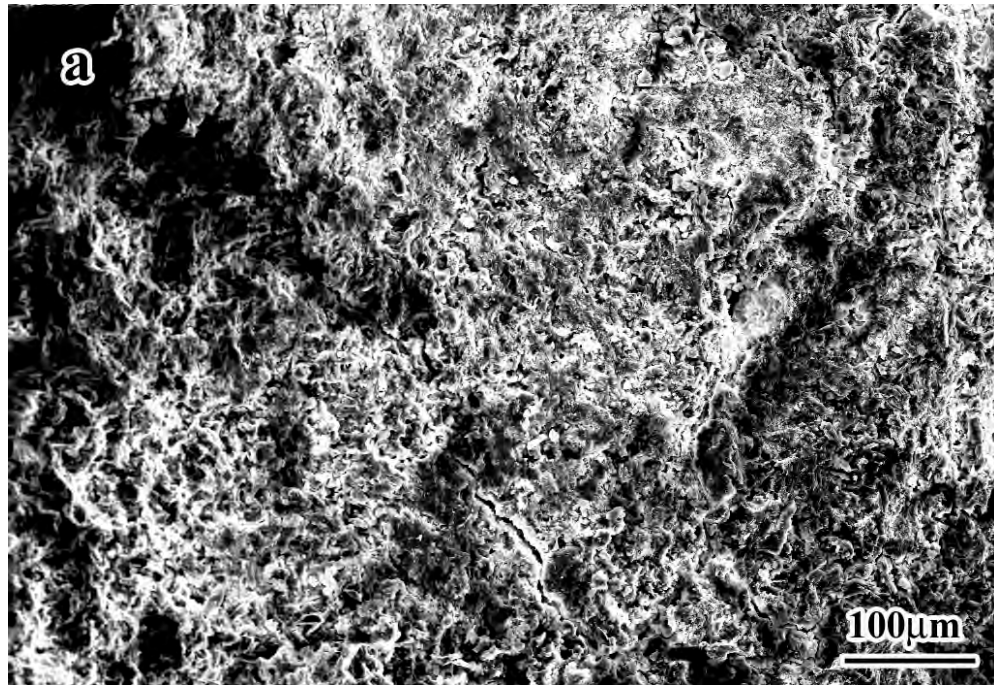


Figure 5- 28 The SEM/EDS result of the concrete samples after 15 F/T and W/D cycles in CaAc₂ with a) SEM image and b) corresponding EDS element distribution results.

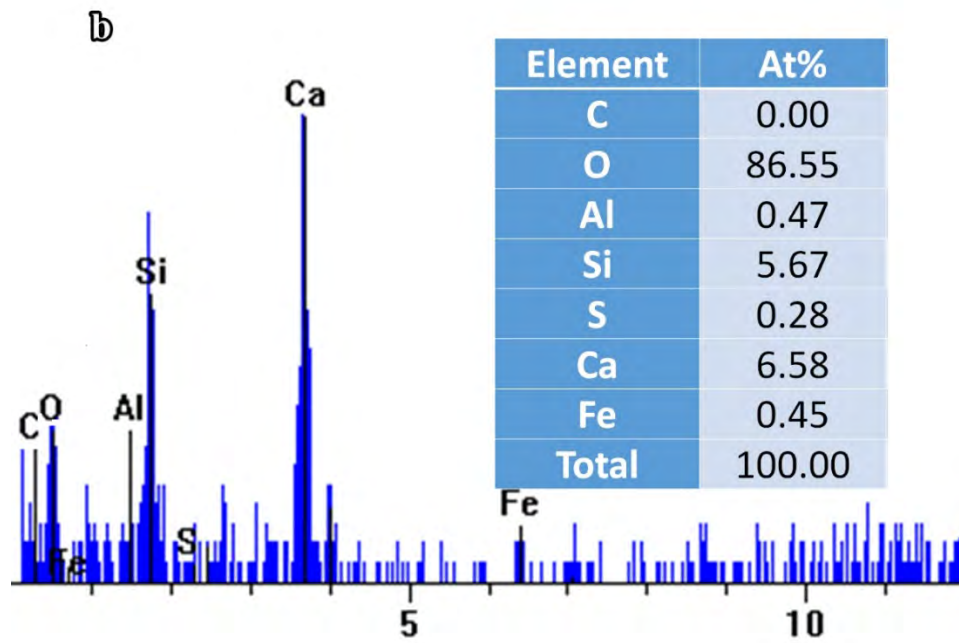
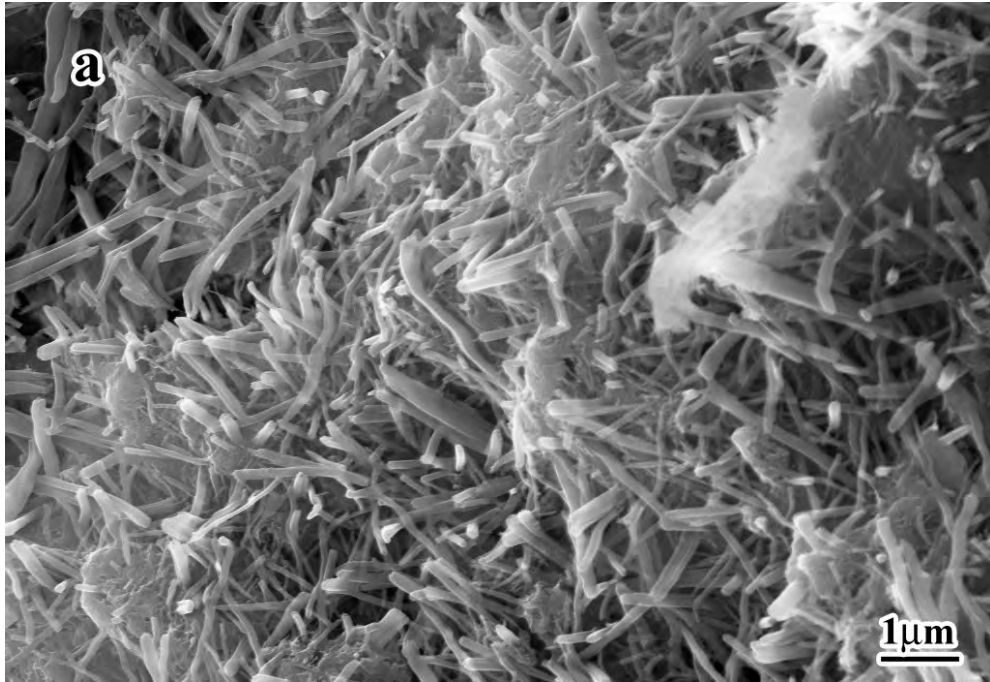
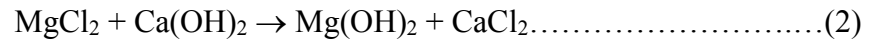
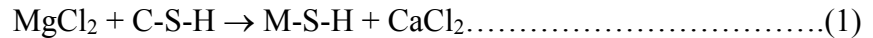


Figure 5- 29 The SEM/EDS result of the concrete samples after 15 F/T and W/D cycles in CaFm_2 with a) high magnification SEM image and b) corresponding EDS element distribution results.

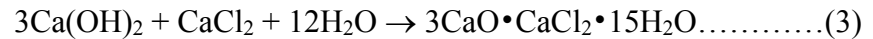
5.3.3 TEM/XRD Analysis of the White Precipitates in the MgCl₂ Solution

After exposure to F/T and W/D cycles in various deicer solutions, only MgCl₂ exposed samples show white precipitates (Figure 5- 30). In addition, due to the disagreement between the splitting tensile strength and the external image of the samples exposed to MgCl₂ solution, further investigation is warranted to looking at the potential deterioration mechanism of the MgCl₂ on the concrete materials.

The aforementioned findings obtained from the cored field concrete decks are consistent with existing laboratory studies that reported the detrimental effect of MgCl₂ on Portland cement concrete (Moukwa, 1990; Spry et al., 1994; Deja and Loj, 1999; Sutter et al., 2008) and with some limited field studies (Cody et al., 1996). As shown in Equation (1), MgCl₂ can react with the cementitious calcium silicate hydrate (C-S-H) present in the cement paste and turn it into non-cementitious magnesium silicate hydrate (M-S-H). As shown in Equation (2), MgCl₂ can also react with another type of cement hydration product, Portlandite (Ca(OH)₂), and produce a crystal known as brucite (Mg(OH)₂). The formation of brucite in confined concrete pores induces great expansive forces and may lead to cracking of the concrete (Wakeley et al., 1992).



A recent laboratory study reported the formation of another potentially detrimental phase, calcium oxychloride (3CaO•CaCl₂•15H₂O), which formed in cement mortars exposed to 15% MgCl₂ solutions for 84 days, as confirmed by optical microscopy, scanning electron microscopy (SEM), and microanalysis (Sutter et al., 2006). The proposed mechanism was based on Equations (1) and (2):



A recent study claimed that, with exposure to MgCl₂, the cementitious materials will interact significantly with MgCl₂, which is similar to Ca(OH)₂ - CaCl₂ - H₂O phase diagram (Farnam, 2015). The products of the chemical reactions between MgCl₂ and the cementitious phase include CaCl₂, brucite, magnesium oxychloride, and calcium oxychloride in concrete. Based on this statement, it was assumed that the formation of calcium oxychloride or magnesium oxychloride, and brucite will consume the solution content to keep cementitious materials unsaturated, which leads to the change of transport paths and damage of concrete.

The petrographic evidence indicated that plate calcium oxychloride crystals and their carbonate-substituted phase precipitated in air voids and cracks by consuming Portlandite. In

addition, Friedel's salt ($3\text{CaO}\cdot\text{Al}_2\text{O}_3\cdot\text{CaCl}_2\cdot 10\text{H}_2\text{O}$) was detected in the specimens analyzed (Sutter et al., 2006). In another laboratory study by the same group, the structures of brucite were also observed in the outer layers of the PCC specimens exposed to concentrated MgCl_2 (Sutter et al., 2008).

Figure 5- 31 shows the XRD pattern of the white precipitates from the MgCl_2 solution with concentration of 20% after 15 F/T cycles of the concrete samples. The results suggest some potential mechanisms of the chemical reaction between the C-S-H binder phase and the MgCl_2 deicer. As can be seen in Figure 5- 31, obvious crystalline peaks of $\text{CaMg}_2\text{Cl}_6\cdot(\text{H}_2\text{O})_{12}$ and NaCl phases can be observed in the white precipitates. In this figure, the main characteristic peaks of the tachyhydrite ($\text{CaMg}_2\text{Cl}_6\cdot(\text{H}_2\text{O})_{12}$) appear at about 18° , 23° and 34° and can be clearly observed, which indicates the formation of this crystal. Note here that the main peaks of NaCl, which might have resulted from the contamination of the solution while moving the samples in and out of the containers, can be also observed at 32° and 45° . It is important to note that, in this XRD pattern, the CaCl_2 and $\text{Mg}(\text{OH})_2$ peaks were not observed, which means that the replacement of Mg to Ca is more complicated than the reaction equations (1) and (2). According to the XRD results shown in Figure 5- 31, the following additional chemical reaction may have occurred:



Figure 5- 32 shows a typical TEM image of white precipitates. As can be seen in this figure, the precipitates show very thin structure and are relatively transparent to the electron beam. As a result, it is very hard to observe the white precipitate under SEM in the concrete samples.

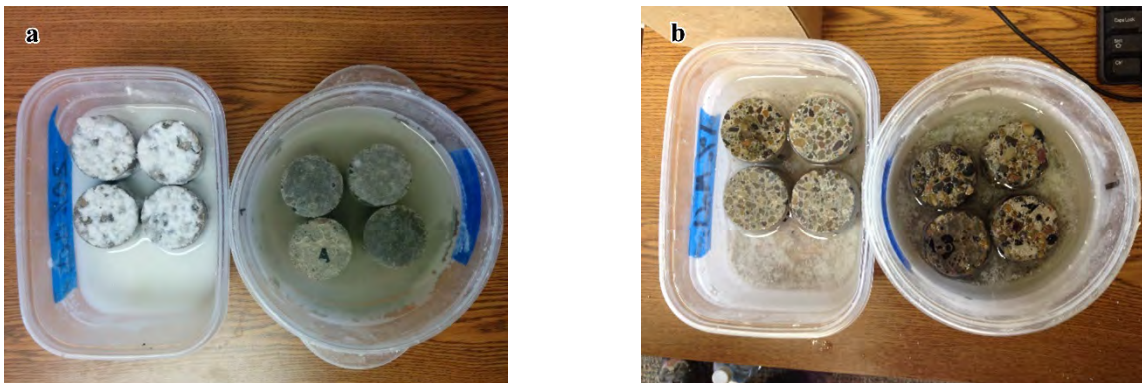


Figure 5- 30 Concrete samples experienced 15 F/T cycles in MgCl_2 (rectangular box) and NaCl (round box) with concentration of a) 20% MgCl_2 and NaCl and b) 1% MgCl_2 and NaCl.

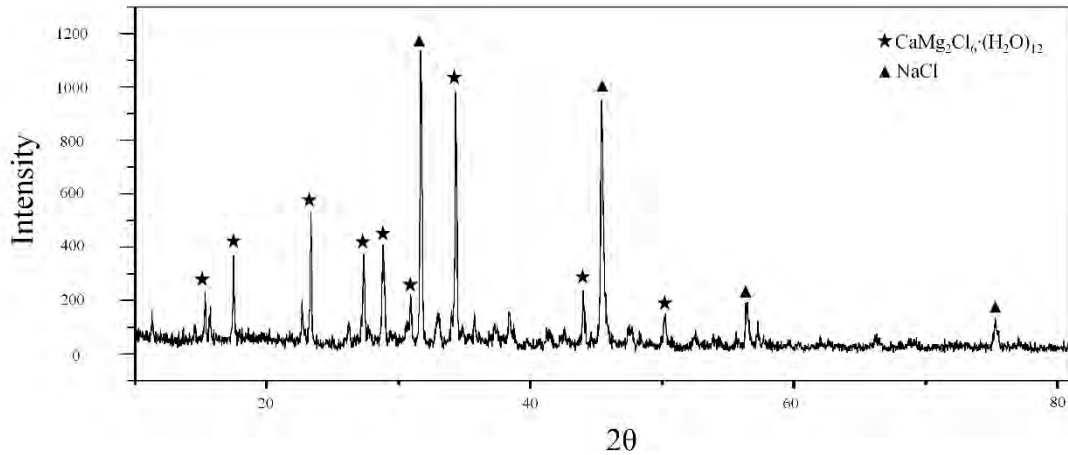


Figure 5- 31 XRD pattern of the white precipitates from the $MgCl_2$ solution with concentration of 20% after 15 times of F/T cycles of the concrete samples.

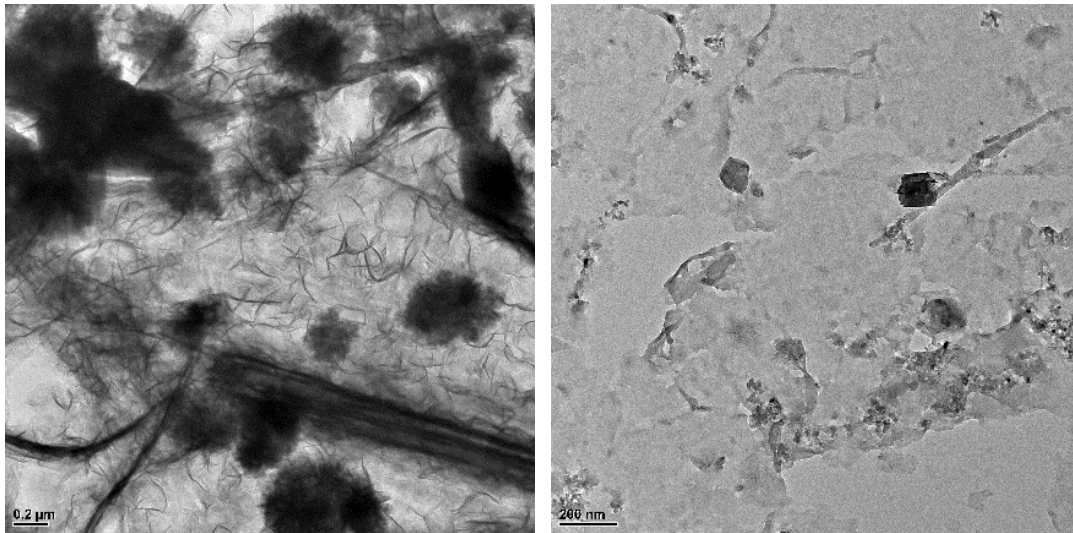


Figure 5- 32 Transmission Electronic Microscopy morphologies of the white precipitates of concrete samples after 15 of F/T cycles in $MgCl_2$ solution

5.4 Key Findings

Of the eight types of deicers, including NaCl, KCl, KAc, KFm, $MgCl_2$, $CaCl_2$, $CaAc_2$, and $CaFm_2$, $CaCl_2$ has the largest ice melting capability at $-25^\circ C$, while the $MgCl_2$ has the lowest ice melting capability at $-25^\circ C$.

The corrosion rates of stainless steel with exposure to various deicers are not very high; they are all in the range of 0.0 ± 0.2 MPY, except $CaFm_2$, which has a relatively high corrosion

rate of 1.12 MPY. The corrosion rates of plain steel with exposure to various deicers are considerably different. All chloride salts have relatively high corrosion rates from about 30 to 48 MPY, while KAc and CaAc₂ have extremely low corrosion rates at about -2.0 MPY. CaFm₂ had a relatively high corrosion rate about 30 MPY. The corrosion rates of the galvanized steel with exposure to various deicers are all relatively high, ranging from 15 to 47 MPY.

All concrete samples exposed to alkali based deicer solutions exhibited severe surface distress, while the samples exposed to alkali earth based deicer solutions showed little surface distress. The concrete samples exposed to KCl solution showed the highest mass loss while the samples exposed to CaCl₂ solution showed the lowest.

The mechanical properties testing results show that the MgCl₂ has a considerable reduction of splitting tensile strengths, even without obvious visible deterioration of the external shape of the samples.

After exposure to F/T and W/D cycles in various deicer solutions, only MgCl₂ exposed samples show white precipitates. In addition, due to the disagreement between the splitting tensile strength and the external image of the samples exposed to MgCl₂ solution, further investigation is warranted to looking at the potential deterioration mechanism of MgCl₂ on concrete materials.

Microstructure analysis demonstrated that the alkali metal based deicers strongly affects the deterioration of C-S-H binder phase in cement paste. CaCl₂ and CaAc₂ have less of an effect on the C-S-H phase than other deicers.

CaMg₂Cl₆·(H₂O)₁₂ is one of the main reaction products when concrete is exposed to MgCl₂.

5.5 References

- Cody, R. D., Cody, A. M., Spry, P. G., & Gan, G. L. (1996). Experimental deterioration of highway concrete by chloride deicing salts. *Environmental & Engineering Geoscience*, 2(4), 575-588.
- Deja, J., and Loj, G. (1999). Effect of cations occurring in the chloride solutions on the corrosion resistance of slag cementitious materials. In *Infrastructure regeneration and rehabilitation improving the quality of life through better construction*. International conference (pp. 603-620).
- Farnam, Y., Dick, S., Wiese, A., Davis, J., Bentz, D., & Weiss, J. (2015). The influence of calcium chloride deicing salt on phase changes and damage development in cementitious materials. *Cement and Concrete Composites*, 64, 1-15.
- Fay, L., & Shi, X. (2012). Environmental impacts of chemicals for snow and ice control: State of the knowledge. *Water, Air, & Soil Pollution*, 223(5), 2751-2770.
- Liu, Y., & Shi, X. (2012). Ionic transport in cementitious materials under an externally applied electric field: Finite element modeling. *Construction and Building Materials*, 27(1), 450-460.

- Moukwa, M. (1990). Characteristics of the attack of cement paste by $MgSO_4$ and $MgCl_2$ from the pore structure measurements. *Cement and Concrete Research*, 20(1), 148-158.
- Neville, A. (1995). Chloride attack of reinforced concrete: an overview. *Materials and Structures*, 28(2), 63-70.
- Shi, X. (2008). Impact of airport pavement deicing products on aircraft and airfield infrastructure, Transportation Research Board.
- Shi, X., M. Akin, T. Pan, L. Fay, Y. Liu and Z. Yang (2009a). "Deicer Impacts on Pavement Materials: Introduction and Recent Developments." *Open Civil Engineering Journal* 3.
- Shi, X., L. Fay, C. Gallaway, K. Volkening, M. Peterson, T. Pan, A. Creighton, C. Lawlor, S. Mumma and Y. Liu (2009b). Evaluation of Alternative Anti-icing and Deicing Compounds Using Sodium Chloride and Magnesium Chloride as Baseline Deicers, Phase I, Colorado Department of Transportation, DTD Applied Research and Innovation Branch.
- Shi, X., Fay, L., Peterson, M. M., & Yang, Z. (2010). Freeze–thaw damage and chemical change of a portland cement concrete in the presence of diluted deicers. *Materials and Structures*, 43(7), 933-946.
- Shi, X., Fay, L., Peterson, M. M., Berry, M., & Mooney, M. (2011). A FESEM/EDX investigation into how continuous deicer exposure affects the chemistry of Portland cement concrete. *Construction and building materials*, 25(2), 957-966.
- Shi, X., Xie, N., Fortune, K., & Gong, J. (2012). Durability of steel reinforced concrete in chloride environments: An overview. *Construction and Building Materials*, 30, 125-138.
- Spry, P. G., Cody, A. M., & Gan, G. (1994). The role of magnesium in concrete deterioration. Department of Geological and Atmospheric Sciences, Iowa State University.
- Sutter, L. and S. Dakota (2008). The deleterious chemical effects of concentrated deicing solutions on Portland cement concrete, South Dakota Department of Transportation.
- Wakeley, L. D., Poole, T. S., Ernzen, J. J., & Neeley, B. D. (1993). Salt saturated mass concrete under chemical attack. *ACI Special Publication*, 140.
- Yu, H., Shi, X., Hartt, W. H., & Lu, B. (2010). Laboratory investigation of reinforcement corrosion initiation and chloride threshold content for self-compacting concrete. *Cement and concrete research*, 40(10), 1507-1516.

CHAPTER 6. LABORATORY INVESTIGATION OF ASPHALT AND HIGH FRICTION PAVEMENT EXPOSED TO CHLORIDE BASED DEICERS

6.1 Introduction

Over the past few decades, various polymers have been used as high friction coating materials to prevent damage to bridge decks and pavements from the effects of deicers and freeze/thaw cycles. Over 2,724 polymer-based overlays have been applied on bridge structures in the United States (Federal Highway Administration, 2010). Since 2008, the use of polymer overlays has increased 24.2%, whereas the use of other surface overlays has decreased every year (Young, 2012).

Polymer based high friction surfaces must satisfy the same requirements as a traditional pavement, including skid resistance, wear resistance, bonding strength, and mechanical properties. Therefore, not all types of polymers can be used as pavement coatings. Epoxy and acrylic polymers are the two main types of polymers that are widely used as coating materials for pavements. This chapter presents information on the performance of these selected polymers as high friction pavement coatings.

6.1.1. Epoxy Resins

Epoxy resins can be used as adhesives to join two surfaces of different components by forming a bond between them. They were commercially introduced in 1946 as adhesives and can be applied in many industrial sectors. Epoxy resins are easily modified to achieve required properties. They are also the most widely used adhesive because many materials can be bonded. In the epoxy industry, the modification is called *formulating* or *compounding*. In the modification process, the curing agent and the reaction mechanisms are the key factors that guarantee the required properties are met at a reasonable cost; therefore, numerous epoxy adhesive formulations can be obtained. Because of the various curing agents and specific formulations, manufacturers can design a wide range of final properties for the resins. Cured epoxies provide outstanding mechanical properties; in addition, they show good resistance to oil, moisture, and many other solvents.

As demonstrated in Figure 6-1, the chemical structure of epoxy represents a broad group of reactive compounds that are characterized by the presence of an oxirane or epoxy ring. This is a three-member ring containing an oxygen atom bonded with two carbon atoms, which have been united with some other elements or groups. More than one epoxy group can be contained in an epoxy resin to form the molecule.

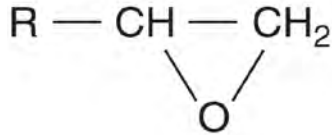


Figure 6- 1 The chemical structure of epoxy resin.

The general formula of an epoxy resin can be expressed as Figure 6-2 (Osumi, 1987). The linear polyether with epoxy groups and the hydroxyl groups along the length of the chain contribute to the chemical resistance, heat resistance, durability, and adhesion. The reactivity of the molecules are governed by the terminal of the molecule and the hydroxyl at the midpoint. The adhesion property of epoxy is governed by the secondary hydroxyl groups located in the molecule chain.

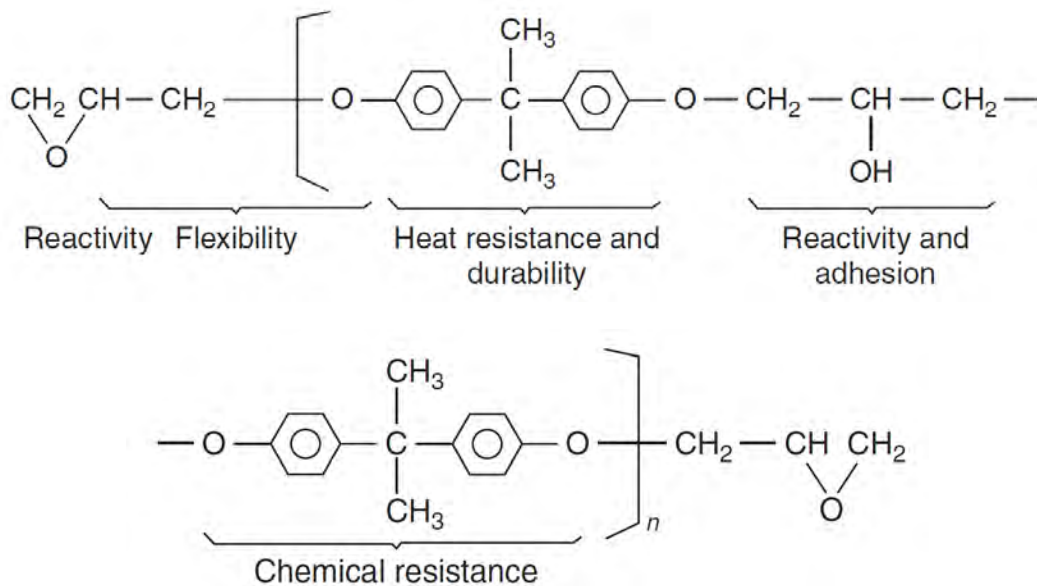


Figure 6- 2 The structure and properties of epoxy resins (Osumi, 1987).

The main mechanism of the epoxy curing is the so-called *ring opening*. In this process, the epoxy group may react in different ways. One is the anionic reaction, and the other one is the cationic reaction. Figure 6-3 shows the anionic mechanism of the ring opening (Lee, 1967). In the cationic reaction, the epoxy group will open and form a new hydroxyl bond by the introduction of an active hydrogen.

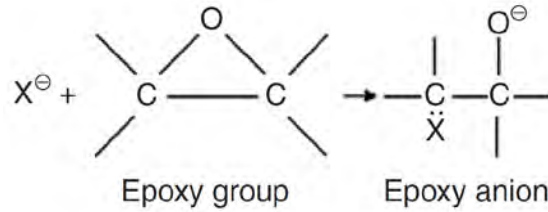


Figure 6- 3 Anionic mechanism of epoxy reaction (Lee, 1967).

The materials react with the epoxy and form the epoxy network called the *curing agent* or *hardener*. The mixing content of the curing agent varies from several percent to as high as 50 percent. A large number of curing agents can react with epoxy to form a crosslink structure. The curing agent, in most cases, will react with the available epoxy or hydroxyl groups. Currently, for commercial epoxies, the following materials are widely used as the curing agent.

- Aliphatic amines and modified aliphatic amines
- Polyamides
- Anhydrides
- Polysulfides and mercaptans

Rigidity is one of the shortcomings of epoxy resins when it is used as coating overlay materials for pavement. Therefore, how to mitigate this problem is the key issue that determines whether or not the epoxy can be applied in the field. Through proper selection of a curing agent, the flexibility of inherently rigid epoxy resins can be improved. By controlling stoichiometric mix ratios between the epoxy resin and the curing agent, or by using flexible molecule curing agents, the epoxy formulation can be changed and the flexibility will be adjusted accordingly. For example, by changing the curing agent from hexahydrophthalic anhydride to hexamineethylenediamine, the impact resistance of a resin system can be doubled and its tensile elongation can be increased accordingly (Epon Resin Structural Resin Manual, 2001).

There are two types of curing methods for current commercial epoxies. The first one is the single component epoxy with heat curing, and the second one is the multiple component epoxy curing at room temperature or at elevated temperatures. In most cases, the heat curing will lead to a relatively higher glass transition temperature and a higher crosslinking density than the ones cured at room temperature. As a result, the epoxies cured at high temperatures will provide a higher shear strength and chemical stability. However, due to their rigidity, their toughness and peeling strength will be lower than those cured at room temperature.

Although some epoxies can be cured as quickly as minutes at room temperature, most of them require relatively longer curing time (18 to 72 h) to obtain full strength. The curing time is

temperature sensitive. It can be shortened by increasing curing temperatures. After curing, the epoxy resins are solid materials with outstanding properties, such as low shrinkage and no volatiles during the curing process, compatible with many types of materials, good mechanical properties, chemically stable, and durable under complex environmental conditions. In addition, the properties of the epoxy resins can be controlled according to the requirements; flexible or rigid; high or low modulus; filled or foamed, conductive or insulative all can be obtained by changing the components of the epoxies.

Apart from the curing time and flexibility, the viscosity of the epoxy resins is another important factor to be considered before it can be applied in the field as the pavement coating. In fact, it is difficult to implement the use of epoxy resins with high viscosity in the field. Currently, commercial epoxy resins are available in either liquid state or solid state. The viscosity of liquid state epoxies can range from water-like to crystalline solids. In most cases, the molecular weight decides the viscosity of the epoxy resins. The higher the molecular weight, the higher the viscosity and the melting point. Other than the molecular weight, the viscosity of the epoxy resins is also governed by the temperature, such that as temperatures decrease, viscosity reduces rapidly.

Epoxy resins were used as pavement coating materials for many years. Most epoxy resin coatings were used as overlays with antiskid or waterproofing functions. Recently, epoxy resin coatings have been used to incorporate the above functions to anti-ice and to create wear resistant surfaces.

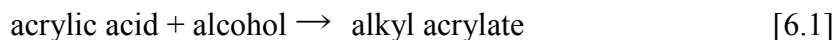
The epoxy coatings for concrete pavement have been extensively studied; however, very limited research has been done on the use of epoxy coatings on asphalt pavement. The following issues have been identified that require additional research. First, the inherent brittleness of cured epoxy resins easily results in cracks on the top of the asphalt pavement because of the mismatch of the deformation capability; 2) the cost of the materials is relatively high if they are adjusted to the required properties; and 3) the curing condition, such as relatively long curing time and high curing temperature, is critical to pavement engineering.

6.1.2. Acrylic Ester Polymers

In 1901, acrylic ester polymers were discovered by Otto Rohm when he was conducting his doctoral research, and they were commercially produced by the Rohm and Haas Co. of Darmstadt, Germany in 1927 (Riddle, 1954). Similar to epoxy resins, acrylic ester polymers can also be used as adhesives to join two surfaces from different components by providing a bond between them.

Figure 6-4 shows the structure of the acrylic ester monomers. The R side chain ester group here determines the final properties of the formed polymers used in various application fields, from

paint to adhesives. In general, the acrylic ester monomers are formed from the reaction between acrylic acid and alcohol as follows:



During the copolymerizing process, the acrylic ester monomers will randomly incorporate themselves to form the polymer chains by the percentage concentration of each monomer. In addition, the acrylic ester monomers can also be copolymerized with methacrylic ester monomers, styrene, acrylonitrile, or vinyl acetate to prepare other products. The final properties of the formed polymers are determined by the molecular weight and the ester side chain of the product. Similar to other polymers, the properties of the acrylic ester polymers can be improved as a function of molecular weight until a threshold is reached. Beyond this threshold, the property improvement will not continue. In general, for acrylic polymers, the threshold molecular weight value is about 100,000-200,000.

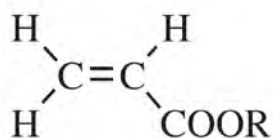


Figure 6- 4 The structure of the acrylic ester monomers (Stone, 2010).

The polymerization of acrylic monomers is based on the chain-growth mechanism. It is realized by the head-to-tail connection of the individual monomer units by breaking the monomer double bond and forming a single bond between the newly incorporated monomer units, shown as Figure 6- 5.

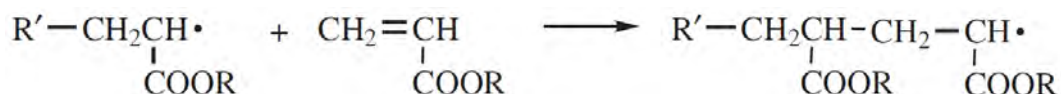


Figure 6- 5 The polymerization mechanism of the acrylic monomers.

The mechanical properties of acrylic ester polymers largely depend on the side chain groups of the ester. If the side chain is H, the poly(acrylic acid) is a brittle material, while the poly(methyl acrylate) is a strong and rubbery material at room temperature. The poly(ethyl acrylate), which has a longer chain length, is more rubbery and extensible. The poly(butyl acrylate)

is tacky at room temperature and can be used as the adhesive. Table 2.1 lists the mechanical properties of acrylic polymers (Stone, 2010). The flexibility of acrylic polymers increases with increasing chain length until it reaches the threshold: poly(n-nonyl acrylate). At this chain length, the side chains will be crystalized and lead to the stiffening of the polymers.

Acrylic ester polymers are chemically stable at aggressive conditions. It is even stable even with exposure to temperatures of 300 °C to 400 °C. This chemical stability guarantees the good durability of the final products. It is also resistant to oxidation and hydrolysis. However, this resistance is not infallible. When exposed to strong acidic or alkaline conditions, the acrylic ester polymers will be hydrolysed to poly(acrylic acid) and alcohol. The resistance to hydrolysis follows the order of butyl acrylate>ethyl ethyl acrylate>methyl acrylate.

The UV radiation resistance is another important factor that determines the durability of the acrylic polymers as pavement coating materials. In general, the acrylic polymers are good at UV resistance; however, if they are incorporated with UV-absorbing monomers, such as styrene, the UV resistance of the resulting products will be considerably decreased and deteriorate rapidly. On the other hand, if the incorporating UV-absorbing monomers are bonded in a non-covalent way, the UV resistance of the resulting polymers will not be affected. For example, hydroxybenzophenone will further enhance the UV resistivity of acrylic polymers (Burgess, 1952).

In pavement engineering, acrylic polymers were widely used as paint materials for pavement markings in past decades. Recently, agencies have started to use them as the overlay materials for color pavements. The acrylic polymer coatings for concrete pavement have been studied as anti-skid overlays (Scholer, 1980). However, the research of acrylic polymers as coating materials on asphalt pavement is also very limited. Except for the relatively low adhesive or bonding strength, when compared with epoxy resins, acrylic polymers have several advantages. First, the flexibility of the cured acrylic polymers is far better than the epoxy resins, which makes capable of matching the pavement deformation during the service time; 2) the chemical and UV stabilities are promising advantages of the acrylic polymers when they are used as overlay materials for pavements; and 3) the relatively low cost guarantees their widely application in pavement engineering.

6.1.3. Advantages and Disadvantages of Various Polymers

Both epoxy and acrylic polymers provide advantages and disadvantages for their use as coating materials for pavements. *Epoxy polymers* typically have several positive benefits including high fatigue strengths, high temperature properties, and chemical stability; however, during installation, the surfaces to be joined have to be carefully cleaned. In addition, generally, the curing time is relatively long and the curing temperature is sometimes high. Apart from the curing problems, the rigidity of the cured epoxy is also a challenge of using epoxy polymers as coating

materials for asphalt pavement. *Acrylic ester polymers* typically have a good plasticity, which is an advantage for the asphalt pavement. It is also chemically stable in aggressive environments. However, neither epoxy nor acrylic polymers are UV resistant. UV ageing is still a critical problem for both of them that needs to be solved.

6.2. Materials and methods

6.2.1 Sample Preparation

For preparation of cement concrete samples, ASTM specification C150-07 Type I/II GU Portland cement from Diamond Mountain, Montana was used. Coarse aggregates (with maximum size of 9.5 mm) and fine aggregates (clean, natural silica sand, maximum size of 4.75mm) were purchased from the JTL Group (Belgrade, MT). A chemical agent, triethylamine (TEA) was used for accelerating the early-age strength of concrete, and a half dosage of air entraining agent was used.

To prepare asphalt concrete, commercial PG 64-22 asphalt was used. The asphalt and aggregates were preheated at 300 °F (150 °C), and the mixture was stirred for 5 minutes, followed by 2 hours at 300 °F (150 °C). After that, the mixture was poured in a mold and pressed to form.

6.2.2 Polymer Coating Procedure

Four types of polymers were utilized as coating materials. For the anti-skid resistant polymer coatings, namely the epoxy and acrylic polymer, the coating thickness was about 2-3 mm, and fine anti-skid resistant silica sand was poured on the coating surface before it fully hardened. After the polymer coating fully hardened, the research team used a vacuum or broom to remove the unbonded aggregates. Of note, to guarantee a good bonding condition, the surface of the sample must be carefully cleaned to remove dirt, which will largely influence the bonding effects of polymer coatings. Methyl methacrylate reactive resin (MMA) and High molecular weight methacrylate polymer (HMWM), which are used as coating to seal cracks, were brushed on the sample surfaces. Unlike the acrylic polymer or epoxy resin, these two polymers were not required to be thick to bond sands due to their low viscosity. No fine aggregates were used in these two coatings.

6.2.3 Bond Strength Testing

Bond strength testing of polymer coatings was performed in accordance with the Bond Strength or Tensile Strength of Concrete Repair and Overlay Materials by Direct Tension (Pull-off Method), shown in Figure 6- 6. Before the testing, a steel brush was used to clean the surface of cement or asphalt concrete samples. The bonding strength of the polymer coatings at -24 °C, -18 °C, -12 °C, -6 °C, 0 °C, 20 °C, 45 °C, and 60 °C was tested.

After the polymer coatings were cured on asphalt concrete for 2 days, the head of the testing device was bonded with the coating using a two components glue. Two hours later, the asphalt concrete was frozen or heated at set temperature for another two hours, followed by the bond strength testing.

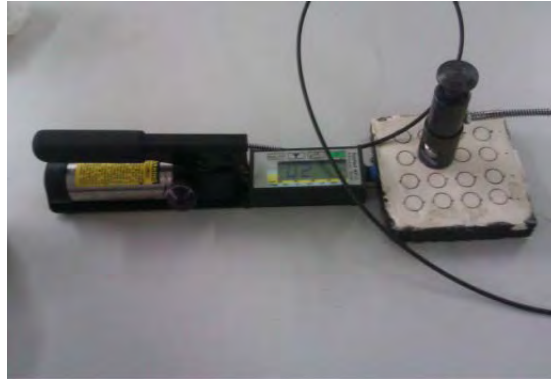


Figure 6- 6 Bond strength tests

6.2.4 Freeze/thaw Resistance Testing

The impacts of the deicers on the coatings were assessed by conducting freeze-thaw tests of concrete samples in the presence of NaCl and MgCl₂ solutions with concentration of 3 wt.% and pure water. The test evaluates the combined effects of deicers and freeze-thaw cycling on the structural integrity of samples with various polymer coatings. Before testing, all surfaces were brushed with polymer coating materials. The samples with 15 exposure cycles were used to simulate the F/T and wet/dry cycles experienced by field conditions in an accelerated manner. Each cycle consisted of 48 hours of fully immersing the samples in the diluted deicer solutions at $-27\pm 5^{\circ}\text{F}$, RH $50\pm 5\%$ followed by 24 hours of thawing and 12 hours of exposing the samples in dry air at room temperature ($73.4 \pm 3^{\circ}\text{F}$, RH $45\pm 5\%$). For the deicer exposure, each sample was placed in a Ziploc bag containing sufficient deicer to avoid water evaporation. The average freezing rate was approximately $0.05^{\circ}\text{C}/\text{min}$ during the first 5 hours and then approximately $0.05^{\circ}\text{C}/\text{min}$ during the subsequent 25 hours. The average warming rate was observed to be approximately $0.01^{\circ}\text{C}/\text{min}$.

6.2.5 Bending Beam Rheometer (BBR) Test

The BBR test was operated according to ASTM D6648-01. The BBR test measures the mid-point deflection of a simply supported prismatic beam of asphalt binder subjected to a constant load applied to the mid-point of the test specimen. A 100-gram load is applied to asphalt binder beams with dimensions of 125mm in length, 6.25mm in width and 12.5mm in height for a total of

240 seconds, and the deflection of the beam is recorded during this period. The primary test results include: creep stiffness of the asphalt binder beam throughout the test. In particular, the creep stiffness and rate of creep stiffness change at 60 sec. are used to grade the asphalt binder. Two test temperatures were used in this study for each asphalt binder. The critical cracking temperature is chosen as the interpolated temperature at which the asphalt binder transitions from failing to passing the Superpave performance criteria.

6.2.6 Surface Friction

The surface friction tests of anti-skid coatings were conducted in accordance with ASTM E303 Standard Test Method for Measuring Surface Frictional Properties Using the British Pendulum Tester. Before the tests, specimens with polymer coatings were kept in an open-air environment for 24 h to keep all test coatings in equivalent curing conditions. The apparatus is shown in Figure 6- 7.

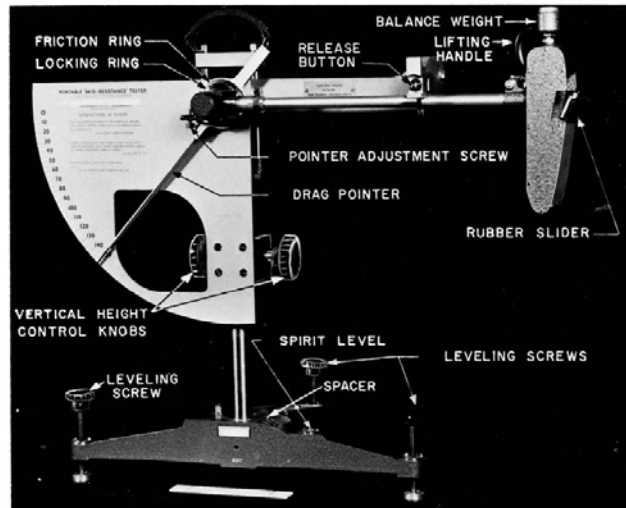


Figure 6- 7 British Pendulum Tester.

6.2.7 Microscopic Characterization

The fracture surface morphology of lab prepared samples was performed on an FEI-Quanta 200F scanning electron microscope. SEM was conducted under an accelerating voltage of typically 20 kV. The X-ray diffraction pattern (XRD) was obtained on a Rigaku D/max-rA X-ray diffractometer with Cu K α radiation ($\lambda = 1.5406 \text{ \AA}$).

6.3. Results and Discussion

6.3.1 Anti-icing performance of asphalt materials exposed to chloride based deicers

Figure 6- 10 displays the creep stiffness testing results of PG 68-22 grade asphalt exposed to chloride based deicers at a) -12 °C, and b) -18 °C. Figure 6- 9 shows the m-values of PG 68-22 grade asphalt exposed to chloride based deicers at a) -12 °C, and b) -18 °C.

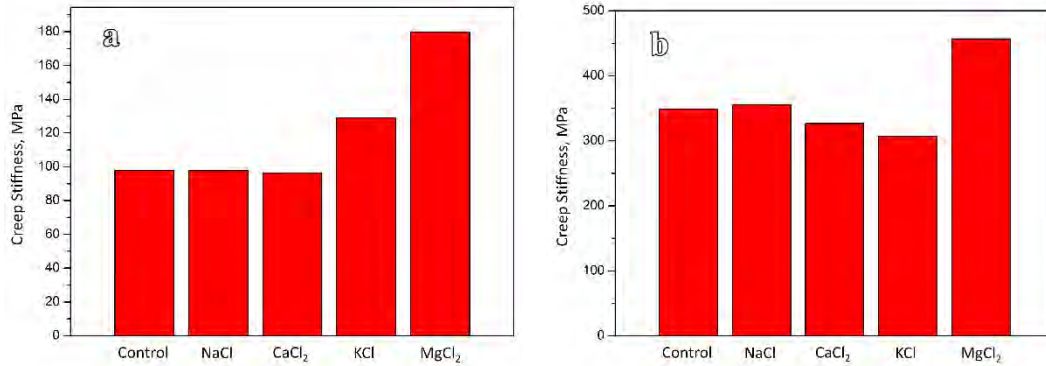


Figure 6- 8 Creep stiffness of PG 68-22 grade asphalt exposed to chloride based deicers at a) -12 °C and b) -18 °C.

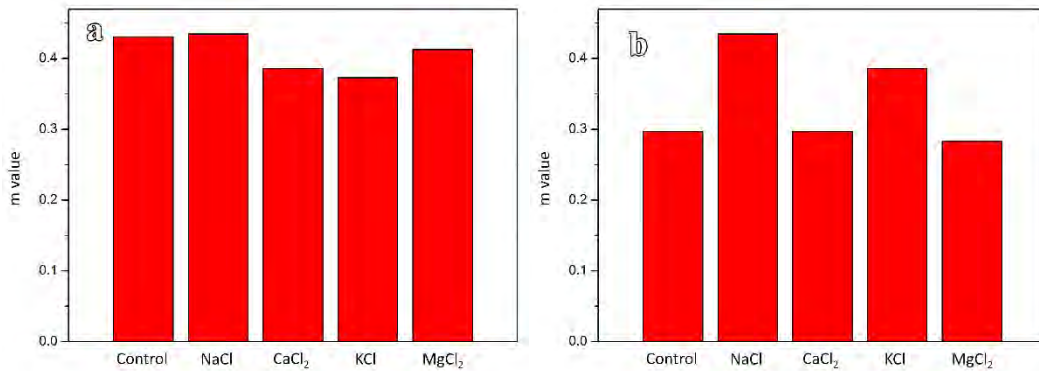


Figure 6- 9 m-values of PG 68-22 grade asphalt exposed to chloride based deicers at a) -12 °C and b) -18 °C

The low temperature performance grade of all of these binders are -22°C. By interpolating temperature from passing to failing the Superpave performance criteria, the continuous performance grade of control binder, binders soaked in the NaCl, CaCl₂, KCl and MgCl₂ are -26.8°C, -26.7°C, -27.0°C, -26.5°C, -24.6°C, accordingly. Therefore, no significant changes was found after 3-day freeze-thaw cycles by using different solutions.

6.3.2 Impacts of Freeze/Thaw Cycles and Deicers on Polymer Coatings

Figure 6- 10 shows external failure images of the acrylic polymer coating on asphalt concrete at various temperatures. As can be seen in this figure, the failure mechanisms can be divided into three types, including the failure of the polymer, the failure of the asphalt, and the failure of both polymer and asphalt.

Of note, three types of failure mechanisms of the coating can be found in all samples tested below $-18\text{ }^{\circ}\text{C}$. At room temperature, however, most of the failures occurred on the polymers, as shown in Figure 6- 10 b). At high temperatures ($>45\text{ }^{\circ}\text{C}$), the failure of acrylic polymer coatings was not observed, and all failures occurred on asphalt materials, shown as Figure 6- 10 c).



Figure 6- 10 External failure images of the acrylic polymer coating on asphalt concrete, a) failure of both polymer and asphalt, b) failure of polymer, and c) failure of asphalt.

Figure 6- 11 and Figure 6- 12 show external images of acrylic and epoxy polymers as coating on asphalt samples before and after 10 F/T cycles. As can be seen in this figure, after 10 F/T cycles, the external dimension of the acrylic polymer coating remains in good shape, while the epoxy coating shows obvious damage, including bubbles and color change.

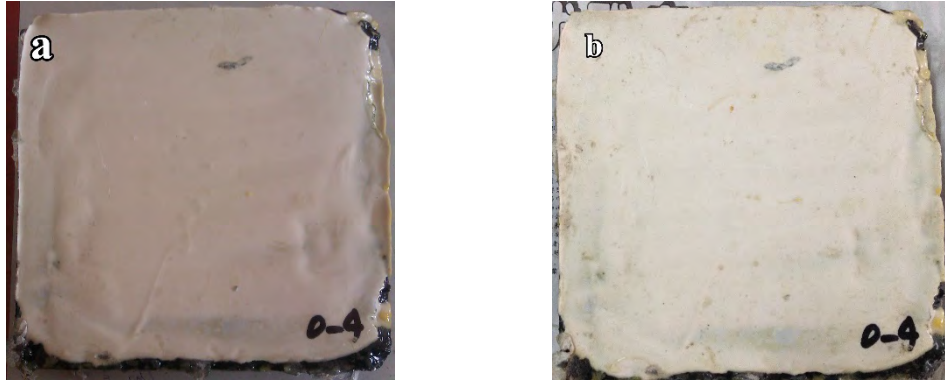


Figure 6- 11 External image of acrylic polymer coating a) before and b) after F/T cycles in water.

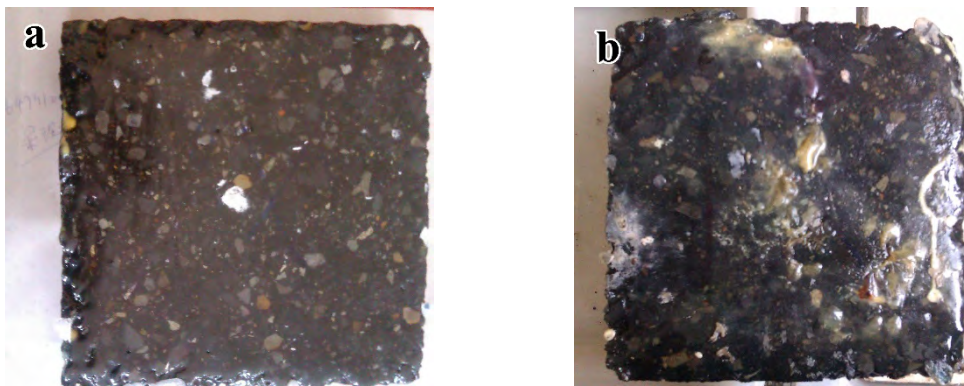


Figure 6- 12 External image of epoxy polymer coating a) before and b) after F/T cycles in water.

Figure 6- 13 illustrates the change in bond strength of acrylic polymers after 15 of F/T cycles in water, 3% NaCl and MgCl₂ solutions. In general, the bond strength of the acrylic polymer stays intact after F/T and W/D cycles in water, NaCl and MgCl₂ solutions; and such bond strength decreases significantly as testing temperatures increase.

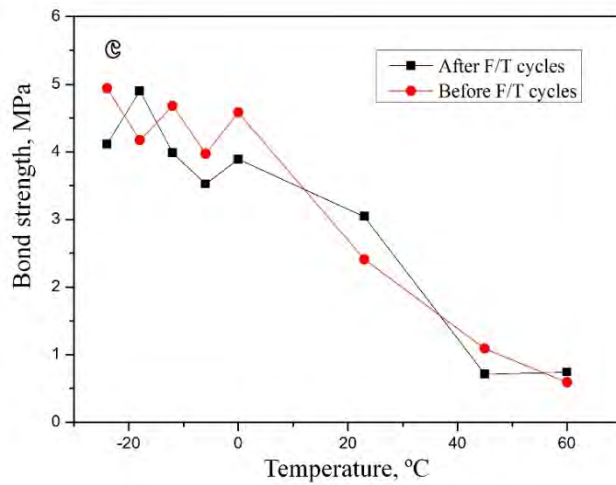
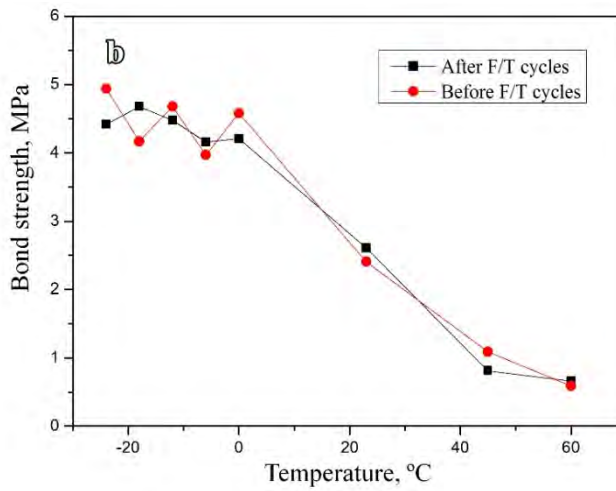
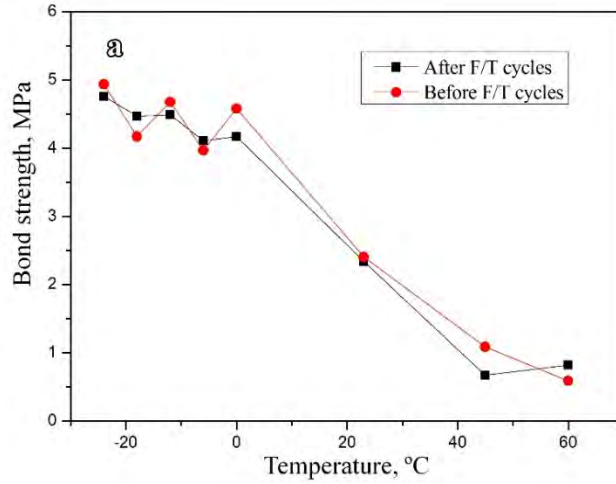


Figure 6- 13 Bond strength of acrylic polymer exposed to a) water, b) NaCl, and c) MgCl₂ solution after 15 F/T cycles at various temperatures.

6.3.3 Abrasion Resistance of Acrylic Polymer Coatings

Figure 6- 14 shows images of the asphalt concrete samples with the acrylic polymer coating before and after abrasion resistance testing. As can be seen in this figure, after the skid testing, although some anti-skid sand at the top layer has been removed, the sands at the bottom of the coating remains in good shape.

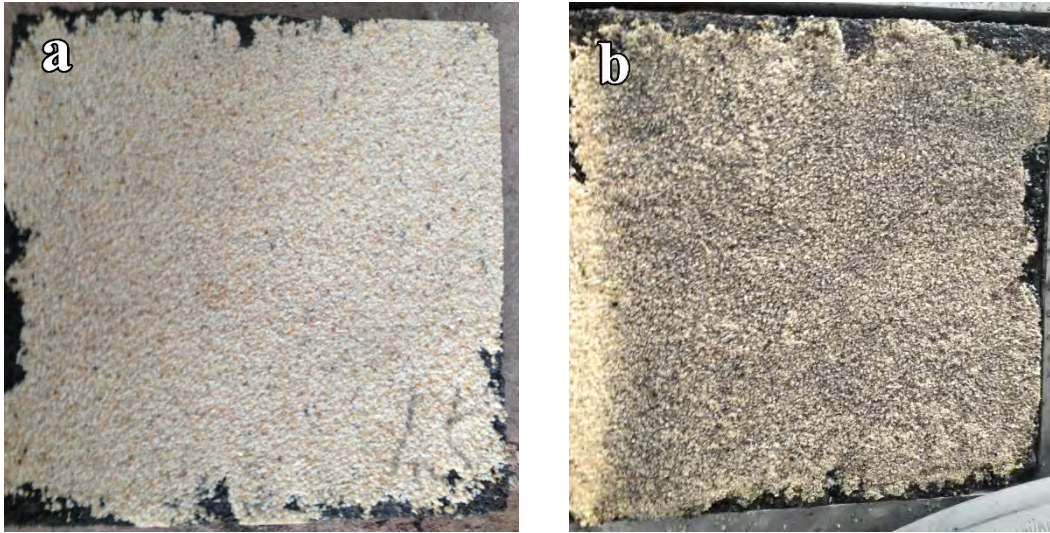


Figure 6- 14 Asphalt concrete samples with the acrylic polymer coating a) before and b) after abrasion resistance testing.

Table 6- 1 lists the BPN values of acrylic polymer coatings before and after 15 F/T cycles exposed to water, NaCl and MgCl₂, respectively. As can be seen in this list, the abrasion resistance of the acrylic polymer coating has no considerable change after F/T cycles in NaCl or MgCl₂ solutions, suggesting a good anti-salt scaling performance.

Table 6- 1 BPN values of acrylic polymer coatings before and after 15 F/T cycles exposed to water, NaCl and MgCl₂ solutions

Samples	BPN
Control Samples	61
Acrylic polymer coatings before F/T cycles	70
Acrylic polymer coatings after F/T cycles in water	65
Acrylic polymer coatings after F/T cycles in 3% NaCl	67
Acrylic polymer coatings after F/T cycles in MgCl ₂	62

6.3.4 Anti-icing Performance of Crack Sealant Polymers

In a laboratory study, two commercial surface treatment products, namely Methyl methacrylate reactive resin (MMA) and High molecular weight methacrylate polymer (HMWM), were evaluated for their effectiveness in protecting concrete from freeze/thaw and wet/dry cycles and exposure to a diluted deicer simulated by 3 wt.% NaCl and MgCl₂ solution. The results indicated that both of the surface treatments exhibited good performance.

Figure 6- 15 shows the splitting tensile strengths of concrete samples coated with MMA and HMWM with exposure to 3,7, and 15 F/T cycles in NaCl and MgCl₂ solutions. Although the splitting tensile strength shows some reduction after 15 F/T cycles in deicer solutions, the coatings can continue to protect the concrete samples from the impacts of deicers along with F/T cycles. As can be seen in this figure, after 3 and 7 F/T cycles, the samples with exposure to NaCl and MgCl₂ solutions show little reduction in splitting tensile strengths in comparison to the control samples. However, after 15 F/T cycles, the splitting tensile strength of the sample exposed to MgCl₂ without coating has a considerable reduction, while those with HMWM and MMA coatings retain better performance than the control sample.

Figure 6- 16 to Figure 6- 19 show the low and high magnification SEM microstructure images of the coatings after 15 F/T cycles with exposure to NaCl and MgCl₂ solution, respectively. As can be seen from these figures, after F/T cycles in deicer solutions, microcracks can be observed in both HMWM and MMA coatings. Even the MMA shows the integrity morphology at low magnification, but the high magnification images illustrate that the nano sized cracks are initiated in both polymer coatings. Figure 6- 15 confirms that the splitting tensile strength of the sample with the MMA coating is higher than the control sample and the sample with HMWM coating. In addition, as shown in Figure 6- 18, with exposure to NaCl solution, the coating surface is not as smooth as other conditions. The high magnification microstructure demonstrated that some crystals with size range from 50-200 nm were precipitated on the coating surface, and the coating becomes porous.

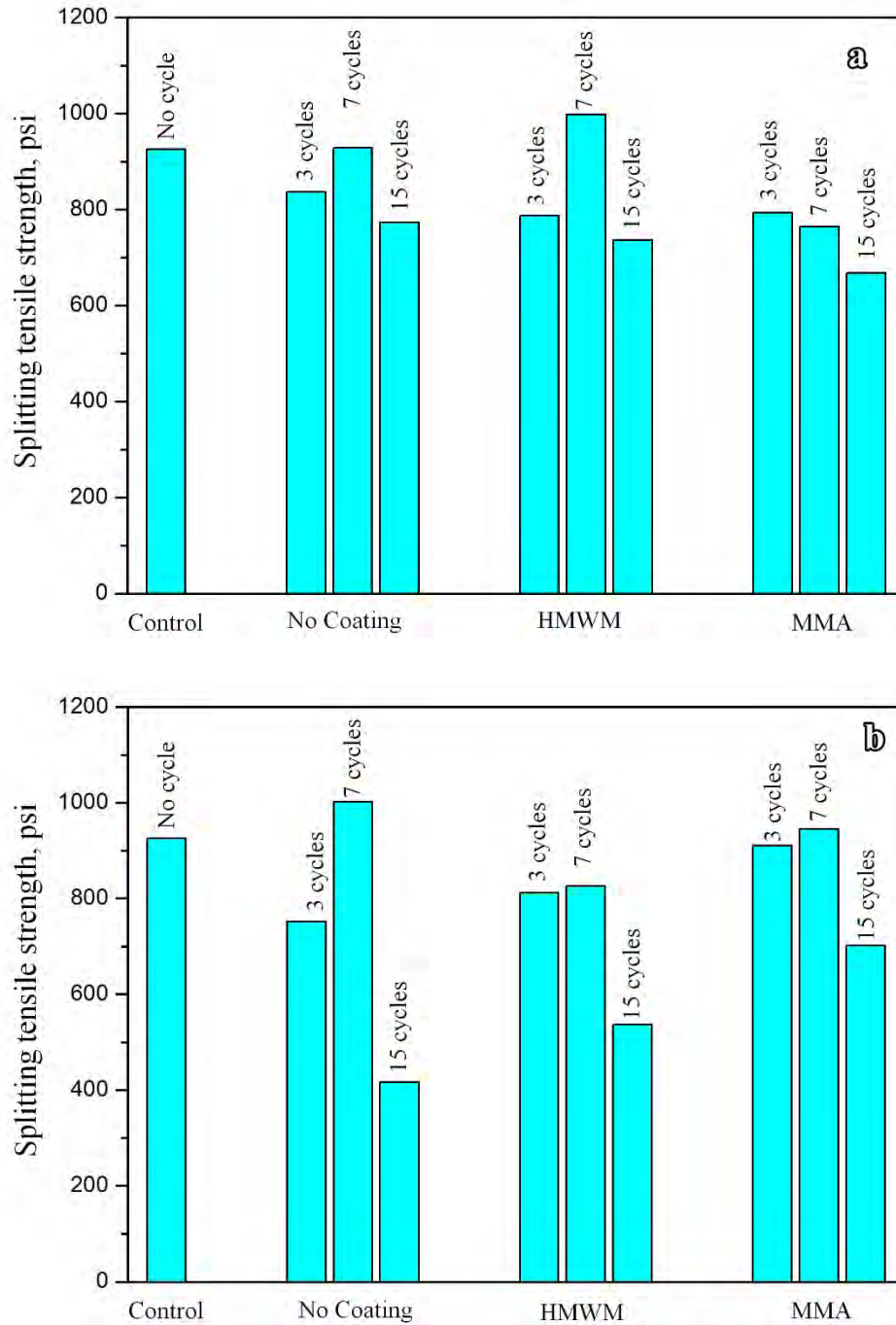


Figure 6- 15 Splitting tensile strength of concrete samples with various coatings with exposure to a) NaCl and b) MgCl₂ solution.

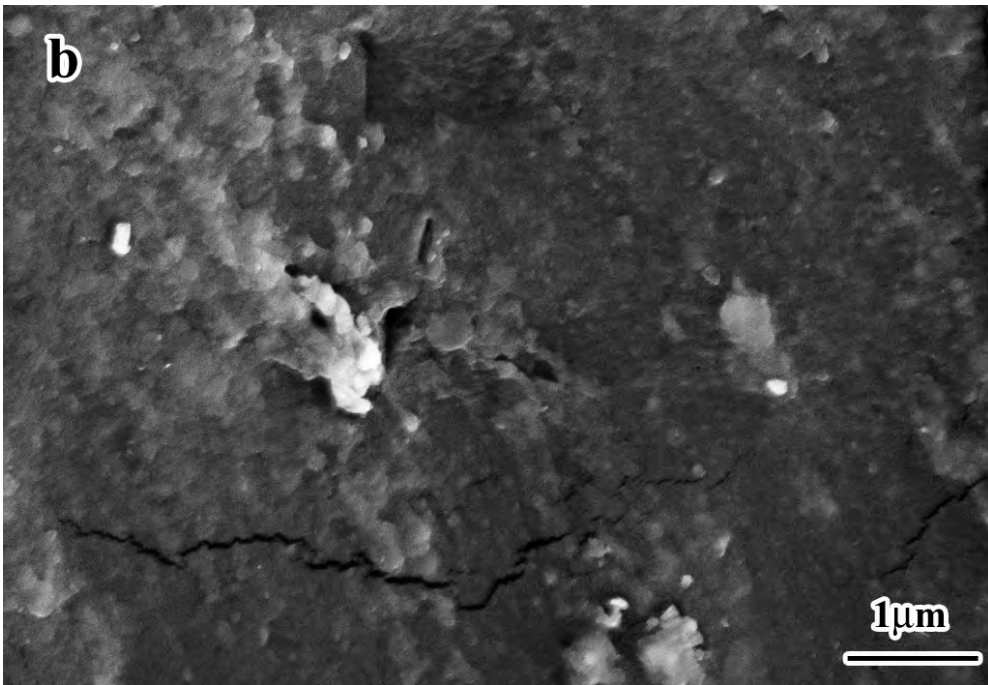


Figure 6- 16 SEM microstructure images of the HMWM coatings after 15 F/T cycles with exposure to MgCl₂ solution a) low magnification, b) high magnification.

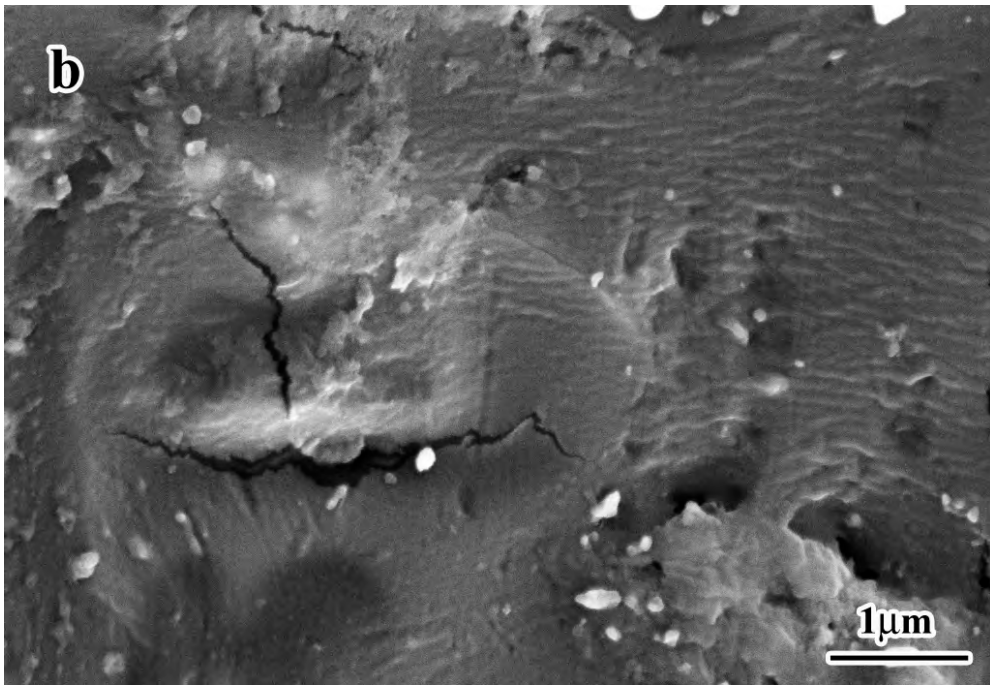


Figure 6- 17 SEM microstructure images of the MMA coatings after 15 F/T cycles with exposure to MgCl₂ solution a) low magnification, b) high magnification.

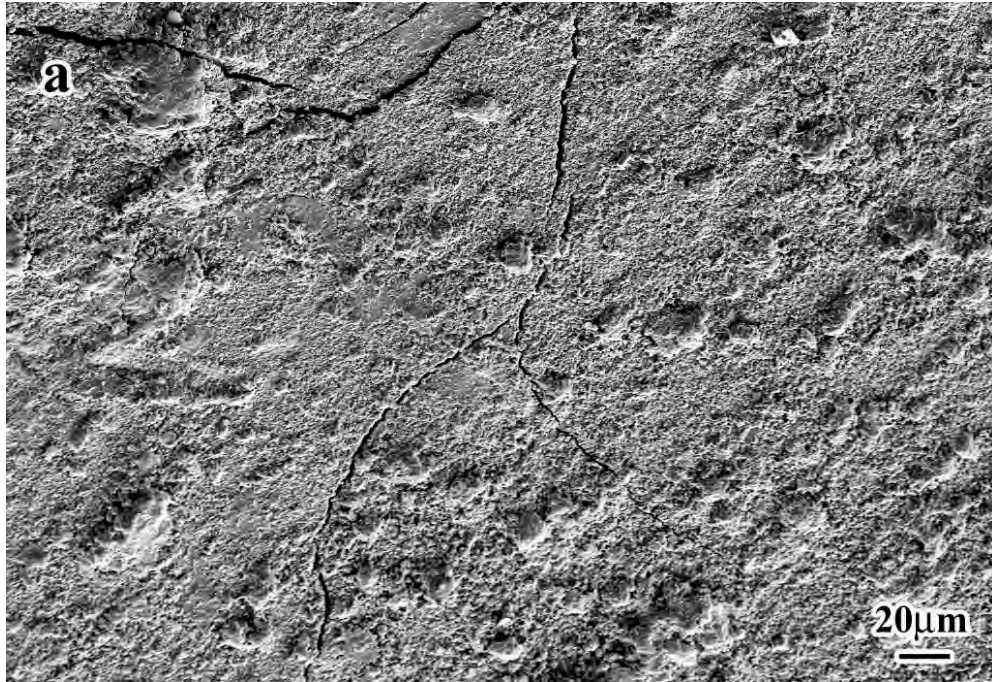


Figure 6- 18 SEM microstructure images of the HMWM coatings after 15 F/T cycles with exposure to NaCl solution a) low magnification, b) high magnification.

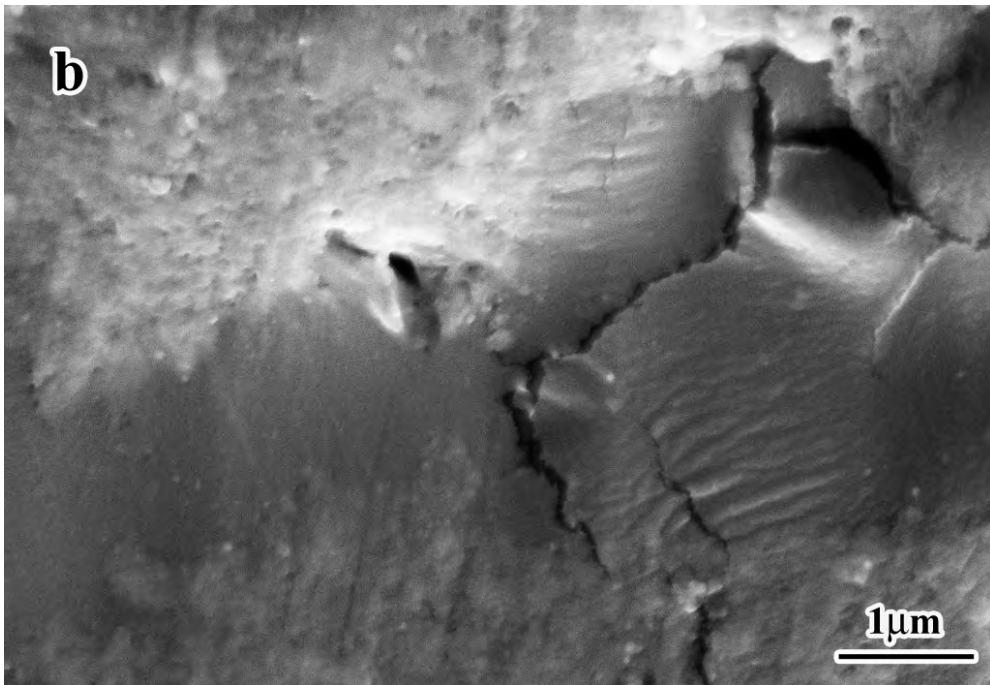


Figure 6- 19 SEM microstructure images of the MMA coatings after 15 F/T cycles with exposure to NaCl solution a) low magnification, b) high magnification.

Of particular note, unlike cement or asphalt materials whose properties are relatively stable, the properties of polymers vary largely with different polymer structures or doping elements. As a

result, the performance of the polymers tested in this chapter only represent the polymers we used, which CANNOT represent other polymer performances.

6.4 Key Findings

The failure mechanisms of polymers can be divided into three types, including the failure of the polymer, the failure of the asphalt, and the failure of both polymer and asphalt. Three types of failure mechanisms of the coating can be found in all samples tested below -18 °C. At room temperature, however, most of the failures occurred on the polymers. At high temperatures (>45 °C), all failures occurred on the asphalt materials.

After 10 F/T cycles in water, the external dimension of the acrylic polymer coating remains in good shape while the epoxy coating shows obvious damage, including bubbles and color change.

The bond strength of the acrylic polymer stays intact after F/T and W/D cycles in water, NaCl and MgCl₂ solutions; and such bond strength decreases significantly as testing temperatures increase.

The BPN values of acrylic polymer coatings before and after 15 F/T cycles exposed to water, NaCl and MgCl₂ show that the skid resistance of the acrylic polymer remains in good shape with exposure to NaCl and MgCl₂ deicers.

After 3 and 7 F/T cycles, the samples with exposure to NaCl and MgCl₂ solutions with HMWM and MMA coatings show little reduction in splitting tensile strengths in comparison with the control samples. However, after 15 F/T cycles, the splitting tensile strength of the sample exposed to MgCl₂ without coating has a considerable reduction, while those with HMWM and MMA coatings have better performance than the control sample.

After F/T cycles in NaCl and MgCl₂ deicer solutions, microcracks can be observed in both HMWM and MMA coatings. The high magnification images illustrate that the nano sized cracks are initiated in both polymer coatings. In addition, with exposure to NaCl solution, the HMWM coating surface is not as smooth as other conditions. The high magnification microstructure demonstrated that some crystals with size range from 50-200 nm were precipitated on the coating surface, and the coating becomes porous.

6.5 References

Burgess, A. R. (1952). U.S. Patent No. 2,615,860. Washington, DC: U.S. Patent and Trademark Office.

Epon Resin Structural Resin Manual-Additive Selection, Resolution Performance Polymers, LLC, Houston, Texas, 2001.

Federal Highway Administration (FHWA). (2010), "Highway bridge by wearing surface. NBI. Inspection and evaluation bridge structures", <http://www.fhwa.dot.gov/bridge/wearing.cfm>.

Lee, H., & Neville, K. (1967). Handbook of epoxy resins.

Osumi, Y., (1987) "One-Part Epoxy Resin". Three Bond Technical News, Three Bond, October, 1.

Riddle E. H., (1954). "Monomeric Acrylic Esters", Reinhold Publishing Corp., New York.

Stone, R.V. (2010), "Acrylic ester polymers". Encyclopedia of Polymer Science and Technology. John Wiley.

Scholer, C. F., & Forrestel, R. R. (1980), "Use of a Very Thin Overlay to Reestablish the Skid Resistance of a Concrete Pavement", Transportation Research Record, (752).

Stone, R.V. (2010), "Acrylic ester polymers". Encyclopedia of Polymer Science and Technology. John Wiley.

Young, L. M., & Durham, S. A. (2012), "Performance of an Anti-Icing Epoxy Overlay on Asphalt Surfaces", Journal of Performance of Constructed Facilities, 27(6), 836-840.

CHAPTER 7. CONCLUSIONS

The coring samples show different mechanical properties. The SEM analysis demonstrates that a large quantity of pores and many small sized “bumpy phases” can be observed in the cement paste of the cored samples, and the quantity of the amorphous binder phase is far less than normal cement paste. The SEM/EDS analysis results confirm the leaching of Ca^{2+} out of the cement paste, which is likely caused by the chemical reaction of MgCl_2 with Ca-rich cementitious phases. This may be a major reason for the reduction of the mechanical strength of the concrete samples cored from these sites.

Eight types of deicers, including NaCl, KCl, KAc, KFm, MgCl_2 , CaCl_2 , CaAc_2 , and CaFm_2 were used to compare their anti-icing performances. It was found that CaCl_2 has the highest ice melting capability, while MgCl_2 has the lowest ice melting capability at -25°C . The corrosion rates of stainless steel with exposure to various deicers are not very high, and were all in the range of 0.0 ± 0.2 MPY, except CaFm_2 , which has a relatively high corrosion rate of 1.12 MPY. The corrosion rates of plain steel with exposure to various deicers are considerably different. All chloride salts have relatively high corrosion rates from about 30 to 48 MPY, while KAc and CaAc_2 have extremely low corrosion rates of about -2.0 MPY. CaFm_2 had a relatively high corrosion rate of about 30 MPY. The corrosion rates of galvanized steel with exposure to various deicers are all relatively high, and ranged from 15 to 47 MPY. All concrete samples exposed to alkali metal based deicer solutions exhibited severe surface distress, while the samples exposed to alkali earth metal based deicer solutions show little surface distress. Concrete samples exposed to KCl solution show the highest value of mass loss, while the samples exposed to CaCl_2 solution show the lowest. The mechanical properties testing results show that MgCl_2 has a considerable reduction of splitting tensile strengths, even without obvious visible deterioration of the external shape of the samples.

After exposure to F/T and W/D cycles in various deicer solutions, only MgCl_2 exposed samples show white precipitates. Microstructure analysis demonstrated that the alkali metal based deicers strongly affect the deterioration of the C-S-H binder phase in cement paste. CaCl_2 and CaAc_2 have less of an effect on the C-S-H phase than other deicers. $\text{CaMg}_2\text{Cl}_6\cdot(\text{H}_2\text{O})_{12}$ is one of the main reaction products when concrete is exposed to MgCl_2 .

The failure mechanisms of polymers as surface treatment methods for asphalt pavement can be divided into three types, including the failure of the polymer, the failure of the asphalt, and the failure of both polymer and asphalt. Three types of failure mechanisms of the coating can be found in all samples tested below 0°F (-18°C). At room temperature, however, most of the failures occurred on the polymers, and at high temperatures ($>113^\circ\text{F}$ (45°C)), all failures occurred on the asphalt materials. After 10 F/T cycles in water, the external dimension of the acrylic polymer coating remains in good shape while the epoxy coating shows obvious damage, including bubbles and color change. The bond strength of the acrylic polymer stays intact after F/T and W/D cycles

in water, NaCl and MgCl₂ solutions; and such bond strength decreases significantly as testing temperatures increase. The BPN values of acrylic polymer coatings before and after 15 F/T cycles exposed to water, NaCl and MgCl₂ show that the skid resistance of the acrylic polymer remains in good shape with exposure to NaCl and MgCl₂ deicers. After 3 and 7 F/T cycles, the samples with exposure to NaCl and MgCl₂ solutions with HMWM and MMA coatings show little reduction in splitting tensile strengths in comparison with the control samples. However, after 15 F/T cycles, the splitting tensile strength of the sample exposed to MgCl₂ without coating has a considerable reduction, while those with HMWM and MMA coatings have better performance than the control sample. After F/T cycles in NaCl and MgCl₂ deicer solutions, microcracks can be observed in both HMWM and MMA coatings. The high magnification images illustrate that the nano sized cracks are initiated in both polymer coatings. In addition, with exposure to a NaCl solution, the HMWM coating surface is not as smooth as other conditions. The high magnification microstructure demonstrated that some crystals with size range from 50-200 nm were precipitated on the coating surface, and the coating becomes porous.



Nevada Department of Transportation
Rudy Malfabon, P.E. Director
Ken Chambers, Research Division Chief
(775) 888-7220
kchambers@dot.state.nv.us
1263 South Stewart Street
Carson City, Nevada 89712